

AD 684945

①

TEXTILE DIVISION  
MECHANICAL ENGINEERING DEPARTMENT  
MASSACHUSETTS INSTITUTE OF TECHNOLOGY  
CAMBRIDGE 39, MASSACHUSETTS

DYNAMIC TESTING OF SMALL TEXTILE  
STRUCTURES AND ASSEMBLIES

FINAL REPORT

BY

J.G. KRIZIK  
D.M. MELLEN  
S. BACKER

DDC  
RECORDED  
MAR 14 1969  
RECORDED  
C

QUARTERMASTER RESEARCH AND DEVELOPMENT CENTER  
TEXTILE CLOTHING AND FOOTWEAR DIVISION  
CONTRACT NO. DA-19-129-QM-1308  
M.I.T.-D.S.R. NO. 8072  
PROJECT 7-93-18-019

This document has been approved  
for public release and sale; its  
distribution is unlimited.

PUBLIC RELEASE AND SALE: ITS DISTRIBUTION  
IS UNLIMITED.

Reproduced by the  
CLEARINGHOUSE  
for Federal Scientific & Technical  
Information Springfield Va. 22151

TD-93-61

THIS DOCUMENT HAS BEEN APPROVED FOR  
PUBLIC RELEASE AND SALE; ITS DISTRIBUTION  
IS UNLIMITED.

DYNAMIC TESTING OF SMALL TEXTILE  
STRUCTURES AND ASSEMBLAGES

TABLE OF CONTENTS

		Page
Section A	INTRODUCTION.	A-1
Section B	FACTORS INFLUENCING STRUCTURAL EFFICIENCY OF TEXTILES.	B-1
Section C	PROBLEMS IN MEASUREMENT OF STRAIN IN IMPACT TESTS ON TEXTILE MATERIALS.	C-1
Section D	IMPACT BEHAVIOR OF SAMPLES TAKEN FROM STORAGE OR FIELD USE.	D-1
Section E	IMPACT BEHAVIOR OF TEXTILE YARNS.	E-1
Section F	IMPACT BEHAVIOR OF MORE COMPLEX TEXTILE STRUCTURES.	F-1
Section G	THE MITEX IMPACT TESTER.	G-1
Section H	OPERATING INSTRUCTIONS FOR THE MITEX IMPACT TESTER.	H-1

## LIST OF FIGURES

	Page
Stress Application across Seam	C-1
Trellis Action of a Textile Fabric	C-2
Strain Pattern in a Textile Fabric	C-3
Load vs. Elongation at Various Gage Length	C-4
Elongation vs. Gage Length	C-5
Load vs. Elongation with Various Jaws	C-6
Schematic of Load-Strain Measuring System for High Speed Testing of Textile Structures	C-7
YSE-VEP 507 - Average Breaking Load of Exposed and Shaded Yarns vs. Exposure Period	D-1
YE-VEP 507 - Breaking Load of Exposed Yarns vs. Exposure Period	D-2a
YS-VEP 507 - Breaking Load of Shaded Yarns vs. Exposure Period	D-2b
YE-VEP 507, - Breaking Load of Exposed Yarns vs. Log. Strain Rate	D-3a
YS-VEP 507 - Breaking Load of Shaded Yarns vs. Log. Strain Rate	D-3b
YSE-VEP 506 - Average Breaking Load of Exposed and Shaded Yarns vs. Exposure Period.	D-4
YE-VEP 506 - Breaking Load of Exposed Yarns vs. Exposure Period	D-5a
YS-VEP 506 - Breaking Load of Shaded Yarns vs. Exposure Period	D-5b
YE-VEP 506 - Breaking Load of Exposed Yarns vs. Log. Strain Rate	D-6a
YS-VEP 506 - Breaking Load of Shaded Yarns vs. Log. Strain Rate	D-6b
YSE-VEP 507 - Average Breaking Strain of Exposed and Shaded Yarns vs. Exposure Period	D-7
Breaking Strain of Exposed Yarns vs. Exposure Period	D-8a
Breaking Strain of Shaded Yarns vs. Exposure Period	D-8b

## LIST OF FIGURES (Continued)

	Page
Breaking Strain of Exposed Yarns vs. Log. Strain Rate	D-9a
YS-VEP 507 - Breaking Strain of Shaded Yarns vs. log. Strain Rate	D-9b
YE-VEP 507 - YS-VEP 507 - Summary of Strain Rate and Exposure Period Effects	D-10
YSE-VEP 506 - Average Breaking Strain Exposed and Shaded Yarns vs. Exposure Period	D-11
YE-VEP 506 - Breaking Strain of Exposed Yarns vs. Exposure Period	D-12a
YS-VEP 506 - Breaking Strain of Shaded Yarns vs. Exposure Period	D-12b
YE-VEP 506 - Breaking Strain of Exposed Yarns vs. Log. Strain Rate	D-13a
YS-VEP 506 - Breaking Strain of Shaded Yarns vs. log. Strain Rate	D-13b
YE-VEP 506 -YS-VEP 506 - Summary of Strain Rate and Exposure Period Effects	D-14
W-VEP 509, W-VEP 510 - Breaking Load and Strain of Exposed Webbing vs. Exposure Period	D-15
The Influence of Strain Rate on Strength	E-1
The Influence of Strain Rate on Extension	E-2
The Influence of Strain Rate on Loop/Straight Strength and Strain Ratio	E-3
Loop Efficiency of Various Yarns as Function of Strain Rate	E-4
Stress vs. Strain, Acetate 900-240-22	E-5
Stress vs. Strain, Arnel 600-160-22	E-6
Stress vs. Strain, Dacron 250-50-0	E-7
Stress vs. Strain, High Tenacity Viscose Rayon (Rayflex No. 1) 600-490-0	E-8
Stress vs. Strain, High Tenacity Viscose Rayon (Rayflex No. 2) 600-234-2.5S	E-9
Stress vs. Strain, Nylon, 210-34-0, Type 305	E-10
Stress vs. Strain, PVA (Vinal Fo) 1000-250-0	E-11

## LIST OF FIGURES (Continued)

	Page
'Z' Twisted Dacron, Nylon and an Experimental Yarn, Stress vs. Strain at 1 in/min.	E-12
'Z' Twisted Dacron, Nylon and an Experimental Yarn, Stress vs. Strain at 200 in/min.	E-13
Loop/Straight Ratio vs. Strain Rate	E-14
Load Extension - Behavior of Parachute Cloth Static vs. Impact	F-1
Yarn Strain Distributions at Failure	F-2
Photographic History of Fabric Failure	F-3
Photographic History of Seam Failure	F-4
Schematic of MITEK Impact Tester	G-1
Instrumentation Block Diagram for MITEK Impact Tester	G-2
Wiring Diagram of Control Switches of MITEK Impact Tester	G-3
Assembly of MITEK Impact Tester	G-4
Structure of MITEK Impact Tester	G-4a
Lower Jaw Displacement as Function of Time	G-5
MITEK Impact Tester Part 1	G-6
MITEK Impact Tester Part 2	G-7
MITEK Impact Tester Part 3	G-8
MITEK Impact Tester Part 4	G-9
MITEK Impact Tester Part 5	G-10
MITEK Impact Tester Part 6a	G-11
MITEK Impact Tester Part 6b	G-12
MITEK Impact Tester Part 7	G-13
MITEK Impact Tester Part 8	G-14
MITEK Impact Tester Part 9	G-15
Panel of MITEK Impact Tester	H-1
Left Side Panel, MITEK Impact Tester	H-2

## LIST OF TABLES

	Page
Tensile Behavior of Nylon Threads (VEP 501)	E-3
Coefficient of Variation in Load-Elongation Tests	E-4
Loop Test Efficiency	E-6
Translation of Yarn Strength into Fabrics	F-2
Fabric and Yarn Particulars of QM Standard & RA #2	F-4
Load-Strain Behavior of QM Fabrics	F-5
Instron and Impact Tests on Ballistic Yarn	F-6
Effect of Strain Rate on Efficiency of Parachute Seams	F-13

SECTION A  
INTRODUCTION

This report presents results of a study of the impact behavior of textiles, conducted by the Textile Division, Mechanical Engineering Department, M.I.T. Principal emphasis of this study was directed towards the high speed mechanical behavior of small textile structures and assemblages, with a view to determining the factors controlling the translation of fiber, yarn, and fabric properties into a product's impact performance.

As a part of this program, a study has been completed on the mechanical behavior of textile materials which have been subjected to long storage periods of complete inactivity or to long service life and hard usage. The purpose of this phase was to establish the utility of impact test behavior, as contrasted to performance in slower speed conventional tests, in detecting actual or latent damage in the textile structure.

In this study, instrumentation and test procedures have occupied the usual high percentage of time consistent with the experimental problems of high speed testing. As a result of the close attention given to experimental problems, several new techniques have been developed which will hold interest for the general field of materials testing at high speeds. A simple effective technique of measuring strain has been invented, one which combines accuracy and reproducibility with low cost. The drop impact testers of the Textile Division Laboratory have been modified for more versatile and controlled impact testing.

A pneumatic-hydraulic test unit has been developed, following earlier designs outlined in a previous M.I.T. Textile Division contract with the Textile Clothing and Footwear Division of the

Quartermaster Research and Development Command. This unit operates at a load capacity of 500 lbs. with testing rates varying from 1 foot/second to 25 feet/second, thus providing an extrapolation of the speeds available in the standard Instron tester. A second model of this (MITEX) unit has been constructed and furnished to the Textile Materials Laboratory at the Q.M. R. & D. Center, Natick.

These new techniques and instruments are described in some detail in the report, and their potential contribution to the field of textile impact testing is demonstrated.

## SECTION B

### FACTORS INFLUENCING STRUCTURAL EFFICIENCY OF TEXTILES

The fibrous forms of many substances are observed to have extremely high tenacities. In some instances technical strengths approaching theoretical limits have been obtained in fiber materials. Varying reasons account for this strength in different substances. Absence of macro and micro cracks are considered to be the reason for the high strength of freshly drawn glass filaments. Elimination of crystal discontinuities or dislocations explains the high strength of metal 'whiskers'. High crystallinity and orientations are attributed as contributing to high tenacity and high modulus of finely drawn organic textile fibers.

The fibrous reinforcement in leaf, stem, trunk, and even animal body tissue is nature's method of forming a relatively soft flexible system endowed with moderately high extensibility and at the same time capable of supporting heavy loads. The inherent slenderness ratio of these fibrous reinforcing elements assures the natural structure of low bending rigidity regardless of their modulus of elasticity in tension or in shear. Such flexibility is, of course, multiplied if the matrix surrounding the fibers has very low shear rigidity and/or readily permits relative movement between fibers during bending of the structure. The ultimate in structural flexibility is achieved when the fibers of a structure are not embedded at all and when the coefficient of friction between the fibers is minimized.

The flexibility considered so necessary in textile structures is accompanied, unfortunately, by a considerable loss of efficiency of translation of the extremely high fiber strengths into yarn

and fabric strengths. Further, there is a loss in fabric strength potential in the fabrication of end items via the sewing process. This inability to translate fiber tenacities into yarn and fabric strength is sometimes due to the inherent weakness of the fiber, to local shear stresses, and to lateral normal pressures, -- as in the case of glass fibers. But in the main, structural strength inefficiencies of textile systems are due to the overwhelming strain inhomogeneities forced on the average yarn or cloth specimen in daily usage.

The twist or the helix angle of fiber in the yarn determines the stress and strain level for each fiber at different yarn strain levels. The crimp inclination angles at load equilibrium determine the local stress level for yarn in a fabric subjected to uniaxial tension or biaxial tension. The degree of yarn flattening likewise influences the local strains in the yarn crown in the stressed fabric. And in bending of fabrics the local twist, the orientation of warp and filling and the mobility of fibers within the yarn and fabric structures all influence the local strain level. Finally, at the joining between fabrics the type of seam, the stitch length and the mobility of yarns in the joined fabrics interact to establish a pattern of local strains.

Where a high degree of strain inhomogeneity is the order of the day, the stress-strain characteristics of the fibers interact with the structural geometry of the fiber assemblage to determine strength efficiency of the system. Maximum strength efficiency can be defined as the case where the fibers working together in the system give rise to a load bearing capacity equal to the sum of the tensile strengths of the

individual fibers tested separately.

The textile structure subjected to a non-homogeneous strain will fail in a stepwise fashion with the failure initiating where the local strain first exceeds the strain to rupture of the fiber present at the point. The failure may propagate from this position leading to early failure of the entire structure. But it is also possible for other regions of the material to reach breaking strains before the initial failure in the system propagates catastrophically to a complete rupture.

Knowledge of the strain inhomogeneity can be used as a basis for calculating the stress distribution in a given structure, as well as the integrated contribution of this stress to tensile resistance in a given direction. The case of twisted yarns has been treated in this way by Platt; the non-woven structure has been studied by Petterson. The experimental confirmations of Platt's and Petterson's analyses were restricted to uniaxial strain. However, Petterson's non-woven fabric analysis affords predictions of general plane stress-strain behavior. While Petterson's experiments did not include biaxial stress, no doubt experiments can be devised to reproduce more complex stress and strain conditions for the non-woven.

The analytical treatment of yarn and non-woven fabric uniaxial strength illustrates the importance of fiber stress-strain properties in the realization of high strength efficiencies. The stress-strain curve which portrays a flat region in the vicinity of rupture assures maximum contribution of fiber strength to fabric strength. This follows from the fact that those fibers which have not quite been strained to break in the system at the time of the initiation of rupture (at a single point of the material) will likely be strained up into the flat region of

their stress-strain curve, and will contribute the major share of their strength at that moment. If their stress-strain curves lacked the broad flat region at rupture then the presence of strain differentials in the system would find many fibers contributing but a small part of their strength potential at the time of failure initiation. Platt has characterized this flat section of the stress-strain curve in terms of its slope and intercept. Clearly a small slope and a large intercept are desirable elements for high strength and strength efficiency in a fibrous structure.

Uniformity in strain to rupture is another extremely important characteristic of the individual fiber in determining its strength transfer efficiency. For if certain fibers in a population have extremely low values of rupture strain, they will fail at an early stage in a strain field which may in itself be fairly homogeneous. And this failure may lead to successive rapid failures of contiguous elements. Actually, the placement of fibers with widely varying rupture strains in a relatively uniform strain field is similar to placement of uniform properties fibers in a non-homogeneous field. The parameter which Platt suggests as most indicative of the fiber's uniformity contribution to strength efficiency is the coefficient of variation of fiber elongation to rupture. And this coefficient has been used effectively in analytical treatment of the uniaxial strength of yarns. Of course, other aspects of non uniformity play an important part in determining fiber strength contribution. For example, the presence of weak spots in the yarn will influence yarn strength, the effect being a function of gage length. Similarly the uniformity or lack of uniformity of cross-section will influence the ultimate stress-strain curve

of the fiber and that of the yarn.

These studies of the influence of non uniformity of fiber properties point the way to numerous other areas of investigation related to the question of strength efficiencies in textiles. For example, the case of parallel fibers considered by Platt can be extended to the treatment of yarns in loose open fabric. The weakest link theory of Peirce can be applied to non-wovens and to textile components subjected to series loading in general. Both approaches are useful in the case of the stressed seam which contains elements of parallel and of series loading.

In the treatment of more complex structures one must account for the presence of complex stresses. The yarn in a close woven fabric can no longer be considered as independent of its neighbor. If the single yarn varies along its length in cross-section, packing factor, or tensile modulus, it is no longer free to obey the simple rules of series loading, i.e. local strain being inversely proportional to local stiffness. For the local strain in the yarn must be consistent with that in the contiguous yarn as determined by the cross thread coupling. The importance of the coupling is dependent on properties of the cross thread, and in particular on the mobility of yarn in fabric.

Failure in a closely woven fabric is likewise influenced by the presence of threads laid perpendicular to the principal direction of tension. If the longitudinal threads are completely uniform in cross-section and in modulus along their length, the first break will occur in the yarn possessing the lowest extension (as tested singly and uniaxially). It is questionable, however, whether the next break will take place in the yarn which has the next lowest extensibility. For as the first yarn ruptures and seeks to discharge its strain-energy it is prevented from freely doing so by the cross yarns which pick up part of

the tensile component necessary to maintain the extension of the first yarn. This tensile component is transferred (as the cross yarns rotate) to the contiguous longitudinal yarns with the major concentrations of stress located at the area of initial rupture. The ability of the contiguous yarn to support the added stress will of course determine whether the break will propagate or whether the system can assume additional boundary extensions leading to failure of the second least extensible longitudinal yarn. The level of stress transfer from one broken yarn to another is dependent on the closeness of weave and frictional resistance of the surrounding matrix, the properties of the cross yarn, and the extensibility of the contiguous yarn. Clearly if the cross yarn has a low modulus and a high rupture strain it can extend sufficiently to accommodate the withdrawal of the broken yarn and permit its discharge of strain energy. On the other hand if the adjacent yarn has a high modulus and a high breaking strength it can likewise accommodate the effects of the nearby failure, this time by shouldering the extra load necessary to keep the ruptured yarn in its extended configuration.

## SECTION C

### PROBLEMS IN MEASUREMENT OF STRAIN IN IMPACT TESTS ON TEXTILE MATERIALS

#### The Need for Impact Tests on Textile Materials

We are all consumers of textile products and as consumers, we are constantly experimenting with fibrous materials in apparel, in household goods, and in selected mechanical usages. We are aware of the 'static' textile properties such as crease resistance, moth resistance, ease of laundering, or 'wash wear' characteristics, warmth without weight, drape, hand, and wear resistance. But little is said in the popular advertising about the dynamic properties of fibrous assemblies, -- of their mechanical behavior under conditions of high speed application of load. Yet tire cords, parachute risers, marine cordage, and aircraft arrester and towing systems are clearly textile applications which require efficient structural behavior under high speed loading conditions. Likewise do ballistic fabrics, safety nets, reinforced helmets and inflatable fabric structures undergo dynamic loading over a wide range of impacting speeds. To assure satisfactory performance of these applications, the textile engineer must study the stress strain behavior of fibers, yarns, and fabrics at high strain rates ranging from a few feet per second to several thousand feet per second.

Satisfactory impact behavior of textile materials is also necessary to meet the demands of industry for higher unit productivity, achieved in most instances by increases in textile process speed. The rash of new fibers which appear yearly on the textile scene cannot survive competition with older fibers if they do not contribute new desirable properties to the consumer item. But first they must survive processing exposure to high speed drawing and spinning, to the rapid accelerations of the winding process and

of weaving, to the tensions and sharp bending of rapid knitting, and to the high velocity, repeated impacts of the modern sewing machine. The textile material must be made before it is sold, and to make it efficiently one must be knowledgeable concerning the interaction of fibers and high speed textile processes.

### Textile Materials -- A Definition

Strict definition of textiles suggests that weaving is a necessary feature of such materials, but the more accepted meaning of the word includes all sheetlike structures which are composed of relatively fine fiber components. The structure may be directly formed of fibers, the so-called non-woven (whose fiber length is several times the length of conventional paper fibers). It may be composed of yarns which have been knit, or woven, braided or knotted and intertwined (in a lace structure). The yarns may have a simple twist structure or may be built up in a compound system with sub units and elementary twisted 'singles'. The important thing to be noted is the fact that a textile itself is rarely a uniform homogeneous material. The single fiber is itself a complicated system from the point of view of its molecular chain structure and its fibrillar formation; the manufactured textile material is doubly complicated by the geometry of its fiber assemblage which interacts with the basic fiber properties in determining mechanical behavior of the end product.

Textile materials are rarely used in flat sheet form. More often they are cut and pieced to approximate three dimensionally curved shapes of the wearer and when this is done, the structural weak point of the system resides in the joint or seam. Thus when impact usage of a fabricated textile system is expected, knowledge must be had of seam behavior under high strain rates, as well as under static test conditions.

### Problems in Measuring Textile Strains

The commonly accepted method of evaluating strain of textile materials under tensile loads is to measure the relative displacement of the two jaws which are clamped on the specimen. In metal, plastic, and rubber specimens, the specimen is frequently thicker or wider at the jaws than at the center span between the jaws, and can therefore withstand considerable clamping force. In textile testing, the yarn or fabric frequently has the same dimensions along the entire specimen length, in jaws and between jaws. In such cases it is important to avoid excessive jaw pressures which may combined with the tension of the free span to create a local stress concentration within the jaw, causing early rupture at a tensile load well below what the textile specimen is capable of handling. And so in clamping textile specimens, one generally lengthens the clamping area and decreases the lateral load per unit length of the sample. This step provides improved breaking load readings but it creates many problems in the accurate measurement of strain. In what follows we shall attempt to describe these textile strain problems together with certain of their solutions. The solutions are in some instances, useful in both static and dynamic tests. In other cases they provide answers satisfactory only for static testing.

1. Complexity of the Textile System. Textile material rarely behaves like an isotropic elastic sheet. It is usually orthotropic, having two principal directions of stiffness, shear rigidity and Poisson, or contraction, ratio. Strain measurement in such a structure is difficult, for the strain of various parts of the textile specimen may differ in a given test. In a twisted yarn or cord the fibers in the center generally have a lower helix angle than the outside fibers and hence are under greater strain

in a tensile test. In a woven fabric, test yarns lying parallel to the loading direction and located at the side of the specimen neck inward while the centrally located yarns remain straight. Thus their strain histories vary during a tensile test. In a seam structure such as is pictured in Figure C-1, the longitudinal stress bearing yarns entering the stitch loop from different positions are under different strains, those at the loop extremities being subjected to higher strain levels and breaking first, those at the loop center undergoing less strain and breaking last.

2. Anisotropy of textile materials. The basic fiber in textile structures is not isotropic, but even if it were, the structural design of yarn and cloth, of itself, induces anisotropic behavior into every textile system. As pointed out above, textile cloths are usually orthotropic in their mechanical properties. The following classical stress strain equations for orthotropic materials have been shown pertinent to behavior of a nonwoven fabric and they suggest some of the difficulties we may have in the valid measurement of stress strain behavior of such a system:

$$\epsilon_x = b_{11} \sigma_x + b_{12} \sigma_y + b_{13} \tau_{xy} \quad (C-1)$$

$$\epsilon_y = b_{21} \sigma_x + b_{22} \sigma_y + b_{23} \tau_{xy} \quad (C-2)$$

$$\gamma_{xy} = b_{31} \sigma_x + b_{32} \sigma_y + b_{33} \tau_{xy} \quad (C-3)$$

where  $\epsilon_x$ ,  $\epsilon_y$ , and  $\gamma_{xy}$  are normal strains and shearstrain in the directions x,y;  $\sigma_x$ ,  $\sigma_y$  and  $\tau_{xy}$  are the normal and shear stresses in the x, y directions. The coefficients 'b' are functions of the principal directional elastic tensile and shear moduli and Poisson ratios of the material. Note that directions x, y are not (in general) the principal directions of the non-woven material. In the case of a uniaxial tensile test wherein the axis of pull, 'y', and the principal direction of the fiber orientation in the non-woven do not coincide, and extension  $\epsilon_y$  exerted on the web by

jaws of the conventional textile test machine, will develop a tensile stress  $\sigma_y$  in the fabric. Because of the free edge  $\sigma_x$  will be zero. But the stress  $\sigma_y$  will be accompanied either by a shear stress  $\tau_{xy}$  (if  $\gamma_{xy} = 0$ , meaning that the jaws are not allowed to rotate) or by a shear strain,  $\gamma_{xy}$ , if the jaws are allowed to rotate (with  $\tau_{xy} = 0$ ). Many tensile testers provide a mixture of these conditions and the observation of their average jaw separation is simply not an adequate strain measurement. Textile fabrics in fact often act like a trellis model loaded off its axes of symmetry, as is shown in Figure C-2 (after Weissenberg C-1, C-2).

3. Jaw Effects -- Restraint. The function of the jaw in a textile tensile test is to clamp the specimen and provide a mechanical connection between it and the moving and fixed cross heads. Many textile specimens subjected to uniaxial pull in the 'y' direction, will show significant contraction in the 'x' direction. In fact Poisson ratios approaching and even exceeding 1.0 can occur in certain cloth constructions. Free contraction of the specimen is prevented at the jaws because of their clamping action and the frequent result of this restraint is a waisted specimen as illustrated (C-1, C-2) in Figure C-3. Clearly the specimen strain is not uniform along its length and jaw displacements do not describe material strains.

4. Jaw Effects -- Slippage. To avoid clamp ruptures numerous special textile jaws have been designed to decrease the unit area pressures required to develop a total frictional force equal to the tension in the specimen. But this reduction in stress concentration is generally accompanied, as has been stated above, by an increase in the working area of the jaw and a lengthening of that section of the specimen which is involved in non homogeneous extension and local slippage. As a result, the jaw to jaw separation

becomes entirely inadequate as a direct measurement of specimen strain.

One move to eliminate such jaw effects on strain measurements was made by Kaswell and Hamburger (C-3) who suggested the technique of measuring the separation of gage marks on the specimen at loads below rupture comparing the values with data on jaw separation, and establishing an effective gage length. This effective length could then serve as the basis for calculating breaking strains from knowledge of jaw separation. Clearly this method was intended to circumvent the need to measure gage mark separation at the moment of specimen rupture, this measurement being an uncertain, if not dangerous procedure for many textiles.

It has also been proposed that the tensile test be run at a fixed strain rate, but with two different gage lengths. One could then take the difference in the extension readings for each load and, attributing this extension difference to the differences in the two gage lengths, one could replot the valid load-strain curve of the material. Still another method uses several different gage lengths in successive tests, then replots the extension at a given load versus gage length. This curve is then extrapolated to zero gage length and the extension intercept is taken to represent both the slippage and extension of the specimen in the jaw. This extension must then be subtracted from the measured jaw separation to give the true strain reading for the chosen load. The procedure is then repeated for other loads to give a table of values of true strain versus specimen load. The extrapolation procedure is illustrated in Figures C-4 & C-5. Figure C-4 shows the load versus jaw movement data plotted for capstan jaw tests of a rayon-cotton webbing, or tape, using gage lengths of 2, 5, 10, 12, and 20 inches. The data of Figure C-4 are cross plotted in Figure C-5 and the elongation curves are extrapolated to zero gage length. These elongation intercepts of Figure C-5 are then plotted back in Figure

C-4 as the 0 gage length (correction) curve -- this curve to be subtracted along the strain axis from each of the other raw data curves of Figure C-4 to give the valid load elongation picture at each gage length tested. It is clear that the uncorrected curves were in error (elongationwise) from over 400% in the case of the 2 inch gage length to about 30% in the case of the 20 inch gage.

The extrapolation method illustrated in Figures C-4 and C-5 is cumbersome and on occasions, unreliable. The method assumes uniformity of specimens (since we are extrapolating and then subtracting from original data from many tests) and it assumes that the rate of load build-up, which can seriously affect slippage and extension of the specimen in the jaws, can be adequately standardized and held constant in the different gage length tests. We have found the technique sometimes inadequate for these reasons, sometimes at slow test rates, sometimes at impact testing speeds. The data of Figures C-4 & C-5 were obtained at a strain rate of 100% per minute. Corresponding tests at 50% per minute strain rate were entirely inconsistent with the 100% per minute data. The 100% rate data were in close agreement with load extension data taken with flat (minimum slippage) jaws and with gage marked capstan jaw tests. (See Figure C-6).

The 'effective gage length' method assumes that the ratio of jaw extension to between-jaw-extension remains constant in the latter part of the tensile test (between the last gage measurement and the rupture point). Further it is dependent on the ability of the operator to judge gage mark separation during the test. In impact tests the behavior in and out of the jaws is not as linear as might be desired, and there is no time for gage mark measurements except by photographic means.

The materials engineer dealing with bulk solids avoids the problems cited above by increasing the cross sectional dimensions of the specimen at the jaws and by limiting his strain

readings to the region of uniform cross section in the middle of the specimen. His strain measuring instruments are hung onto the specimen and consist of mechanical or optical levers, mechanical-electrical devices, or all electric (as for example the bonded wire strain gage) systems. Such devices cannot be used in measurements of textile structures because of the unusual flexibility of these materials leading to an inability to sustain the weight of the strain gage without bending or because of the interference of the forces necessary to activate the strain gage, with the accurate reading of the textile load. Further, the high strains involved in textile systems (often up to 50%) preclude use of the common strain gage designed for metal systems. Finally, the presence of high level strain energy at rupture in the textile structure frequently induces severe lash back which invites damage to expensive instruments and poses a safety problem for laboratory personnel. These objections to use of bulk material methods of strain measurement of textile structures apply in both 'static' and 'dynamic' tests. In fact, all the strain measurement problems cited above for slow speed textile tests apply to an even greater extent in high speed testing of textiles.

#### Strain Measurements in Impact Testing

Clearly the difficulties of fastening flexible, yet very strong textile structures to a jaw system, are accentuated in higher speed tests. But it is worth noting that the reaction of textile materials to stress concentrations differs in high vs. low speed tests. A fabric or yarn which ruptures within a flat jaw at low testing speeds often ruptures between the jaws in an impact test, and capstan jaws can sometimes be done away with to provide a reliable strain reading based solely on jaw movement data. The opposite is sometimes true. But this must be checked for each individual case. The cotton-rayon tape represented by the data

of Figure C-4 was tested both at slow speeds and at high speeds. Flat jaw movement data at slow speeds was used since it did not involve jaw breaks at strain rates of 6% per minute and of 250% per minute. The 100% per minute corrected capstan data derived from Figure C-4 was consistent with these two flat jaw rates (6% and 250% per minute). However the 50% per minute corrected-capstan readings were anomolous. (See Figure C-6).

Where direct strain readings on the sample are desired, there arises an additional problem in high speed testing of textiles, namely the inertial effects of the strain measurement system. The element attached to the specimen must have a small mass lest its resistance to acceleration during the test interfere with valid readings of specimen stress. A small linear differential transformer has been used successfully as a strain measuring element in static textile testing systems. But the presence of large deformations, large strains, and high rupture energies precluded widespread use of the linear differential transformer as a strain gage in high speed textile tests.

A reasonable solution to the direct strain measurement problem for textile impact tests is the use of magnetic tapes as the strain record. A procedure developed in the Textile Laboratories at M.I.T. (by JGK) involves the prerecording on a standard high fidelity magnetic tape of a sine wave whose wave length can be selected from tape to tape. The tape is mounted in the impact test with one end fastened (sewed or stapled) to a point on the specimen, then run over a specially designed record-reproduce magnetic head, with the other end of the tape hanging freely. When the specimen point moves, it pulls the tape with it, and the tape motion is detected at the magnetic head.

The schematic appearance of the system is shown in Figure C-7. The mass of the tape is negligible (0.1 grams per foot) and the

resistance to its movement over the magnetic head is adjusted to less than one pound at test speeds of 40 feet per second. The resolution of tape reading can reach  $10^{-3}$  inches without difficulty. The upper limit of strain reading (and displacement measurement) is infinite for practical purposes. The limits of speed for which the tape movement can be effectively read out in an oscilloscope are 0.5 inches per second to 100 feet per second.

Two or more tapes can be used at one time to describe the displacement history of any designated pair of gage marks, and the differences between these two displacements at any time furnish data on the local strain of that portion of the specimen. Two point impact strain readings have been found entirely feasible on many textile structures of sheet form. Impact strain measurements on yarn specimens have been taken with a single tape attached to the moving flat jaw in cases where jaw breaks did not occur. This latter tape also provides a check on test velocities. The use of two point strain reading for impact tests on twisted structures (such as ropes) has been found possible but the torsional rotation of the rope during the test has interfered significantly with the reliability and reproducibility of the results. An example of successful two point strain reading taken at impact speeds on the cotton-rayon tape referred to above, is shown in Figure C-6.

The strain readings obtained with the magnetic tape system eliminate the effects of the strain inhomogeneity in the region of the jaws. However the stress concentrations of such regions may still seriously effect the maximum load readings obtainable for a given textile specimen. Also, to avoid penetration of the strain inhomogeneity into the center of the specimen it is often necessary to use a specimen length 6 to 10 times its width. This implies use of considerable quantities of material for testing, and sometimes exceeds the dimensions (with jaw travel) of the

testing machine. A far better method for eliminating the jaw restraint on sample contraction, has been proposed by Weissenberg (C-1, C-2) who uses slanted jaws placed parallel to the predetermined lines of zero elongation in the material.

Finally it should be noted that anything the magnetic tape can do in measuring impact strains can be done by photography, though usually with considerably more effort. In high speed tests above 100 feet per second the tape is no longer a suitable device, and as speeds of test approach ballistic velocities, it is doubtful that any system can compete with the photographic method. But within the range of 0.5 inches per second to 100 feet per second, the tape method holds promise of simplicity, low cost, and versatility in strain measurements on textile materials.

### References-Section C

- C-1. Weissenberg, K. The Use of a Trellis Model in the Mechanics of Homogeneous Materials, Journal of the Textile Institute, 40, T89-110 (1949).
- C-2. Chadwick, G.E., Shorter, S.A. and Weissenberg, K. A Trellis Model for the Application and Study of Simple Pulls in Textile Materials, Journal of the Textile Institute, 40, T111- T160 (1949).
- C-3. Kaswell, E.R., and Hamburger, W.J., Use of Effective Gage Length in Elongation Measurement, Rayon Textile Monthly 23, No. 11, 1943.

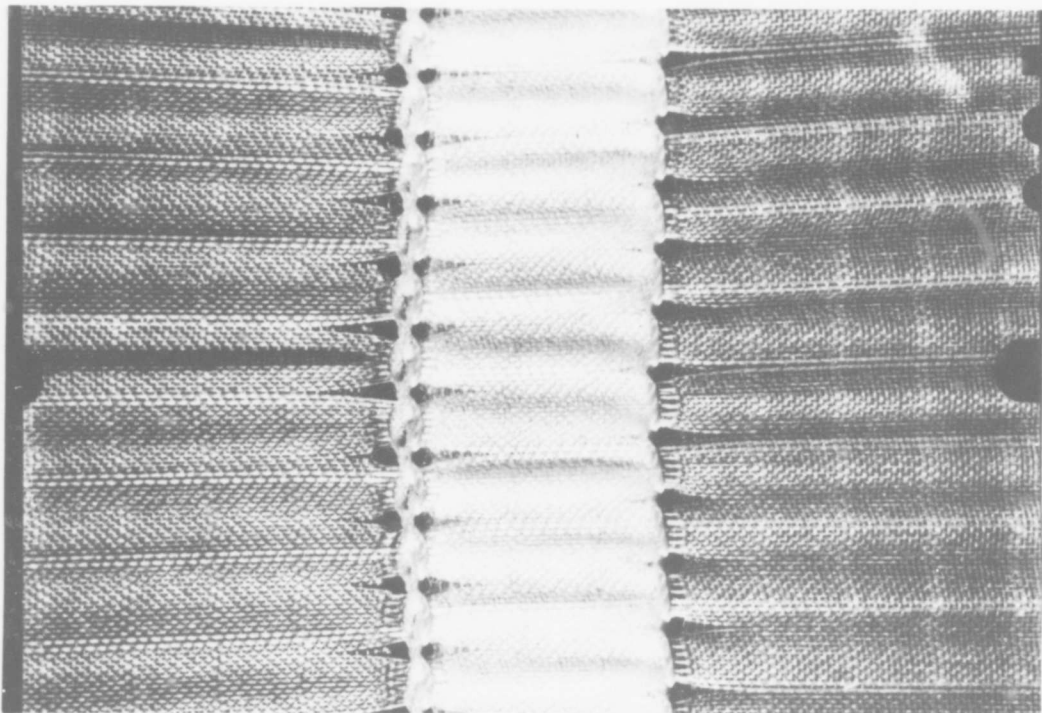


Figure No. C-7

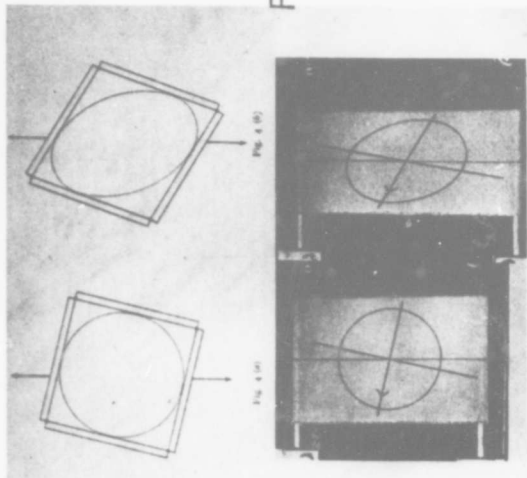


Figure No. C-2

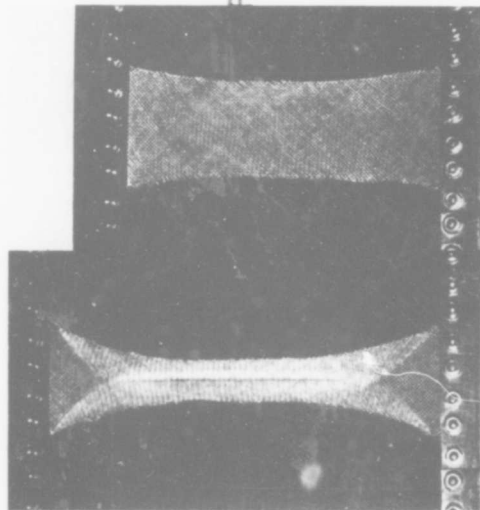


Figure No. C-3

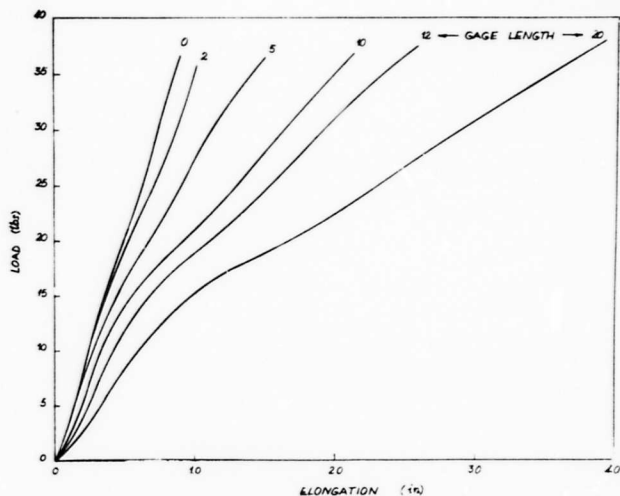


Figure No. C-4

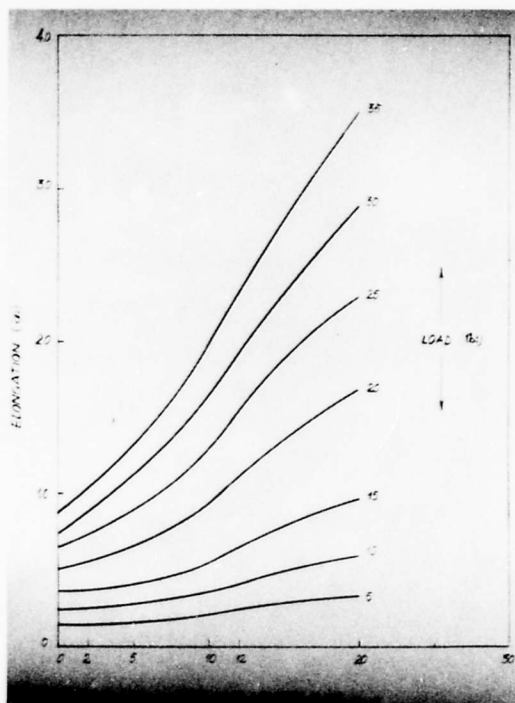


Figure No. C-5

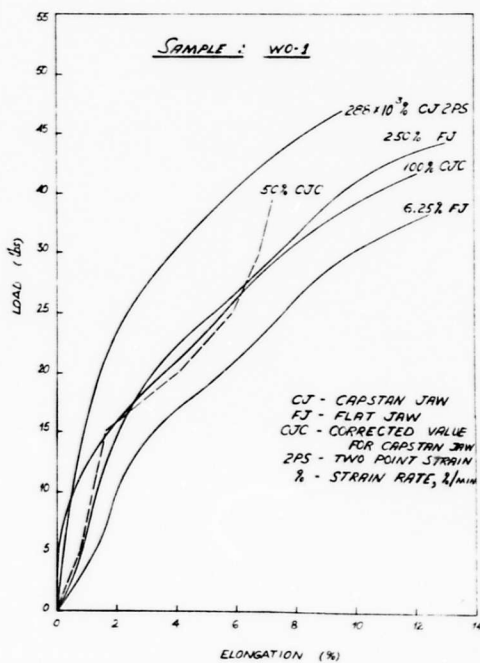
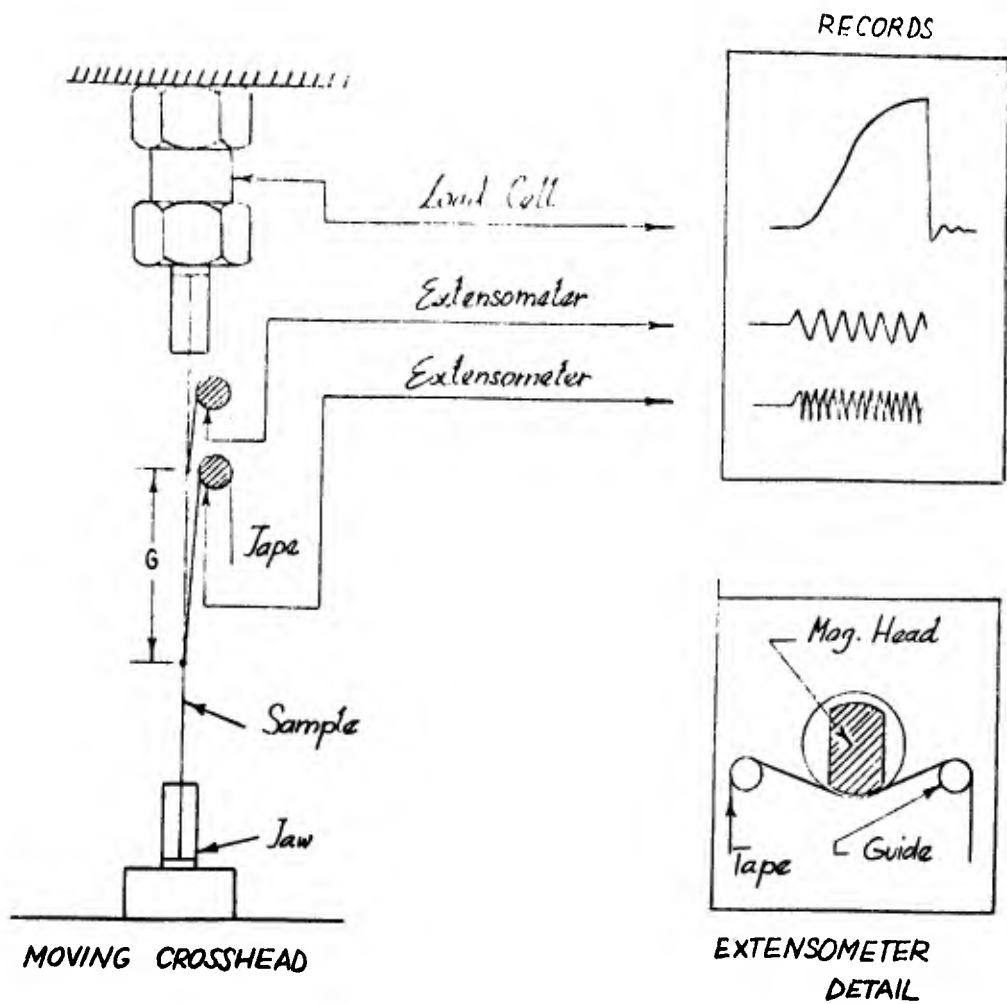


Figure No. C-6



G — Gage length for Strain

*Schematic of Load-Strain Measuring Systems for High Speed Testing of Textile Structures*

*Fig. C-7.*

## SECTION D

### IMPACT BEHAVIOR OF SAMPLES TAKEN FROM STORAGE OR FIELD USE

The effect of storage under ideal conditions and of weather exposure must be fully evaluated before one can establish safe limits for parachute service life. Accordingly considerable time in the current program has been devoted to the study of changes in mechanical properties of exposed and aged samples of parachute components. Impact loading is a common occurrence in usage of parachutes. It follows that mechanical behavior of the parachute and its components should be studied at impact test speeds as well as at static speeds conventional in the textile testing laboratory. Three different test units were utilized in the program: a yarn test at 40 ft./sec. jaw speed; a yarn test at varying speeds from 1.0 ft./sec. to 20ft./sec., and a fabric test at 20 ft./sec. The first and last test conditions were achieved through use of a falling weight tester designed and constructed in the Slater Memorial Textile Research Laboratory, M. I. T. during World War II and modified considerably for the current programs. The second test conditions were provided with the MITEX cylinder impact tester designed and constructed in the Textile Division Laboratories

The study of aged and weathered samples can best be understood as directed towards answering the following questions:

1. How does weathering exposure decrease the mechanical properties of nylon parachute components? Do high speed tests show greater effects than do slow speed tests? Or is it possible that changes which appear to be insignificant in static tests (such as are carried out in routine laboratory

evaluation) may have profound effects on the dynamic behavior of the component in question, either by itself or in structural combination with other materials?

2. How important is strain rate in a tensile test? What general effects are noted for strain rate versus strength, for strain rate versus extension at rupture?

3. How do dyed nylon samples behave in weathering exposure as compared to undyed (natural) samples? Are these differences magnified or suppressed in impact tests as contrasted with static tensile tests?

In order to provide answers to these questions tests were conducted on the following webbings and on yarns taken from the webbings:

- VEP 506 Webbing, Nylon Tubular, Natural 1-inch width.  
MIL-W-5625 FSN 8305-268-2452 (4000 lbs. break).
- VEP 507 Webbing, Nylon, Tubular 1-inch width OD #613  
MIL-W-5625 FSN 8305-268-2455 (4000 lbs. break).
- VEP 509 Webbing, Textile, Woven, Nylon, Type I, Natural  
9/16 in., MIL-W-4088 FSN 8305-263-3639  
(400 lbs. break).
- VEP 510 Webbing, Textile, Woven, Nylon, Type I, OD  
#613, 9/16 in., MIL-W-4088B FSN 8305-260-6909  
(400 lbs. break)

The webbings were tested in their original unexposed state, although these controls were manufactured, according to data furnished by the QMC, between 1951 and 1954. In addition the same webbings were exposed to sunlight for the following periods:

4 days (A3)	21 days (A7)
7 days (A4)	28 days (A8)
14 days (A6)	42 days (A9)

Other designations to be included in the following data are:

- W standing for tests on the full webbing.
- Y standing for tests on the yarns taken from a given webbing.
- $Y_e$  relating to tests on yarns taken from exposed side of webbing.
- $Y_s$  tests on yarns taken from the shaded side of exposed webbing.

Tests on yarns taken from samples VEP 506 and 507 are reported in Figures D-1 - D-14 inclusive. Each point plotted in these figures represents an average of either 4 or 5 tests on samples taken from one side of the webbing. Figure D-1 shows the effect of weathering on dyed yarn strength (VEP 507). The strength of the average exposed and shaded yarns is shown first. A separate graph (Figure D-2a) shows the change in strength of the directly exposed yarns taken from the webbing. Separate curves on each graph show the strength measurements taken at 12.5%, 125% and  $3.6 \times 10^5\%$  per minute strain rate respectively. Yarn samples were tested in flat jaws with strain readings based on displacement of the moving jaws. Figure D-2b shows the change in strength with weathering of the yarns on the shaded side of the webbing, measurements being taken at the three indicated strain rates. Figure D-3a, b shows a load versus strain rate for the exposed and for the shaded yarns, with separate curves for each duration of exposure. All three figures are consistent in suggesting that static tests show considerably greater differences for the effect of weathering than do dynamic tests of strength. In fact the dynamic strength results do not point to deterioration of the nylon in weather, even though considerably loss in strength is noted in static Instron tests.

Figure D-4 shows the loss in average yarn strength (shaded and exposed) with weathering of the natural nylon webbing (VEP 506). Figure D-5a, b shows the strength losses of exposed and shaded yarns separately. Load versus strain rate for the exposed and shaded VEP 506, natural samples are shown in Figure D-6a, b. Again it is seen that dynamic test results do not suggest the extent of damage which the yarn has incurred as a result of weather exposure. In fact a gain in strength of weathered samples is reported at dynamic conditions of tests.

Figure D-7 shows the effect of weathering on elongation to rupture of the dyed webbing yarns, averaging exposed and shaded side data. Figure D-8a, b separates the elongation to rupture data for the exposed and shaded yarns taken from the weathered VEP 507 webbing. In general it is noted that elongations to rupture in the dynamic tests run far below their static counterparts. But again the dynamic tests do not show the effect on elongation to rupture which one observes in the Instron test data for the dyed specimens. Figure D-9a, b shows the effect on elongation to rupture of strain rate for the exposed and for the shaded yarns. The curves for various exposures are plotted separately on these figures. The grouping of the curves at high test rates for each graph underline the tendency of the high strain rate to minimize the evidence of damage due to weather exposure. A summary graph of the data discussed above is presented in Figure D-10, which forcefully illustrates the points mentioned above. High strain rates minimize the extent of damage measured for directly exposed yarns.

Figure D-11 shows the effect of weathering on elongation to rupture of the natural webbing yarns, averaging exposed and shaded data. Figure D-12a, b shows separately the exposed yarn and shaded yarn elongation-to-rupture behavior. Figure D-13a, b

shows the exposed and shaded strain behavior as a function of strain rate. The static tests all show an increase in elongation after 7 and 14 days of webbing exposure but the elongation after 28 days falls to about the original (control) value. The dynamic tests of elongation show little evidence of any change with exposure, although all dynamic extensions fall below their static counterparts. The summary curves for yarns taken from the VEP 506 natural webbing are presented in Figure D-14. Samples VEP 509 and 510 are much lighter in weight and in breaking strength than the 506, 507 series. Tests on the entire webbings have been completed for several degrees of weather exposure.

Instron tests for strength retention versus exposure time for these lighter weight webbings were reported by Dr. Yelland in a paper given on Deterioration Problems in Organic Fibers during the summer program on Materials for Parachutes given at M.I.T. during 1959. These data can be compared now to the tests run at impact speeds on the MITEK machine. The impact data are reported in Figure D-15 and show losses in strength of the undyed sample VEP 509 to be considerable after 30 or 40 days. But these losses are not as great as those reported by Dr. Yelland in the Instron tests at low speeds. The dyed sample (VEP 510) was not observed to lose impact strength with weather exposure, although the Yelland data showed between 15 and 20 % strength loss measured at slow speeds for the 30 - 40 day weather exposure. As for elongation to rupture, the impact tests of the natural webbing showed a slight loss while the dyed samples showed, if anything, a slight gain in elongation to rupture with progressive weather exposure. The data reported for strain of the 509, 510 webbings is based on 2 point strain measurements rather than on jaw displacement values. As such, they are more reliable

than the jaw displacement data. But the tests on the original (control) 509 and 510 materials were actually run on 'similar' fabrics supplied by Dr. Yelland (designated as VEP 588 and 587 respectively). Due to limited supply of samples the VEP 509, VEP 510 data is based on one test at each level of exposure to sun light.

APPENDIX D-1  
SAMPLES OF THREAD FURNISHED TO MIT, UNDER  
CONTRACT DA19-129-QM-1308

VEP 506 A-3 (96 hrs. exposure)

Samples marked with "E" on side exposed to direct radiation. In four samples, exposed side carries identification yarn; in two samples, identification yarn is on side not directly exposed.

VEP 506 A-4 (7 days' exposure)

Samples marked with "E" on side exposed to direct radiation. Four samples carry identification yarn on exposed side; in fifth sample, identification yarn is on side not directly exposed.

VEP 506 A-6 (14 days' exposure)

Samples marked with "E" on side exposed to direct radiation. In one sample, exposed side carries identification yarn; in other four samples, identification yarn is on side not directly exposed.

VEP 507 A-3 (4 days' exposure)

Samples marked with "E" on side exposed to direct radiation. One sample carries the black identification yarn on the exposed side; in the other three samples, this yarn is on the unexposed sides.

VEP 507 A-4 (7 days' exposure)

Samples marked with "E" on side exposed to direct radiation. Two samples carry the black identification yarn on the exposed side; in the other four samples, this yarn is on the unexposed side.

VEP 507 A-6 (14 days' exposure)

Samples marked with "E" on side exposed to direct radiation. Two samples carry the black identification yarn on the exposed side; in the other three samples, this yarn is on the unexposed side.

APPENDIX D-1

SAMPLES OF THREAD FURNISHED TO MIT, UNDER  
CONTRACT DA19-129-QM-1308 (Cont'd)

VEP 509 A-3 (4 days' exposure)

Two samples marked with "E" on side exposed to direct radiation.

VEP 509 A-4 (7 days' exposure)

Three samples marked with "E" on side exposed to direct radiation.

VEP 509 A-6 (14 days' exposure)

One sample marked with "E" on side exposed to direct radiation.

VEP 509 A-7 (21 days' exposure)

Two samples marked with "E" on side exposed to direct radiation.

VEP 509 A-8 (28 days' exposure)

One sample marked with "E" on side exposed to direct radiation.

VEP 509 A-9 (42 days' exposure)

Two samples marked with "E" on side exposed to direct radiation.

VEP 510 A-3 (4 days' exposure)

Two samples marked with "E" on side exposed to direct radiation.

VEP 510 A-4 (7 days' exposure)

One sample marked with "E" on side exposed to direct radiation.

VEP 510 A-6 (14 days' exposure)

Seven samples marked with "E" on side exposed to direct radiation.

APPENDIX D-1

SAMPLES OF THREAD FURNISHED TO MIT, UNDER  
CONTRACT DA19-129-QM-1308 (Cont'd)

VEP 510 A-8 (28 days' exposure)

One sample marked with "E" on side exposed to direct radiation.

VEP 510 A-9 (42 days' exposure)

Two samples marked with "E" on side exposed to direct radiation.

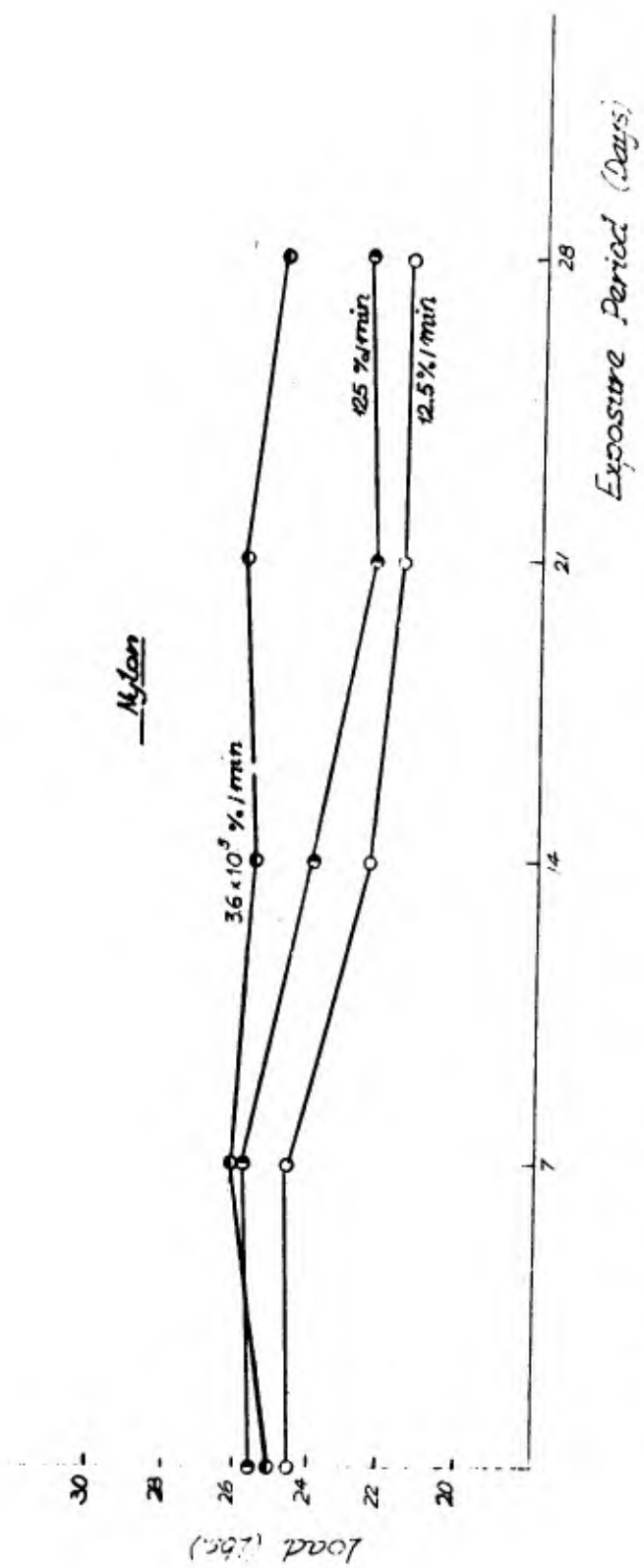


Figure:D-1. Yse-VEP 507 - Average Breaking Load of Exposed and Shade Yarns vs. Exposure Period.

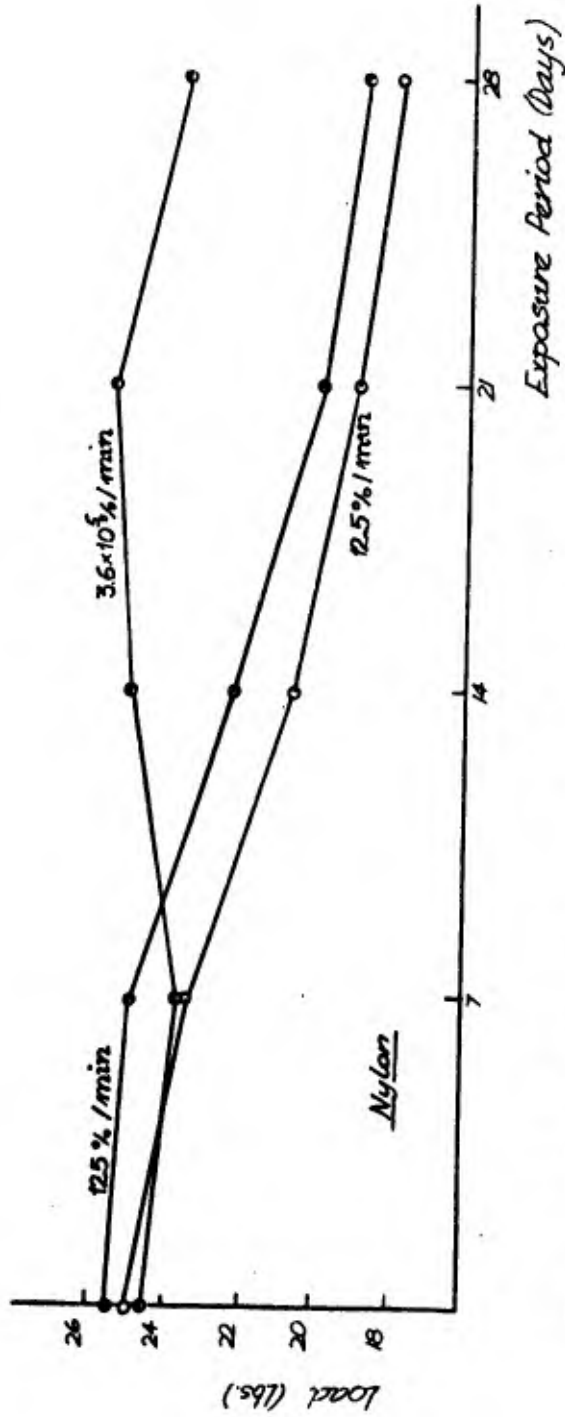


Figure D-2a. Ye-VEP 507 - Breaking Load of Exposed Yarns vs. Exposure Period.

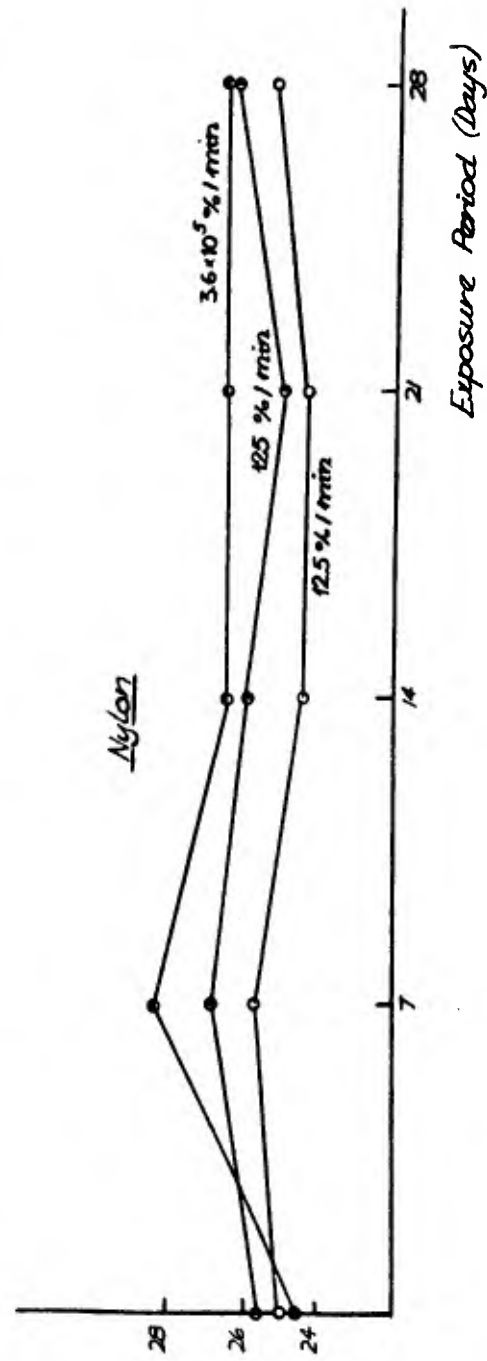


Figure D-2b. Ys-VEP 507 - Breaking Load of Shade Yarns vs. Exposure Period.

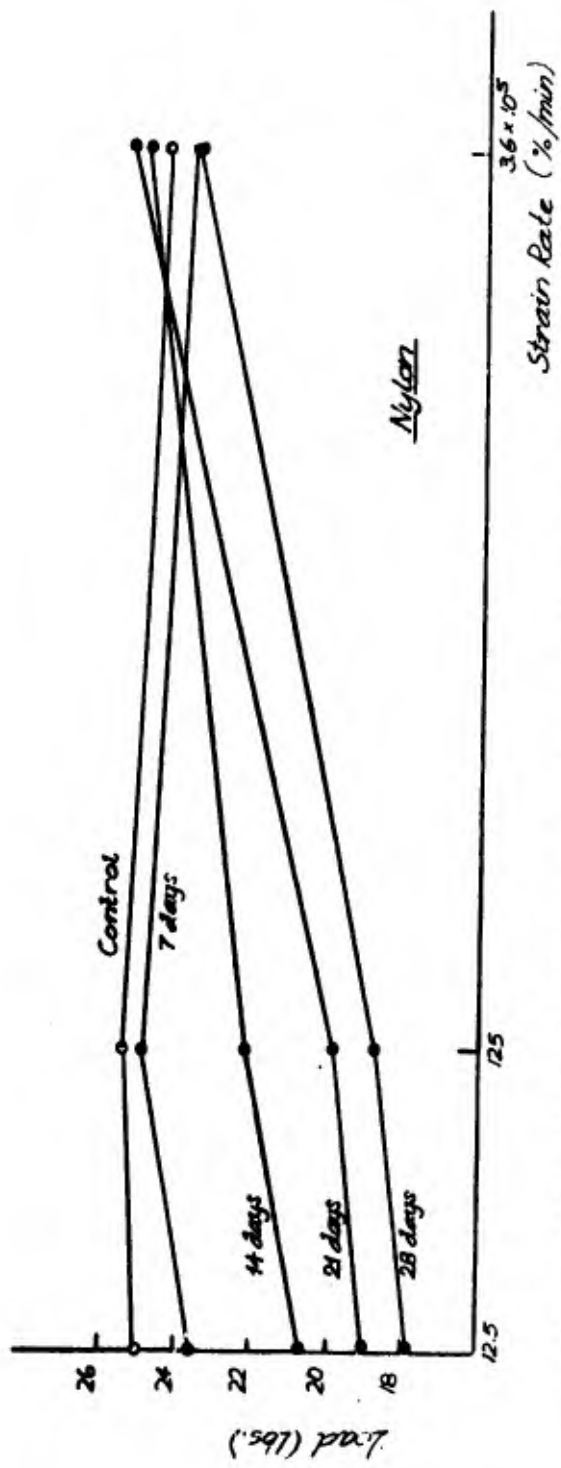


Figure D-3a. Ye-VEP 507 - Breaking Load of Exposed Yarns vs. Log. Strain Rate.

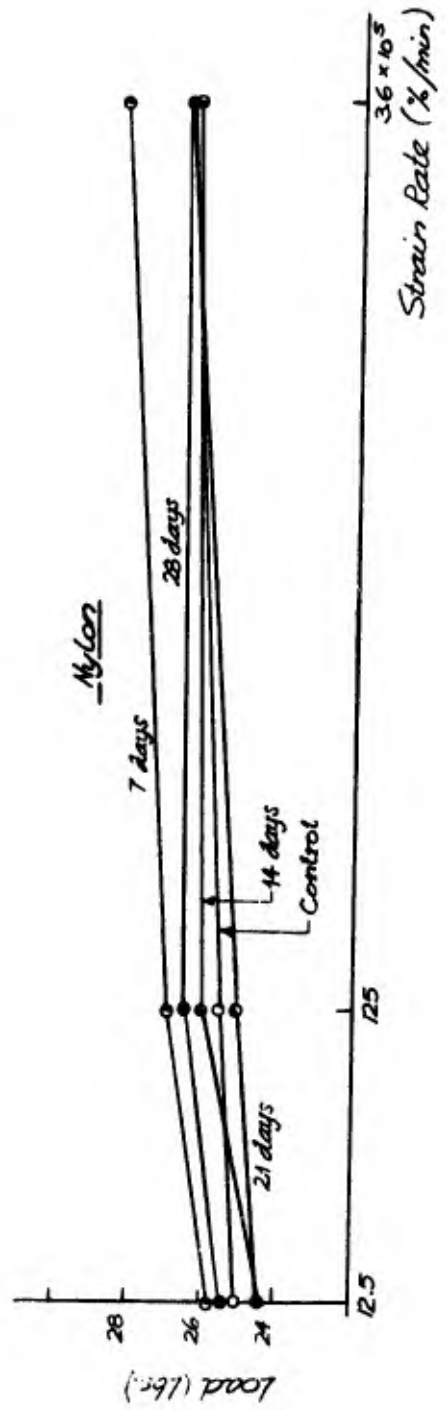


Figure D-3b. Ys-VEP 507 - Breaking Load of Shade Yarns vs. Log. Strain Rate.

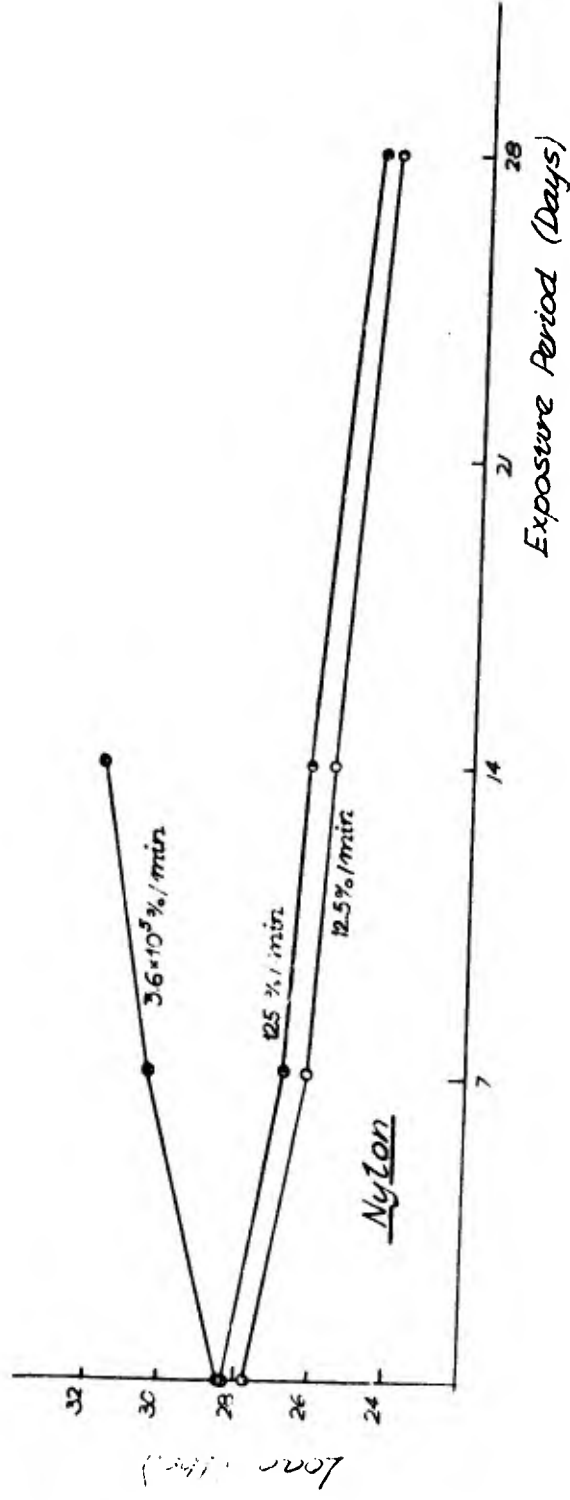


Figure D-4. Yse-VEP 506 - Average Breaking Load of Exposed and Shade Yarns vs. Exposure Periods.

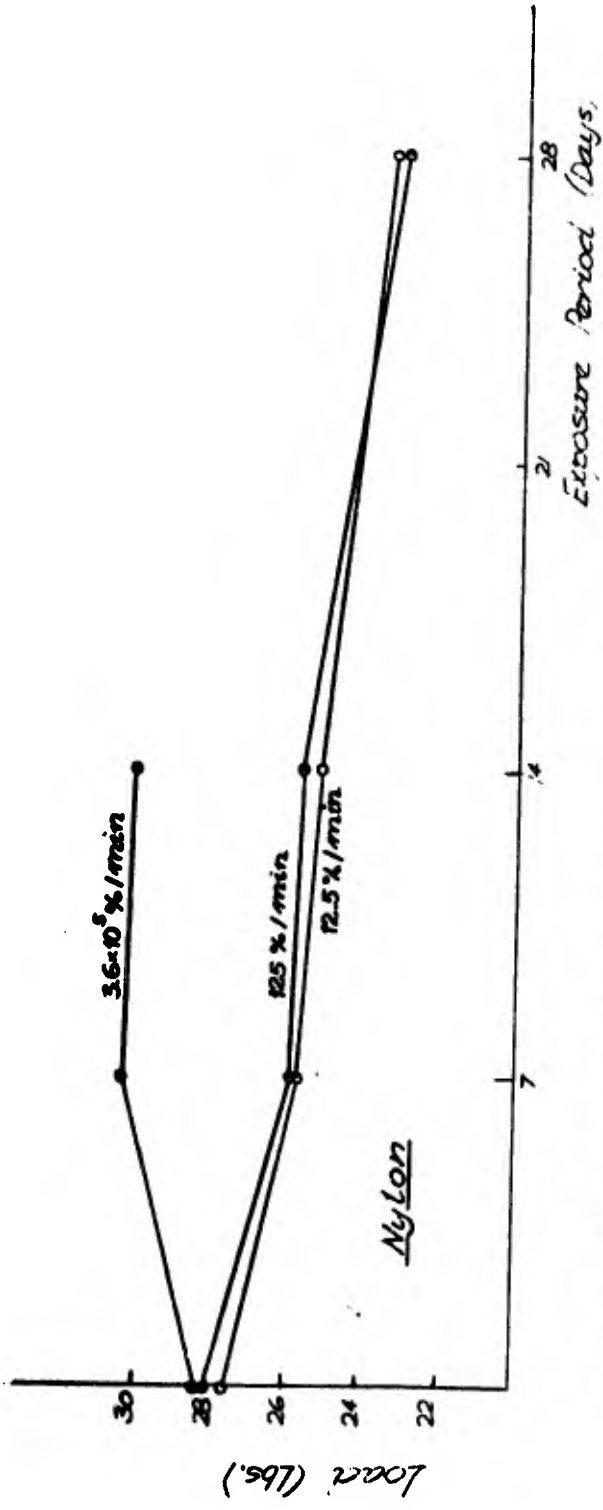


Figure D-5a. Ye-VEP 506 - Breaking Load of Exposed Yarns vs. Exposure Period.

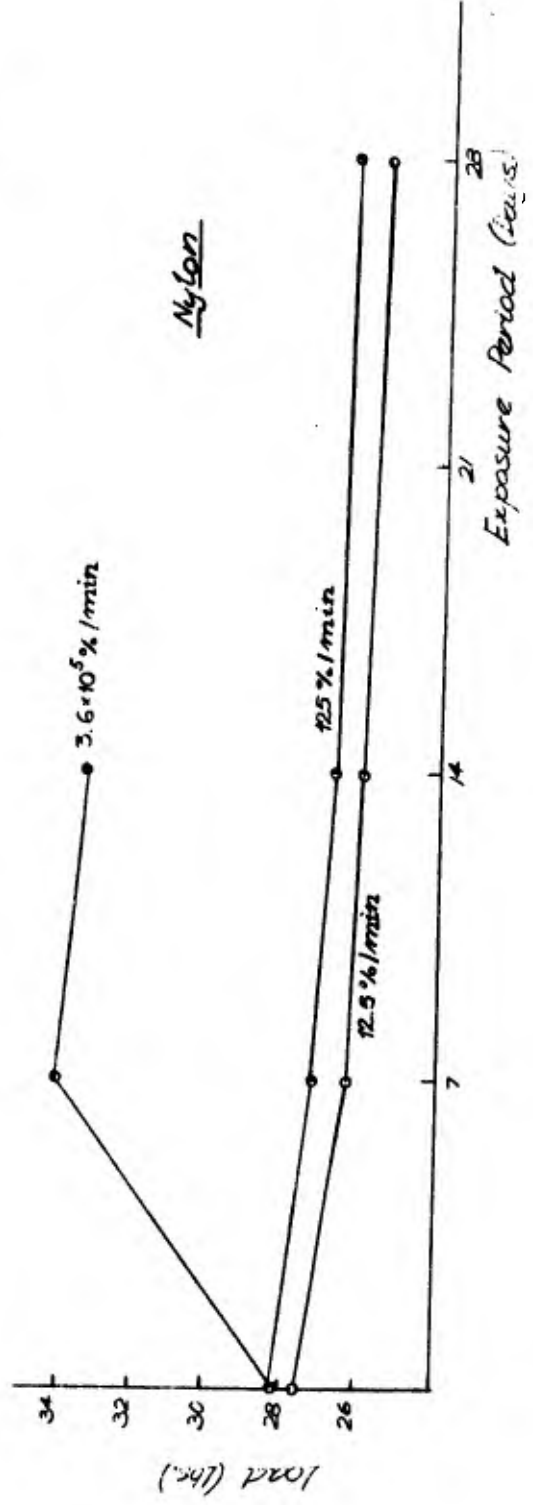


Figure D-5b. Ys-VEP 506 - Breaking Load of Shade Yarns vs. Exposure Period.

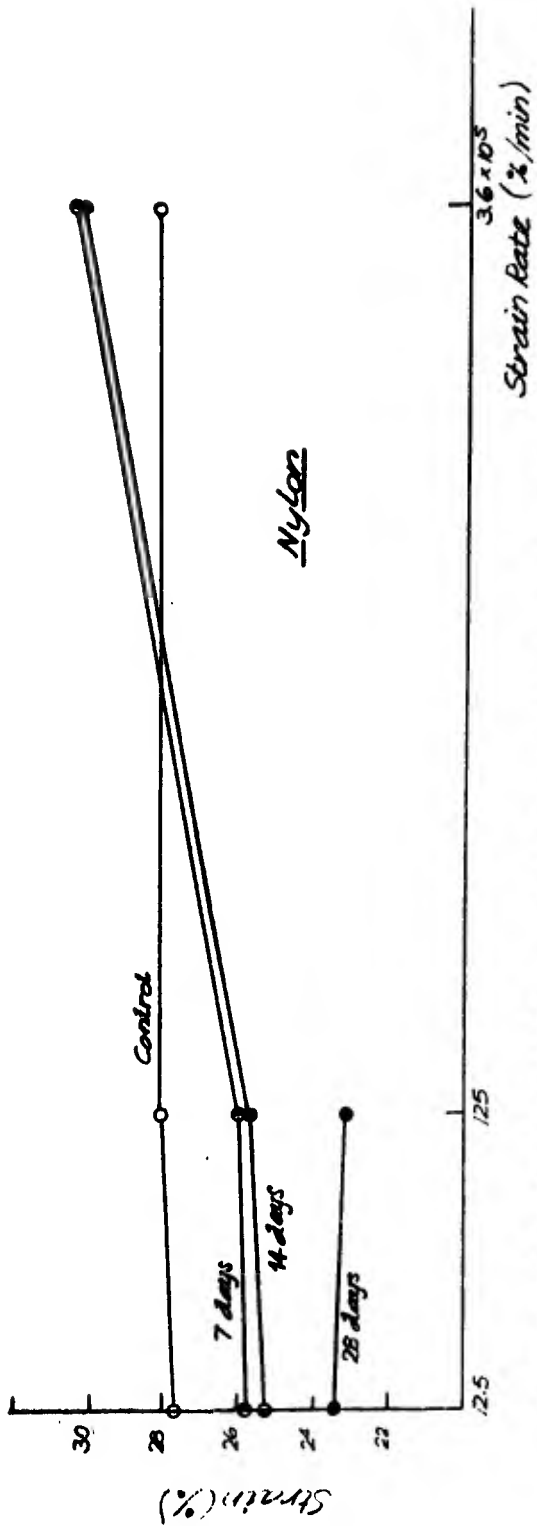


Figure D-6a. Ye-VEP 506 - Breaking Load of Exposed Yarns vs. Log. Strain Rate.

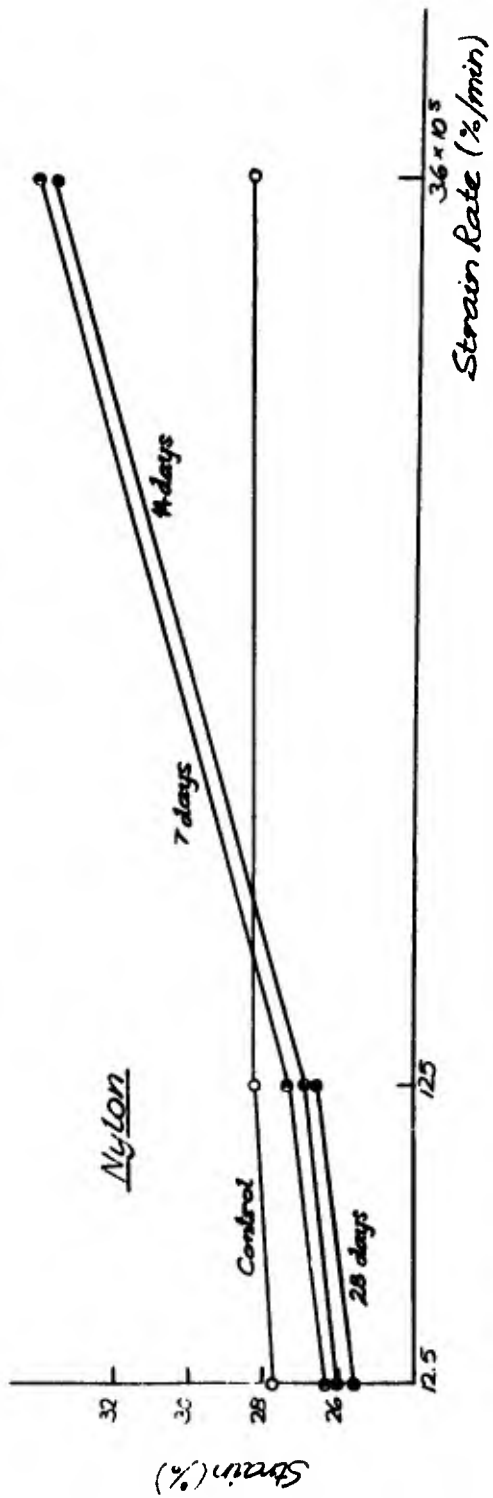


Figure D-6b. Ys-VEP 506 - Breaking Load of Shade Yarns vs. Log. Strain Rate.

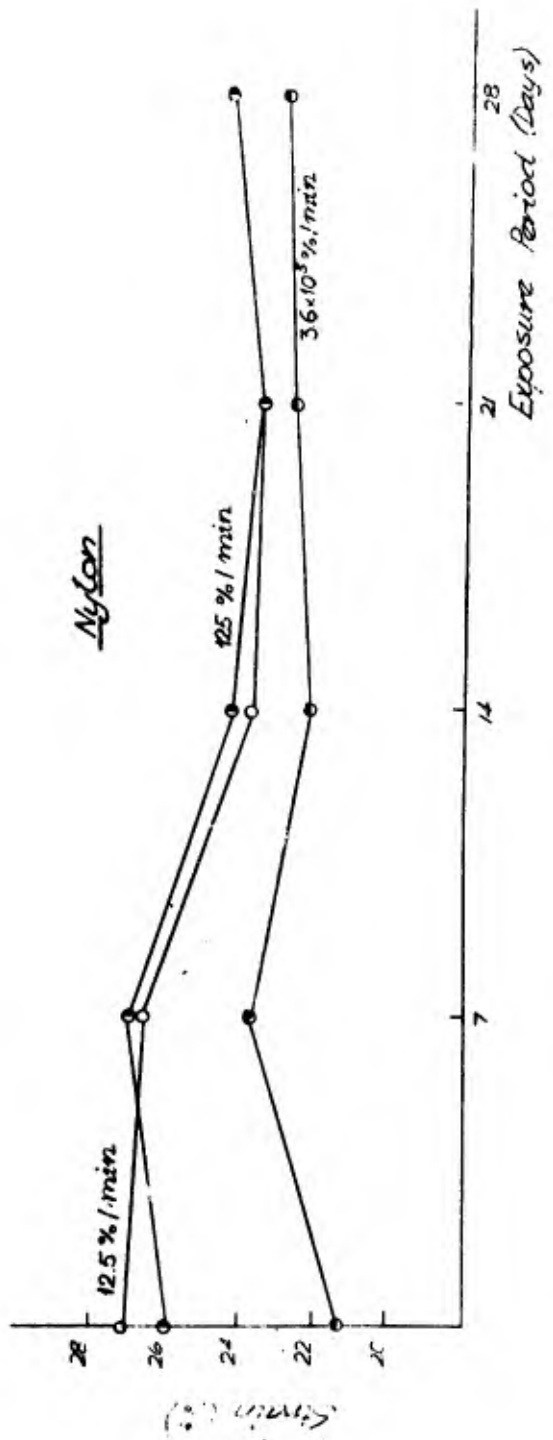


Figure D-7. Yse-VEP 507 - Average Breaking Strain of Exposed and Shade Yarns vs. Exposure Period.

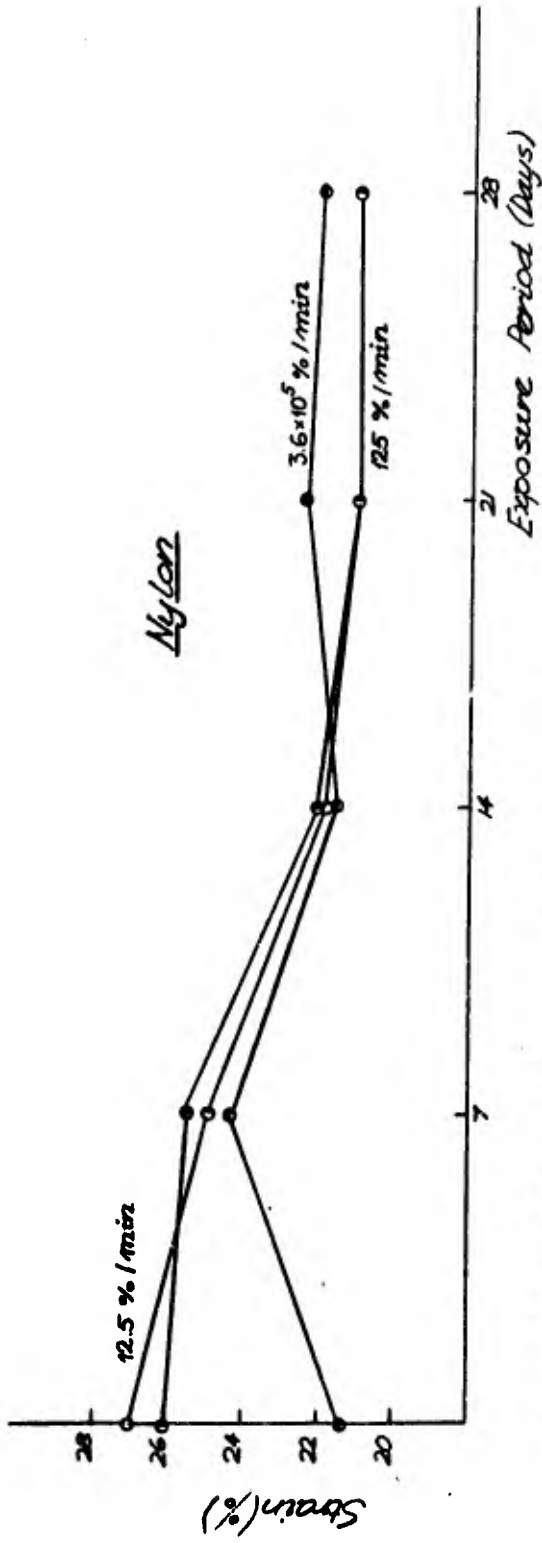


Figure D-8a. Ye-VEP 507 - Breaking Strain of Exposed Yarns vs. Exposure Period

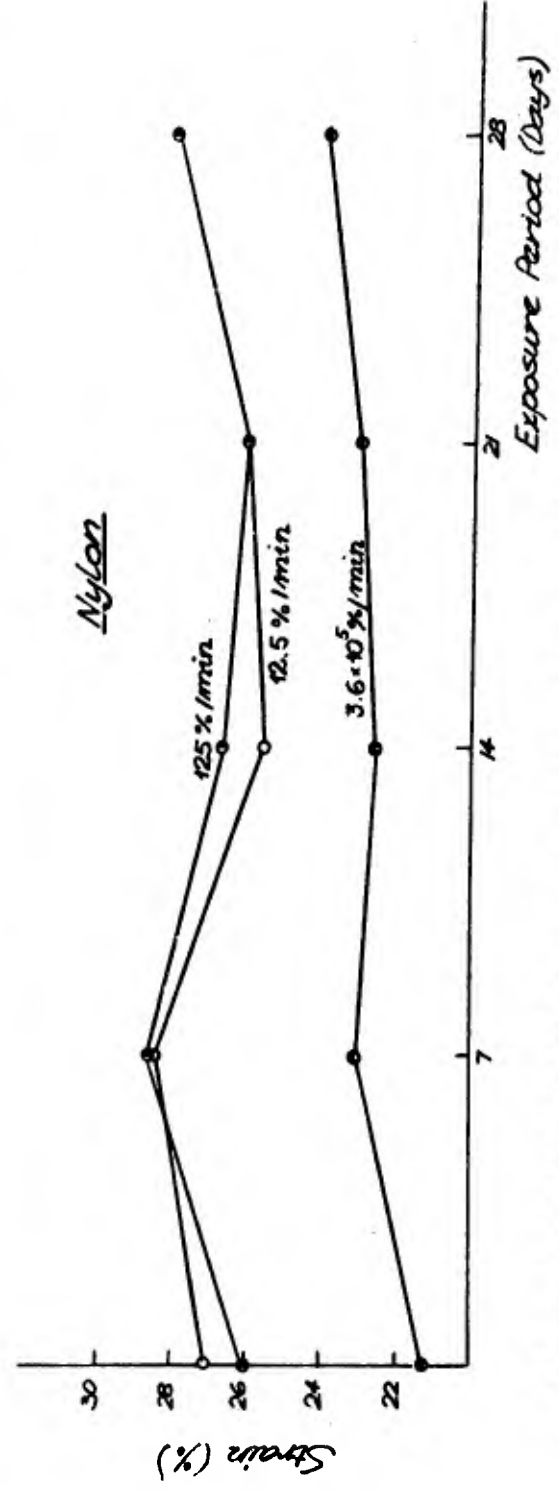


Figure D-8b. Ys-VEP 507 - Breaking Strain of Shade Yarns vs. Exposure Period.

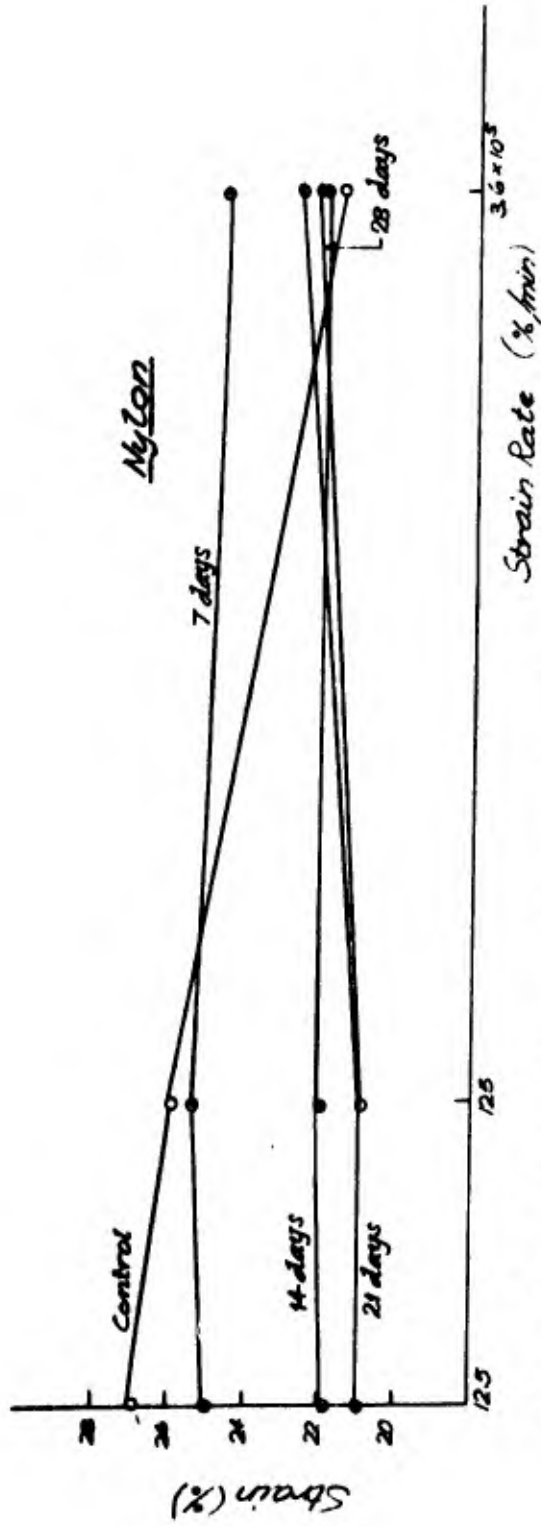


Figure D-9a. Ye-VEP 507 - Breaking Strain of Exposed Yarns vs. Log Strain Rate .

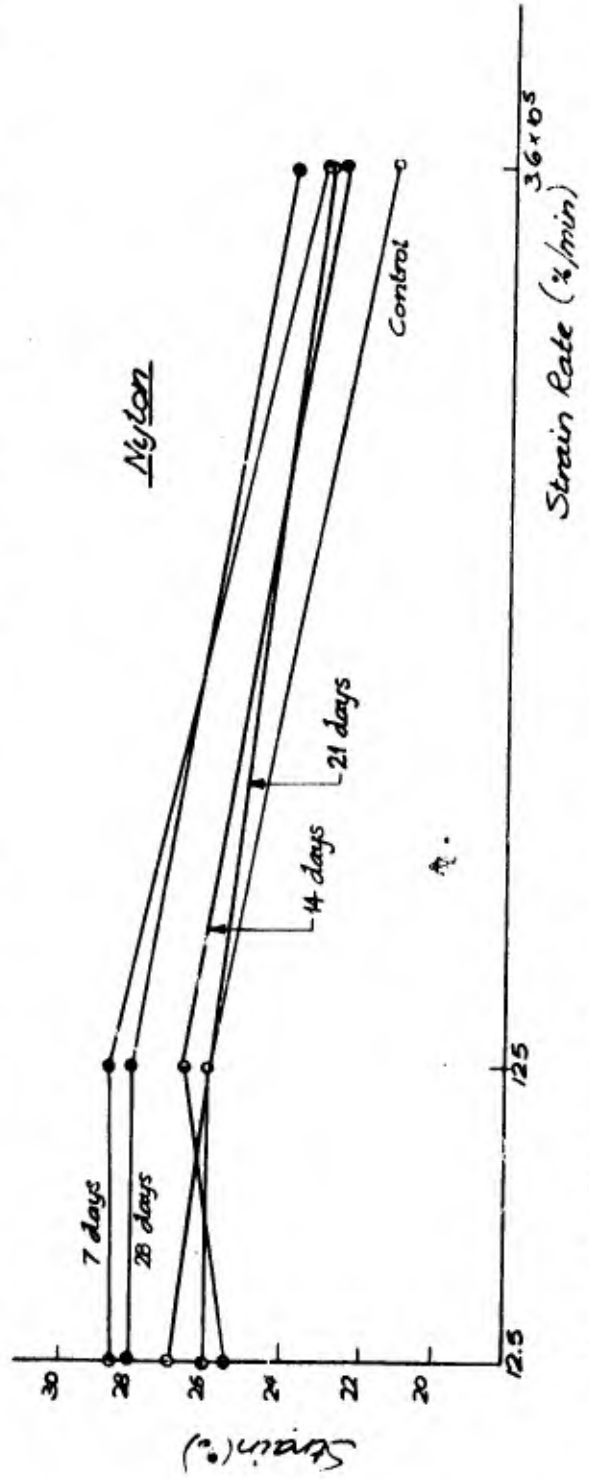
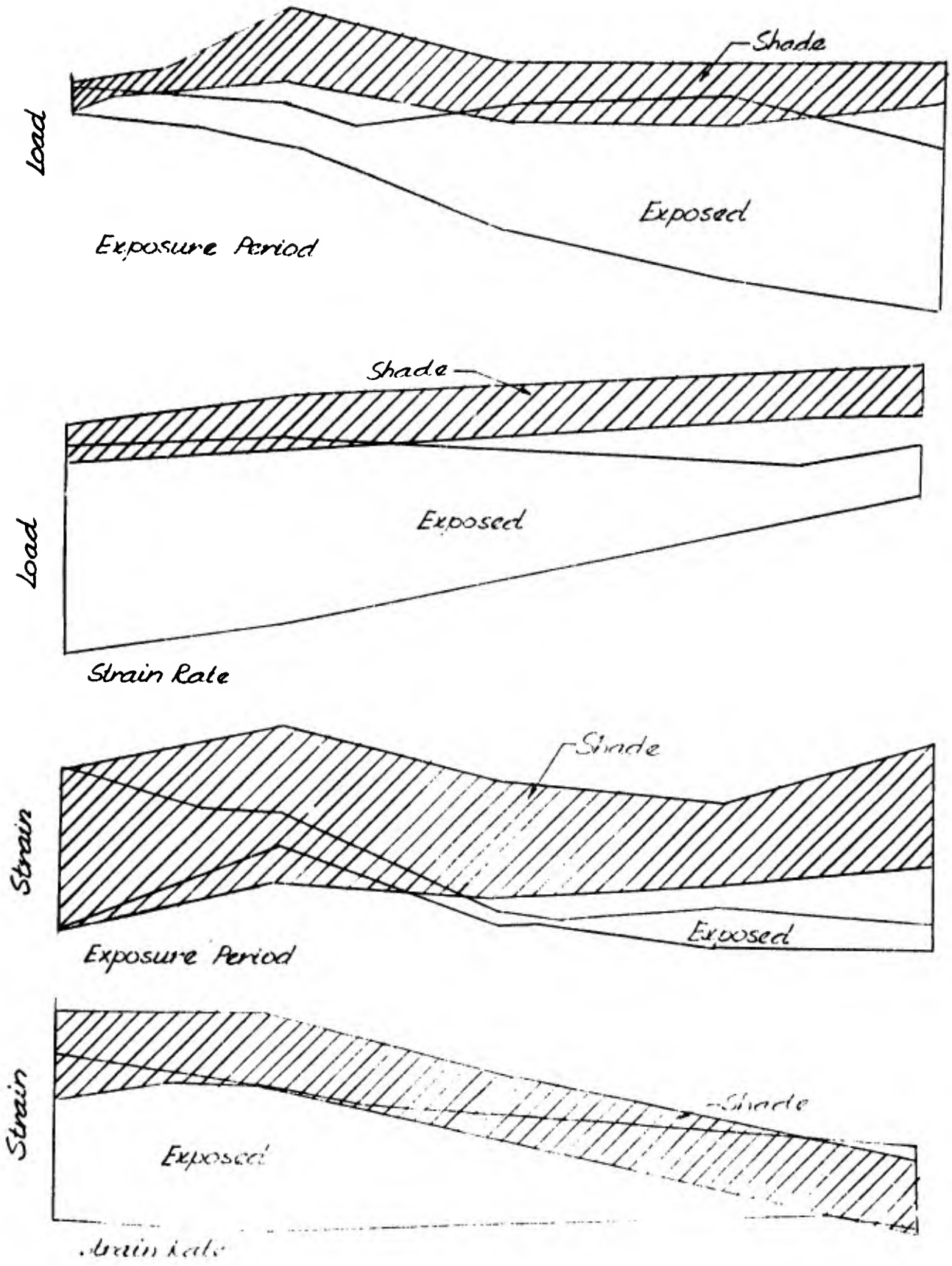


Figure D-9b. Ys-VEP 507 - Breaking Strain of Shade Yarns vs. Log Strain Rate .

Nylon



FigureD-10. Ye-VEP 507, Ys-VEP 507 - Summary of Strain Rate and Exposure Period Effects.

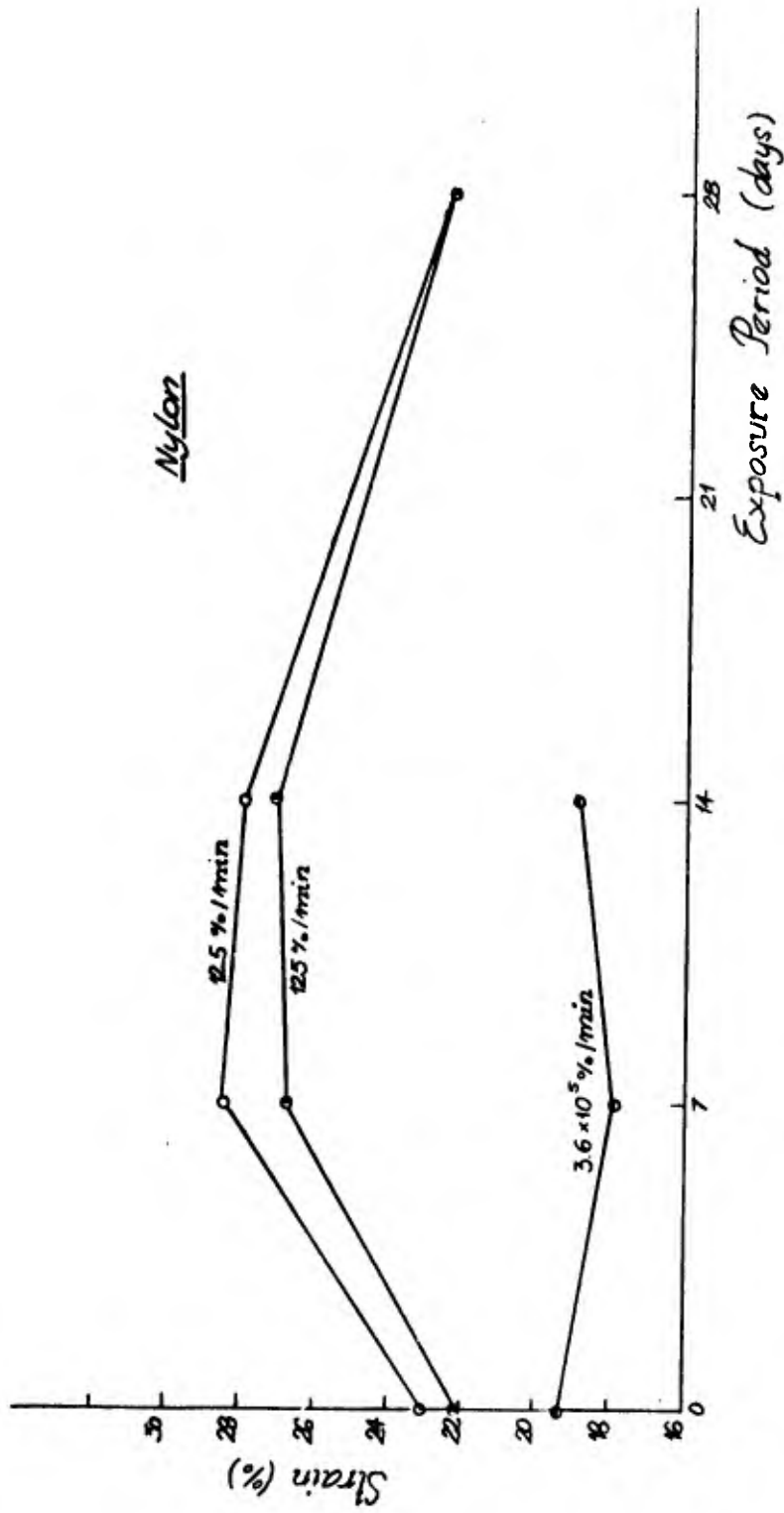


Figure D-11. Yse-VEP 506 - Average Breaking Strain Exposed and Shade Yarns vs. Exposure Period.

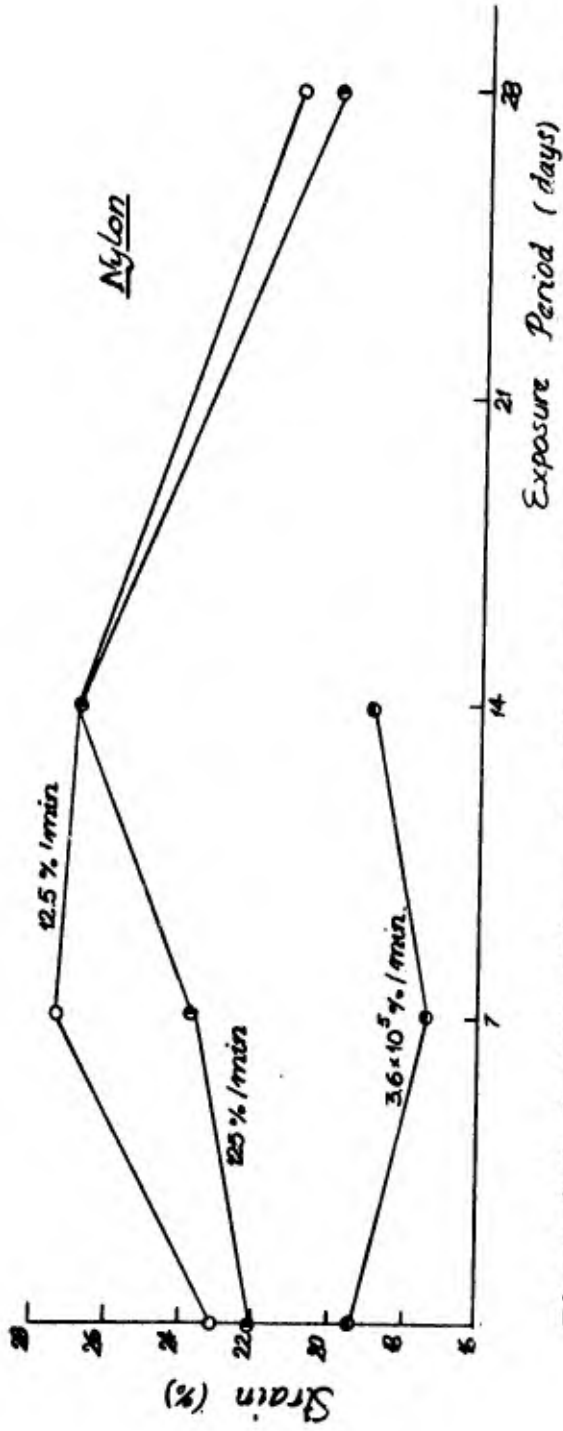


Figure D-12a. Ye-VEP 506 - Breaking Strain of Exposed Yarns vs. Exposure Period.

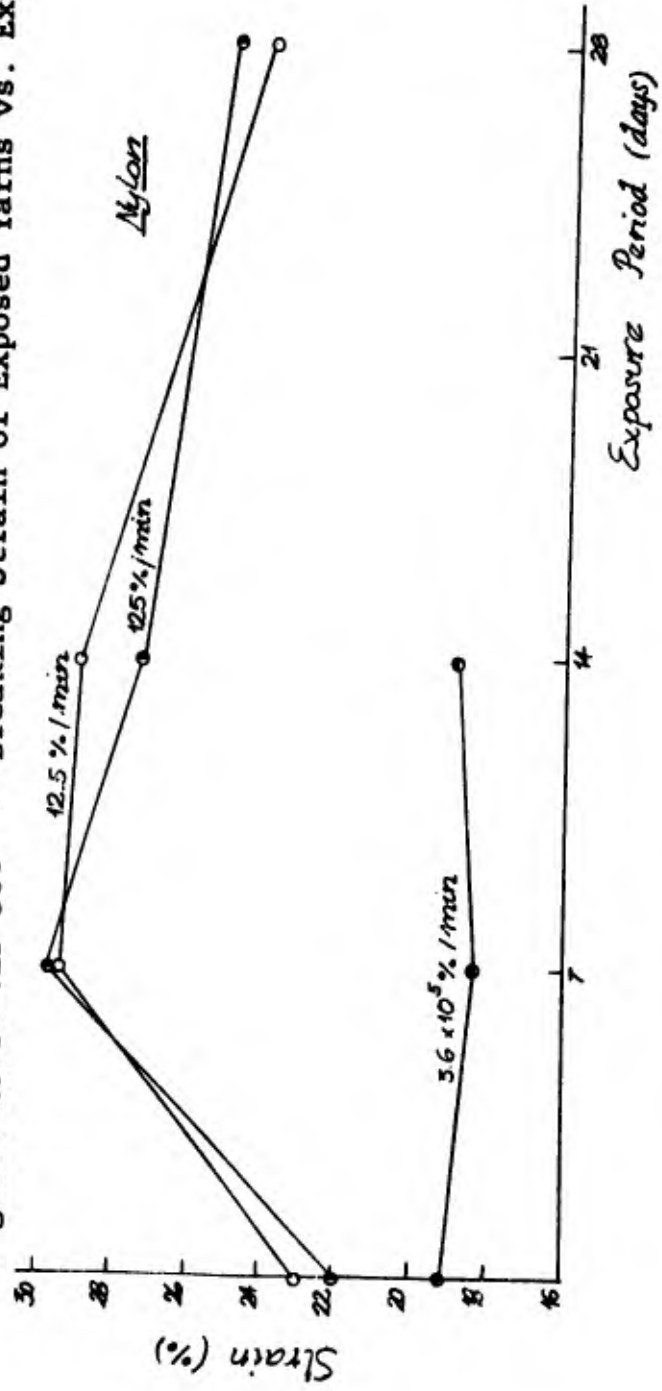


Figure D-12b. Ys-VEP 506 - Breaking Strain of Shade Yarns vs. Exposure Period.

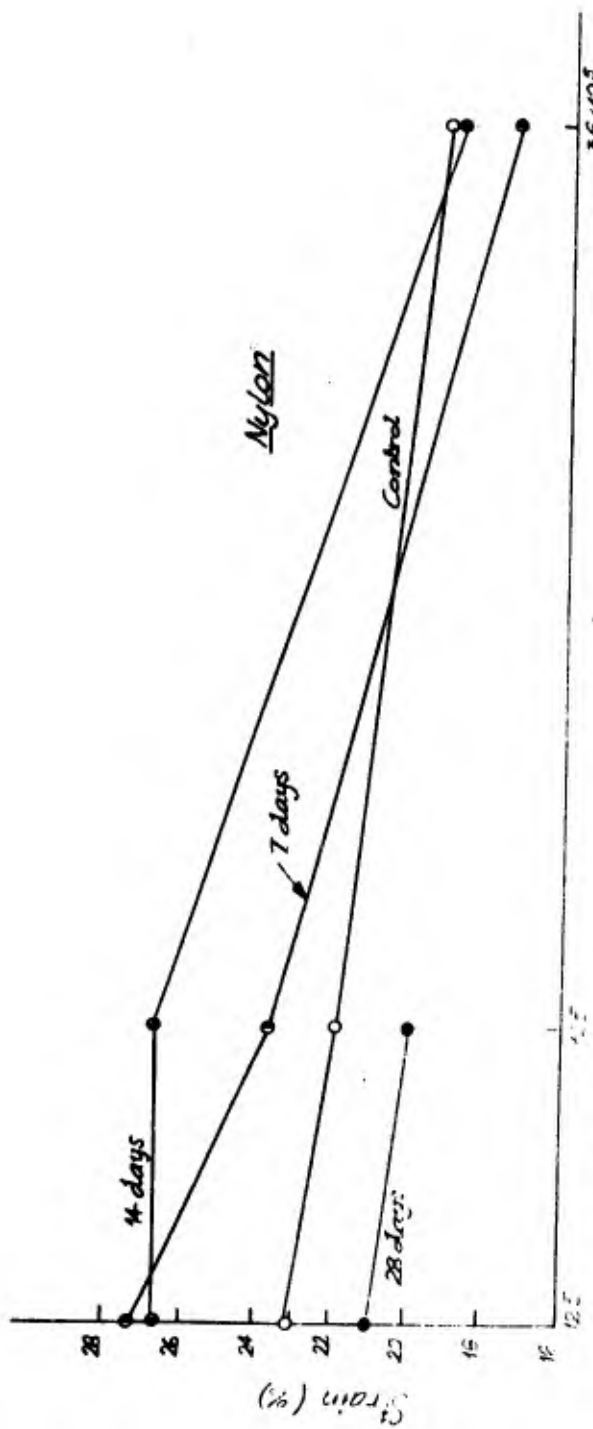


Figure D-13a. Ye-VEP 506 - Breaking Strain of Exposed Yarns vs. Log. Strain Rate.

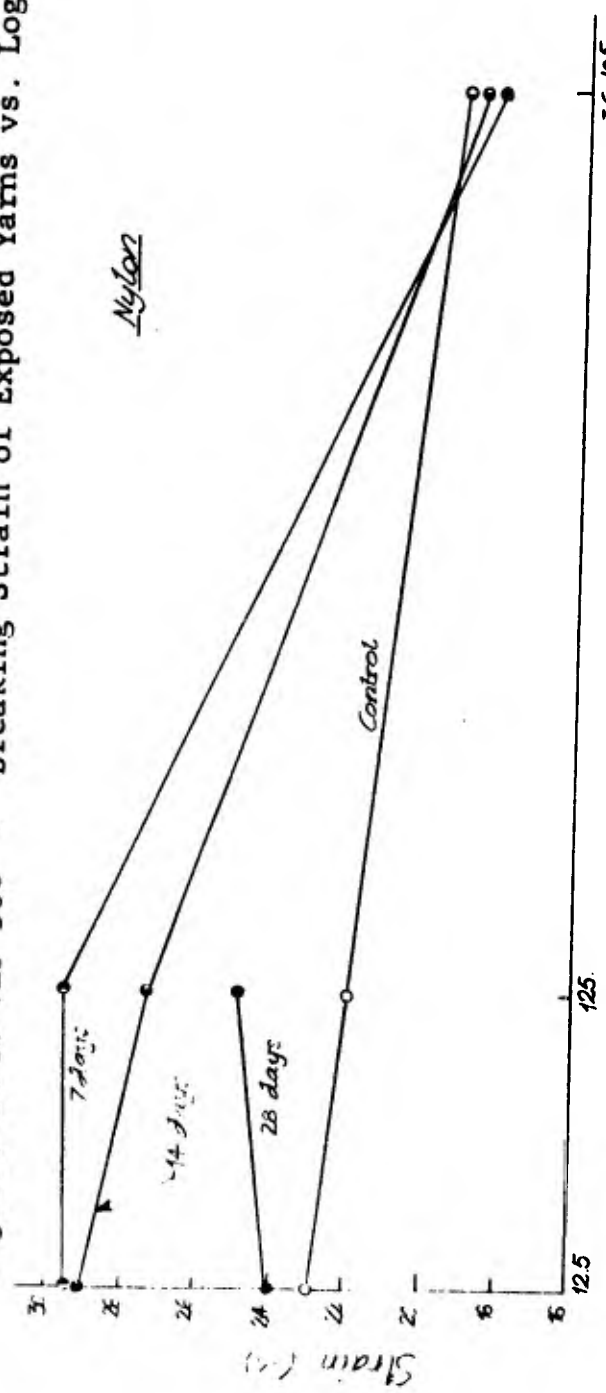


Figure D-13b. Ys-VEP 506 - Breaking Strain of Shade Yarns vs. Log. Strain Rate.

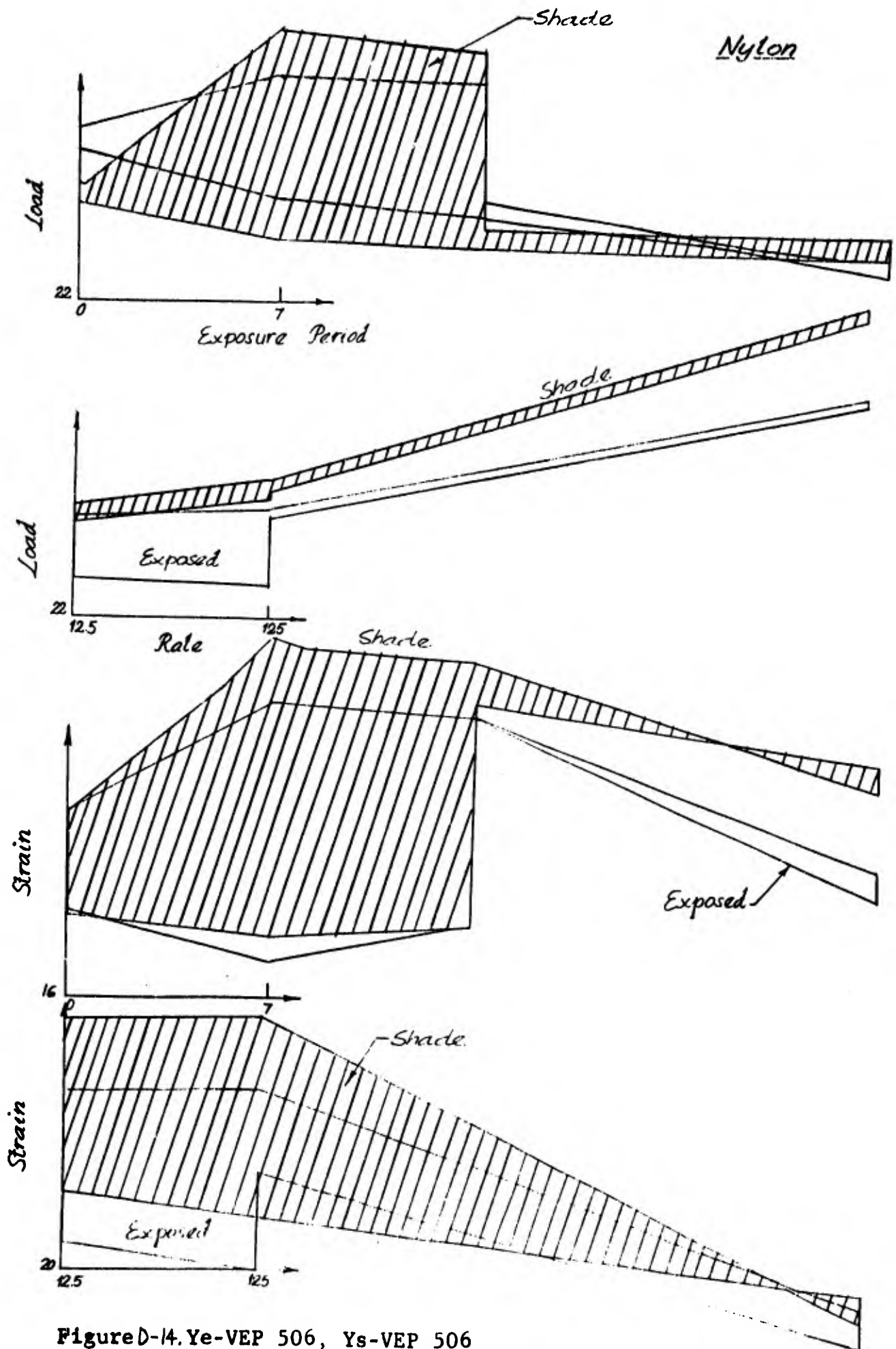


Figure D-14. Ye-VEP 506, Ys-VEP 506  
 Summary of Strain Rate and Exposure Period Effects.

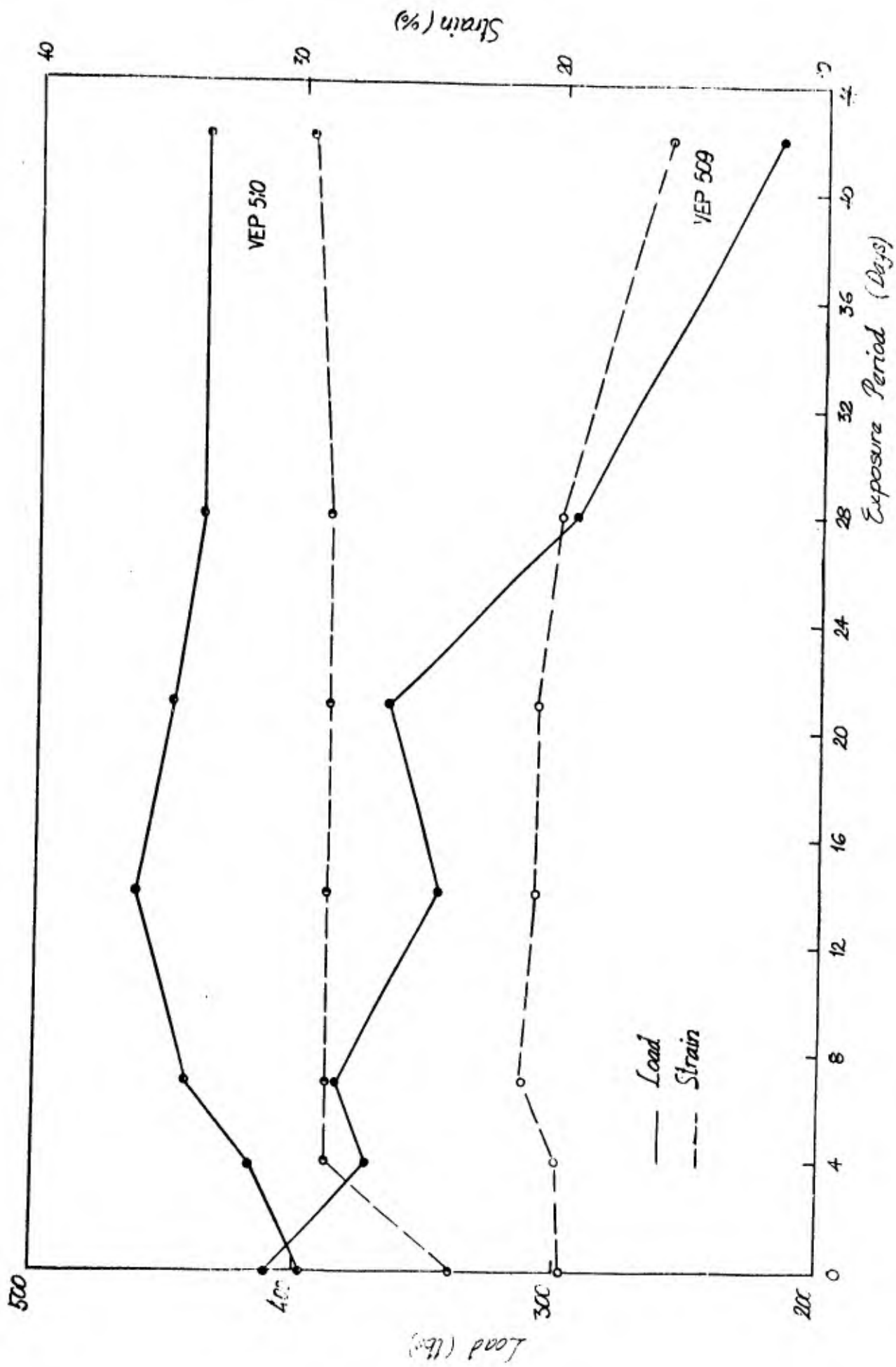


Figure D-15. W-VEP 509, W-VEP 510 - Breaking Load and Strain of Exposed Webbing vs. Exposure Period.

SECTION E  
IMPACT BEHAVIOR OF TEXTILE YARNS

As was pointed out in Section B, the presence of strain inhomogeneities in the loading of textile specimens accentuates the importance of particular factors related to structural efficiencies. These include:

- a. Shape of the yarn stress strain curve
- b. Variation in yarn elongation to rupture
- c. Frictional behavior of the yarn
- d. Structural tightness of the weave
- e. Interaction of yarn and fabric geometry
- f. Variation of the above with strain rate

As a base point in the comparison of yarns and fabrics which differ in respect to items a-f above, an extensive evaluation has been undertaken on a standard sample of nylon thread (VEP 501, Size A, Type I, MIL-T-7807) with comparisons being made between behavior in straight tensile tests and simple loop tests. The gage lengths involved were all 8 inches. Both straight and looped samples (at least 6 samples for each condition of test) were pulled at 2.5, 25, 250, and 300,000% strain per minute. The summary of load and elongation measurements is presented in Table E-1 together with the calculated values of standard deviations for strength and extension. The influence of strain rate on strength of straight and looped thread is pictured in Figure E-1. Figure E-2 shows the influence of strain rate on extension of the two specimen configurations. Figure E-3 points up the effect of strain rate on the loop-to-straight-specimen ratios of strength and extension. The steady and significant increase of breaking load of both straight and looped specimens is observed as the strain rate is increased. The pattern of

strain-at-rupture effects is uncertain and it cannot be said on the basis of the data available, that specimen extension changes significantly as the strain rate is varied over 5 decades. This is true for both straight and looped samples. It follows that since the effect of strain rate is similar for both sample configurations, the ratios of loop: straight strength and extension will be essentially constant with strain rate, as seen in Figure E-3. Finally, it appears in Table E-1 that the variability of the breaking strength of straight and looped samples is not affected as much by strain rate as is the variability of extension at rupture. This becomes more evident when one calculates the coefficients of variation for strength and extension as shown in Table E-2. The significance of the high variability in breaking strain under conditions of stress concentration at high strain rates should become evident in parallel loading tests of looped specimens.

TABLE E-1

Tensile Behavior of Nylon Thread (VEP 501)Single Yarn Tests\*

Strain Rate % per min.	Load (lbs)	Load (St.Dev.)	Strain	Strain (St.Dev.)
2.50	2.65	.072	.158	.0075
25.0	2.96	.067	.161	.0098
250	3.06	.019	.155	.0099
300,000	3.60	.200	.160	.020

Loop Tests\*

Strain Rate	Load (lbs)	Load (St.Dev.)	Strain	Strain (St.Dev.)
2.50	1.98	.110	.1134	.004
25.0	2.27	.176	.120	.004
250	2.27	.251	.130	.005
300,000	2.78	.240	.135	.012

Loop: Straight Test Ratios\*

Strain Rate	Load	Strain
2.5	.75	.85
25	.77	.75
250	.74	.84
300,000	.77	.84

\*All results are based on a minimum of 6 tests

TABLE E-2

Coefficient of Variation in Load-Elongation Tests

Looped Yarn Tests of VEP 501

Strain Rate (%/min)	Load (lbs)	Strain
2.5	2.77	3.33
25	3.87	3.16
250	5.54	3.84
300,000	4.32	0.64

Single Yarn VEP 501

Strain Rate (%/min)	Load (lbs)	Strain
2.5	2.71	4.74
25	2.26	6.08
250	.62	6.39
300,000	5.55	12.50

Further yarn tensile and tensile-loop tests have been conducted on other yarns whose mechanical properties vary significantly from those of nylon. The other materials studied have included cotton and fiberglas. Data on these yarns are presented in Table E-3 and plotted (in comparison with nylon) in Figure E-4 where it is seen that both nylon and cotton show little strain rate effect on loop efficiency, but fiberglas shows a marked improvement in loop efficiency at the higher strain rates. The striking feature of the data plotted in Figure E-4 is the overall low loop efficiency of the glass yarn, -- a feature consistent with its high modulus and stiff elastic behavior near rupture. A most interesting feature in the high efficiency loop tests -- nylon and cotton, is the fact that the cotton yarn demonstrates higher structural efficiency in the loop than does the nylon. Evidently nylon's higher tenacity and higher elongation to break as compared to cotton do not provide the dominant factors influencing these relative loop test efficiencies. The high performance of the cotton can be attributed to factors of gage length, high variability, packing factor, and friction. That is to say, for staple (the cotton) versus filament (the nylon) loop tests, the gage length plays an important part in controlling the mechanism of yarn rupture and in determining the location of break. The packing factor and friction influence the level of strain and strain inhomogeneity and the degree of strain relief at the critical point of the loop. But more will be said about the complexities of loop testing in section F.

TABLE E-3

LOOP TEST EFFICIENCY

Cotton Yarn and Loop

Jaw Speed	<u>Yarns</u>		<u>Loop</u>			Strain Ratio
	Breaking Load (lbs.)	Breaking Elongation (inches)	Breaking Load (lbs.)	Breaking Elongation (inches)	Loop Efficiency	
0.1 in/min.	3.46 (5)	0.89" (5)	6.1 <sup>#</sup> (5)	0.82" (5)	89.7%	0.921
1.0 in/min.	3.70 (5)	0.9" (5)	6.4 <sup>#</sup> (5)	0.79" (5)	86.48%	0.877
10 in/min.	3.74 (5)	0.86" (5)	7.3 (5)	0.83" (5)	97.6%	0.965

# 6

Fibre Glass Yarn and Loop

Jaw Speed	<u>Yarns</u>		<u>Loop</u>			Strain Ratio
	Breaking Load (lbs.)	Breaking Elongation (inches)	Breaking Load (lbs.)	Breaking Elongation (inches)	Loop Efficiency	
0.1 in/min.	13.2 (5)	2.84% (5)	6.35 <sup>#</sup> (5)	1.19%	24.05%	0.67
1.0 in/min.	11.45 (5)	2.65% (5)	8.05 <sup>#</sup> (5)	1.44%	35.15%	0.543
10 in/min.	13.6 (5)	2.95% (5)	8.05 <sup>#</sup> (5)	1.71%	29.59%	0.579

( ) indicates the number of observations averaged

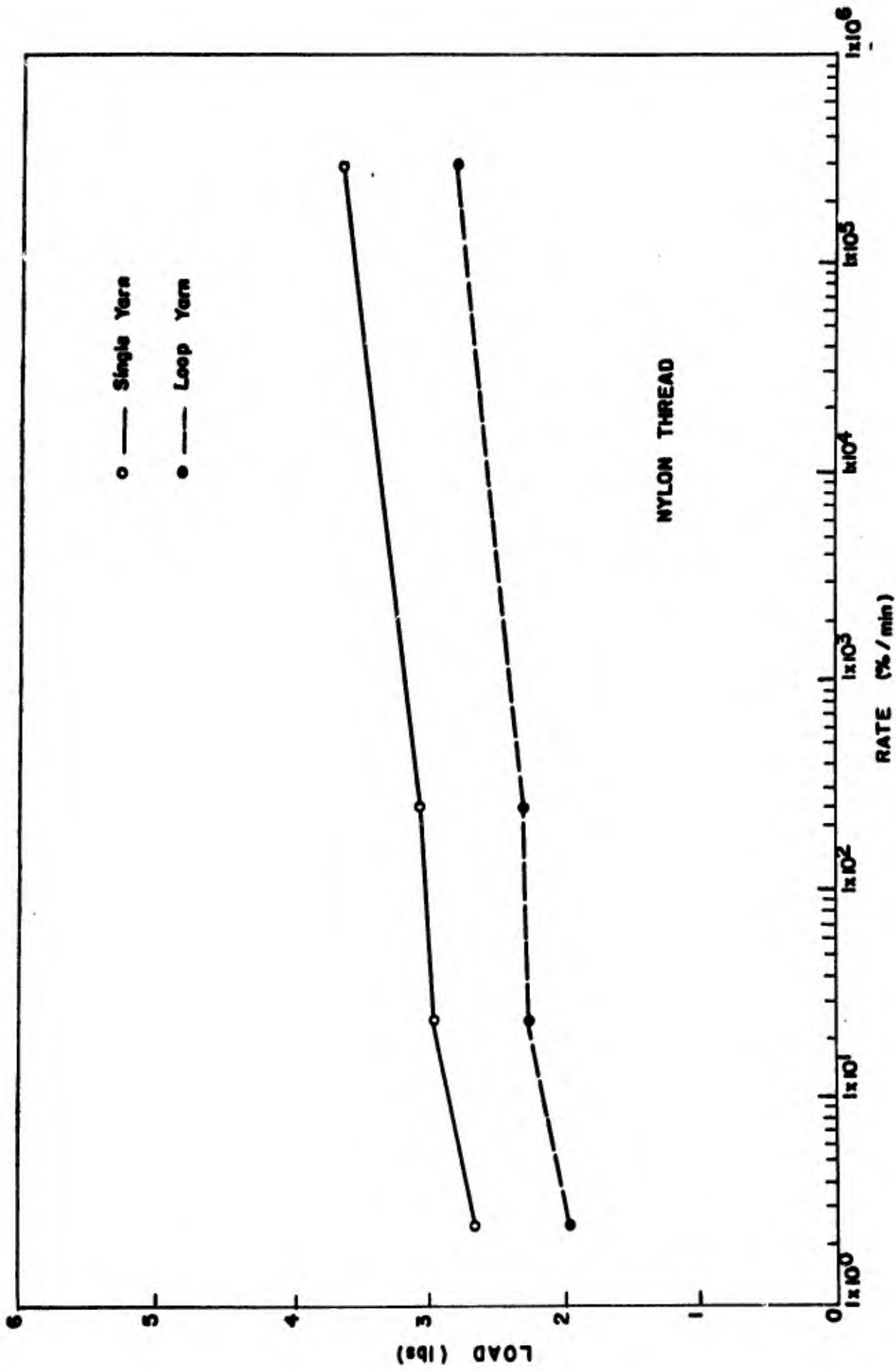
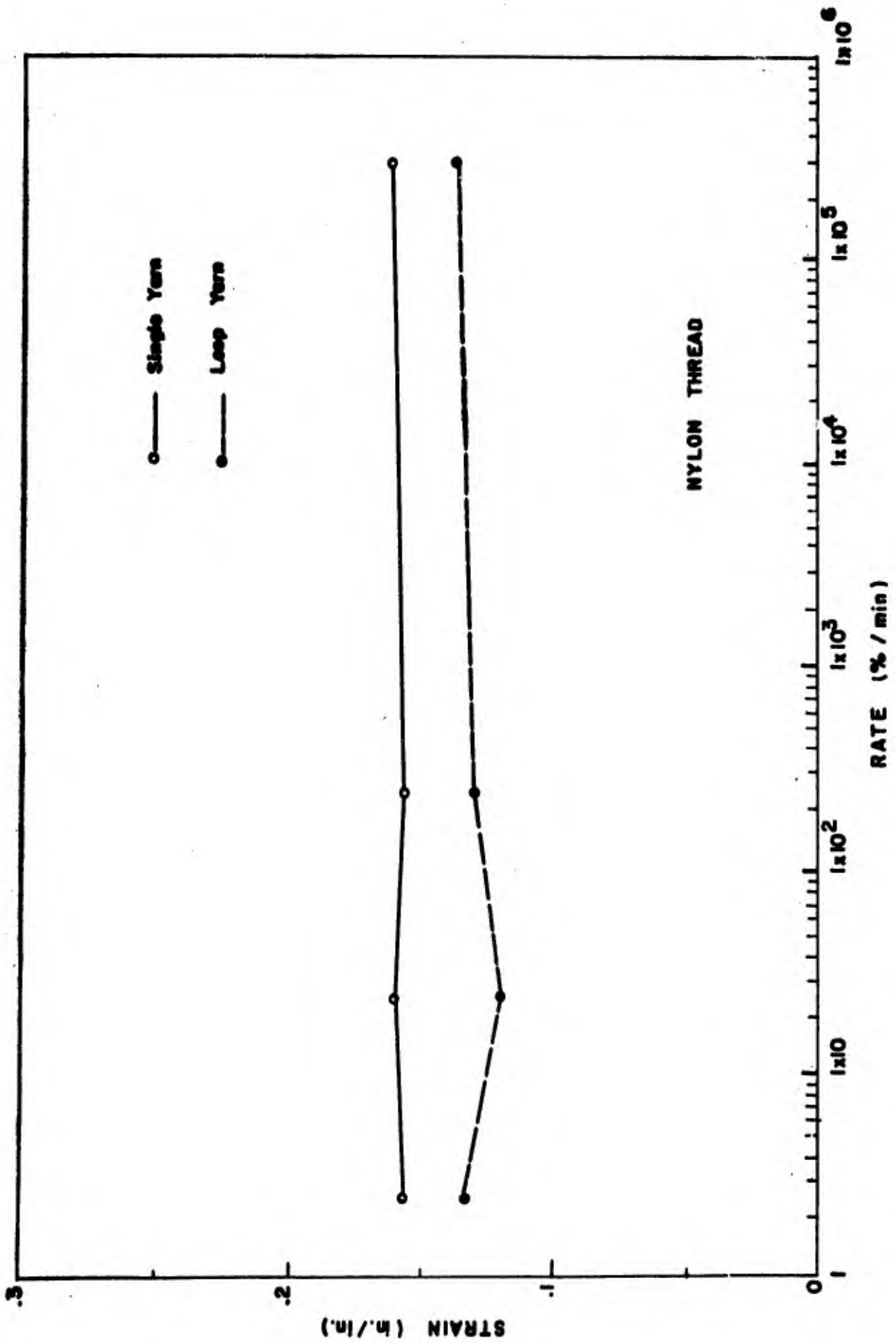


FIGURE E-1. THE INFLUENCE OF STRAIN RATE ON STRENGTH



**FIGURE:E-2. THE INFLUENCE OF STRAIN RATE ON EXTENSION.**

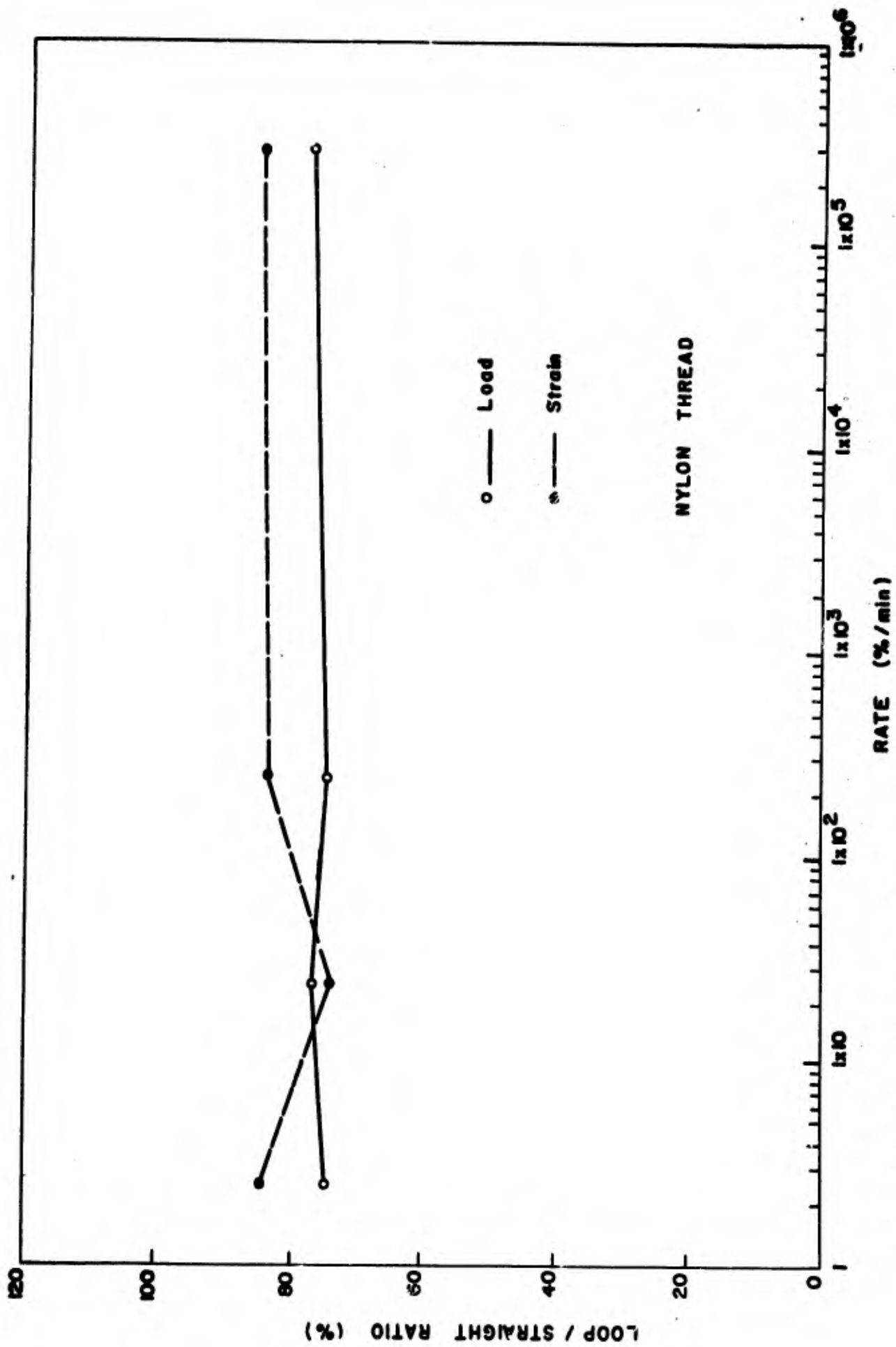


FIGURE-E-3. THE INFLUENCE OF STRAIN RATE ON LOOP / STRAIGHT STRENGTH AND STRAIN RATIO.

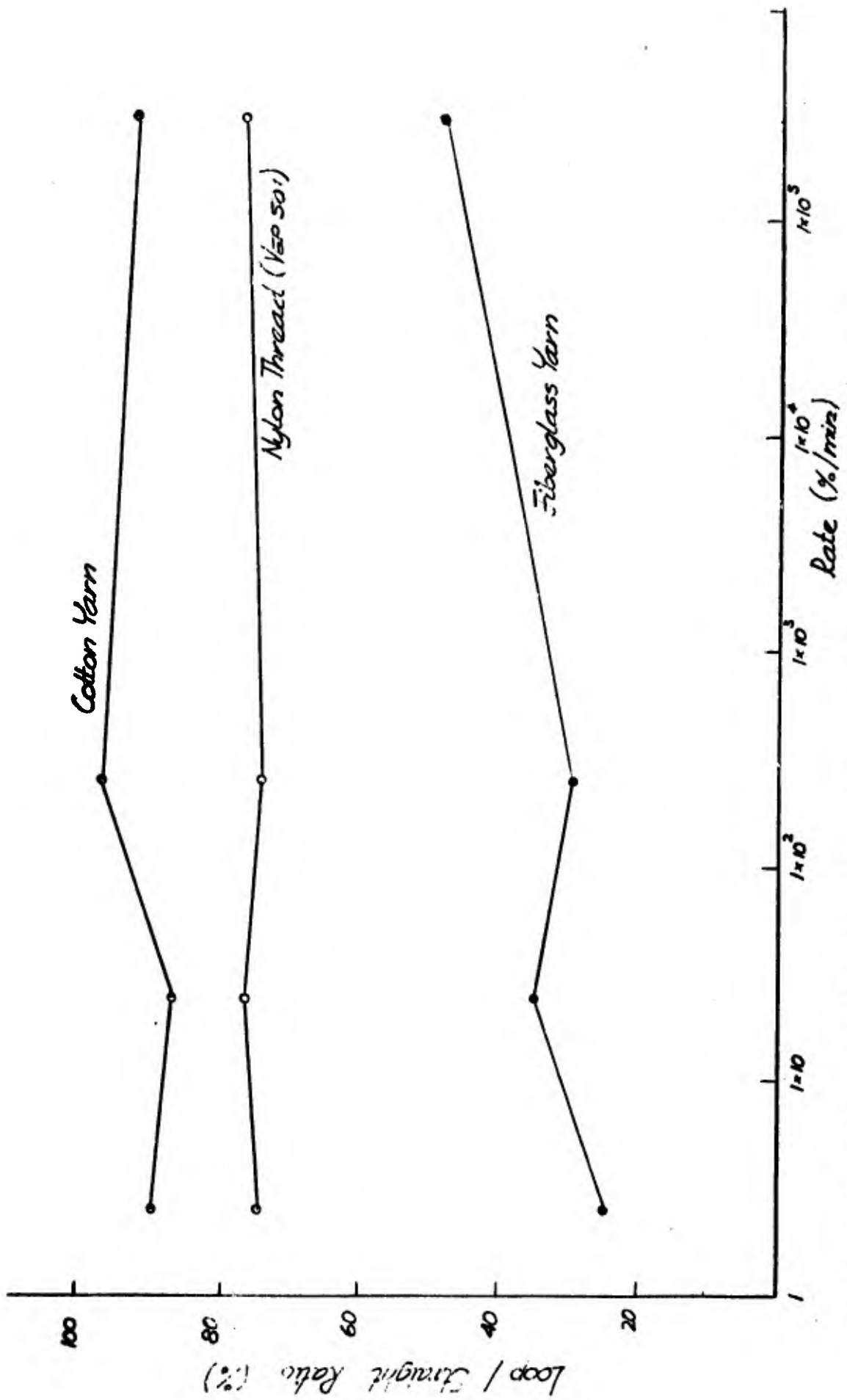


Figure E-4. Loop Efficiency of Various Yarns as Function of Strain Rate.

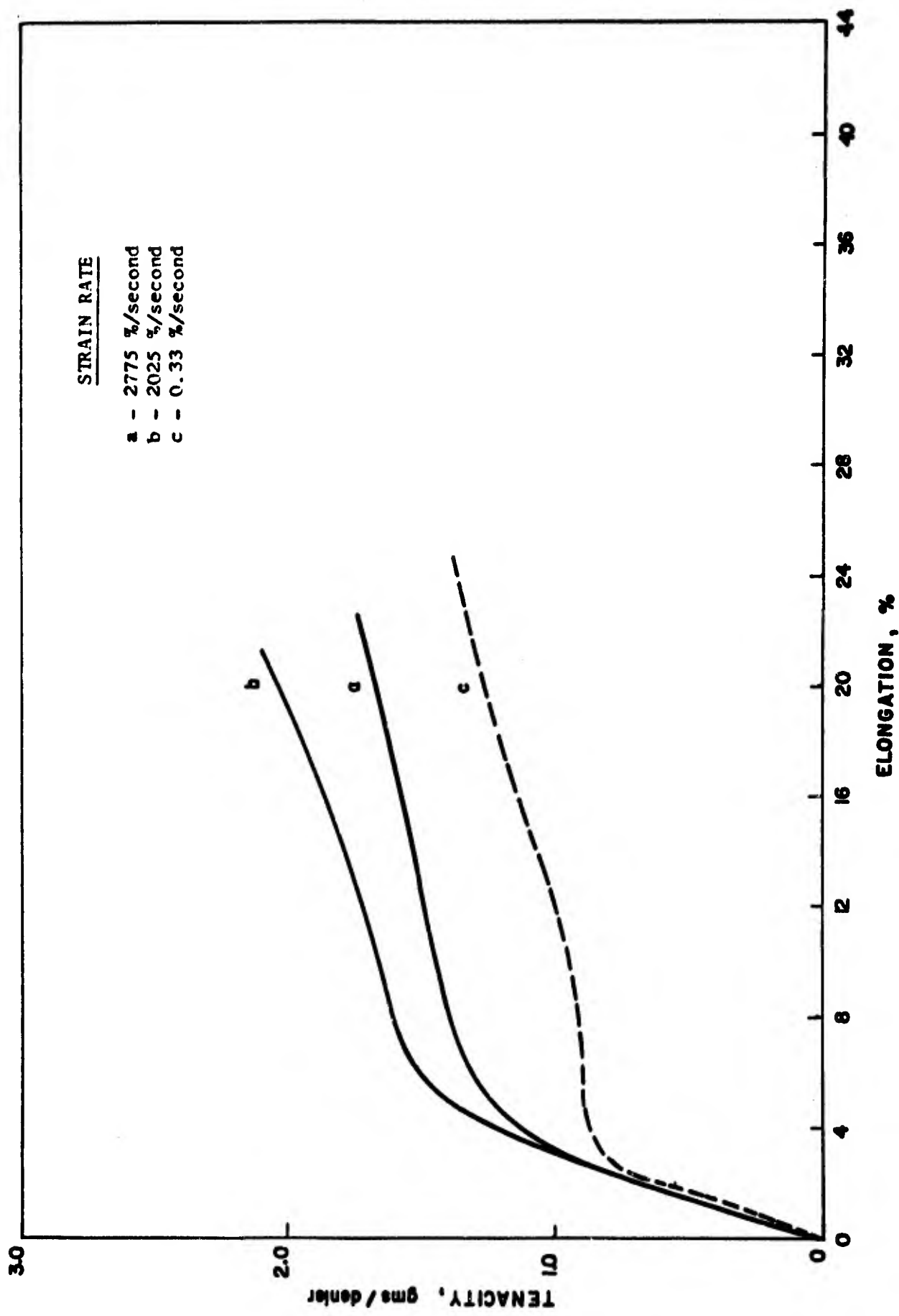


FIGURE E-5 : STRESS vs. STRAIN, Acetate 900 - 240 - 2z

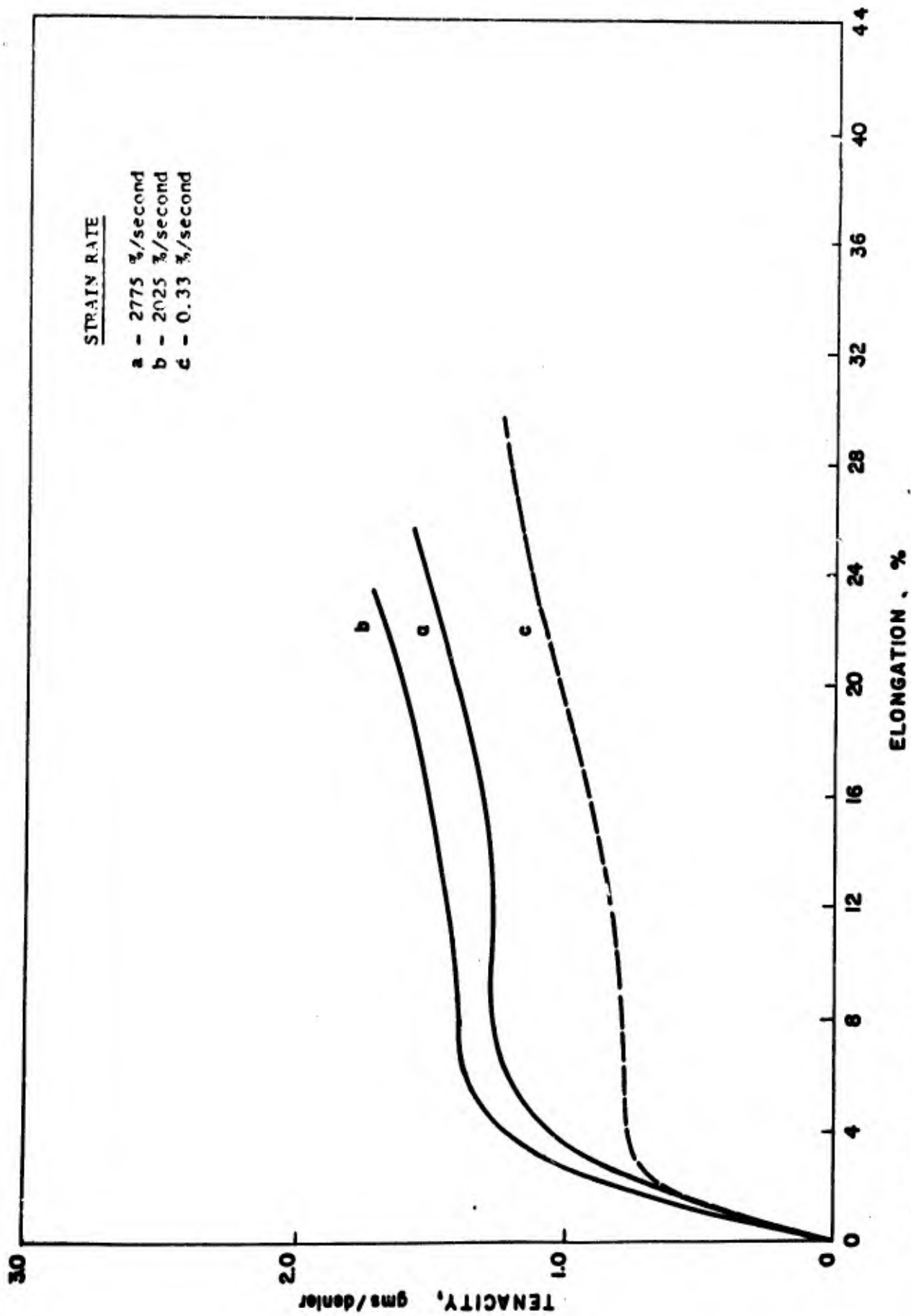


FIGURE E-6 : STRES VS. STRAIN, Arnel 600 - 160 - 2z

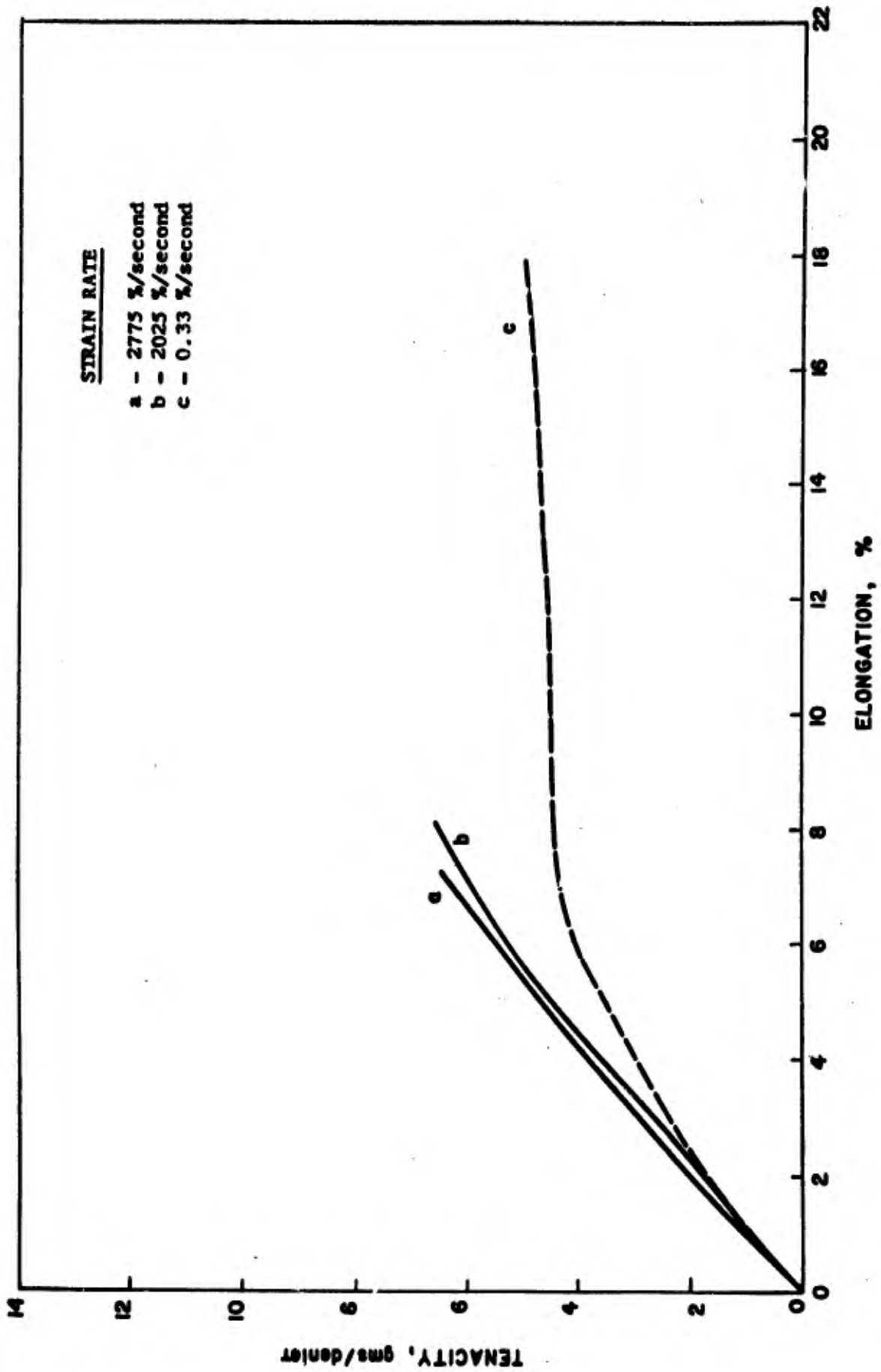


FIGURE E-7 : STRESS vs. STRAIN, Dacron, 250 - 50 - 0, Type 55

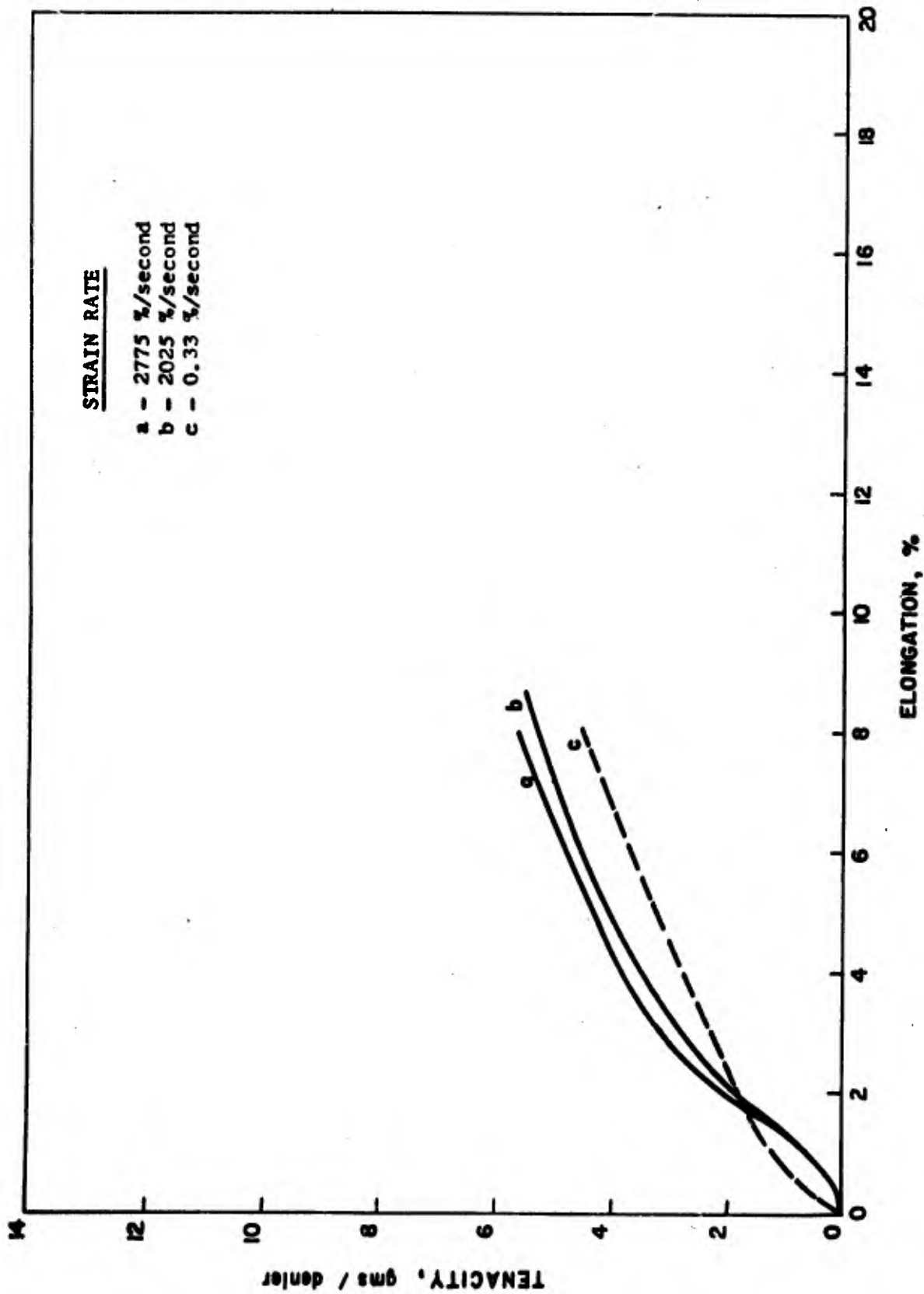


FIGURE E-8 : STRESS vs. STRAIN, High Tenacity Viscose Rayon (Rayflex No. 1), 600 - 490 - 0

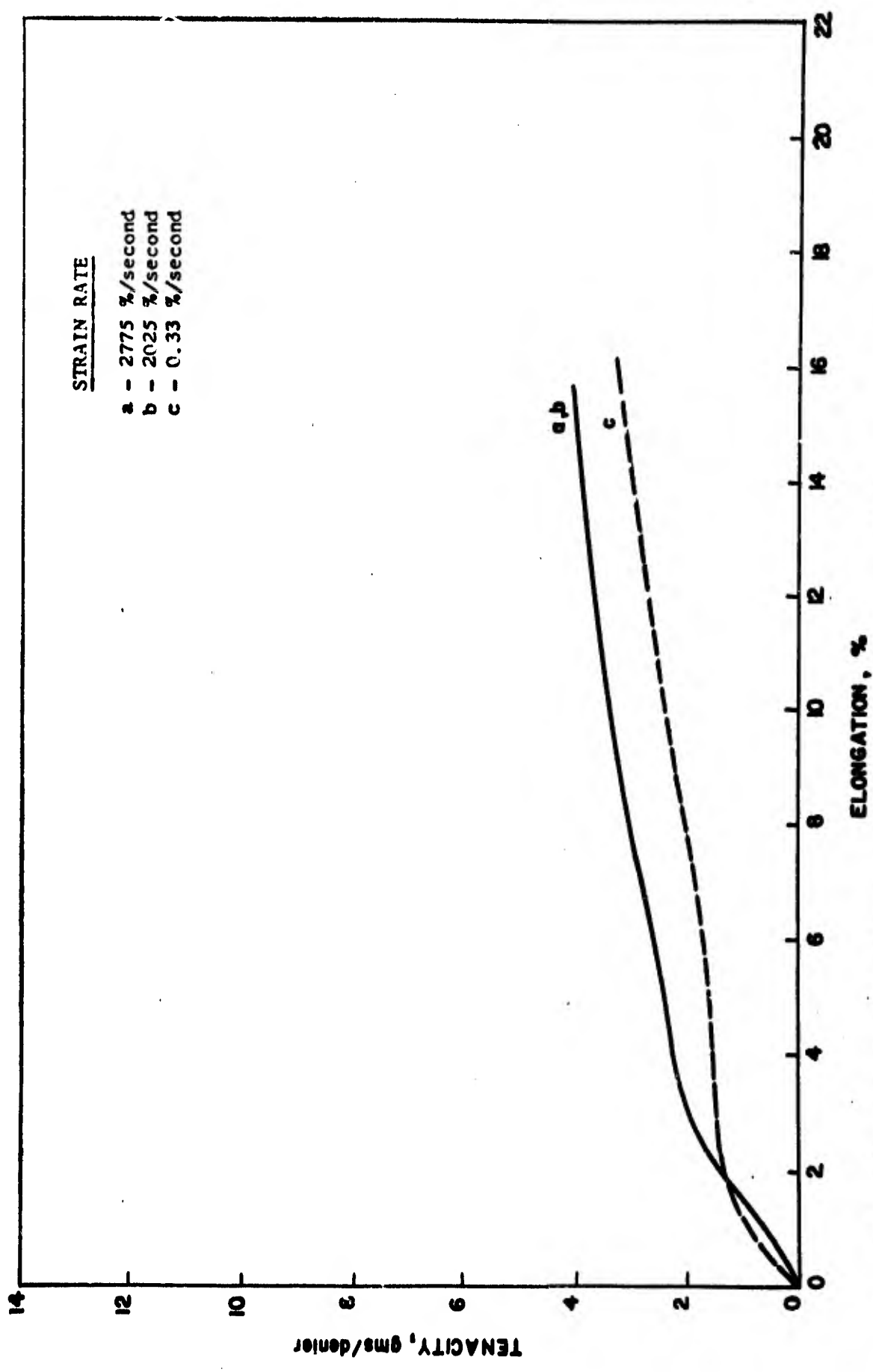


FIGURE E-9 : STRESS vs. STRAIN, High Tenacity Viscose Rayon (Rayflex No. 2), 600 - 234 - 2.5s

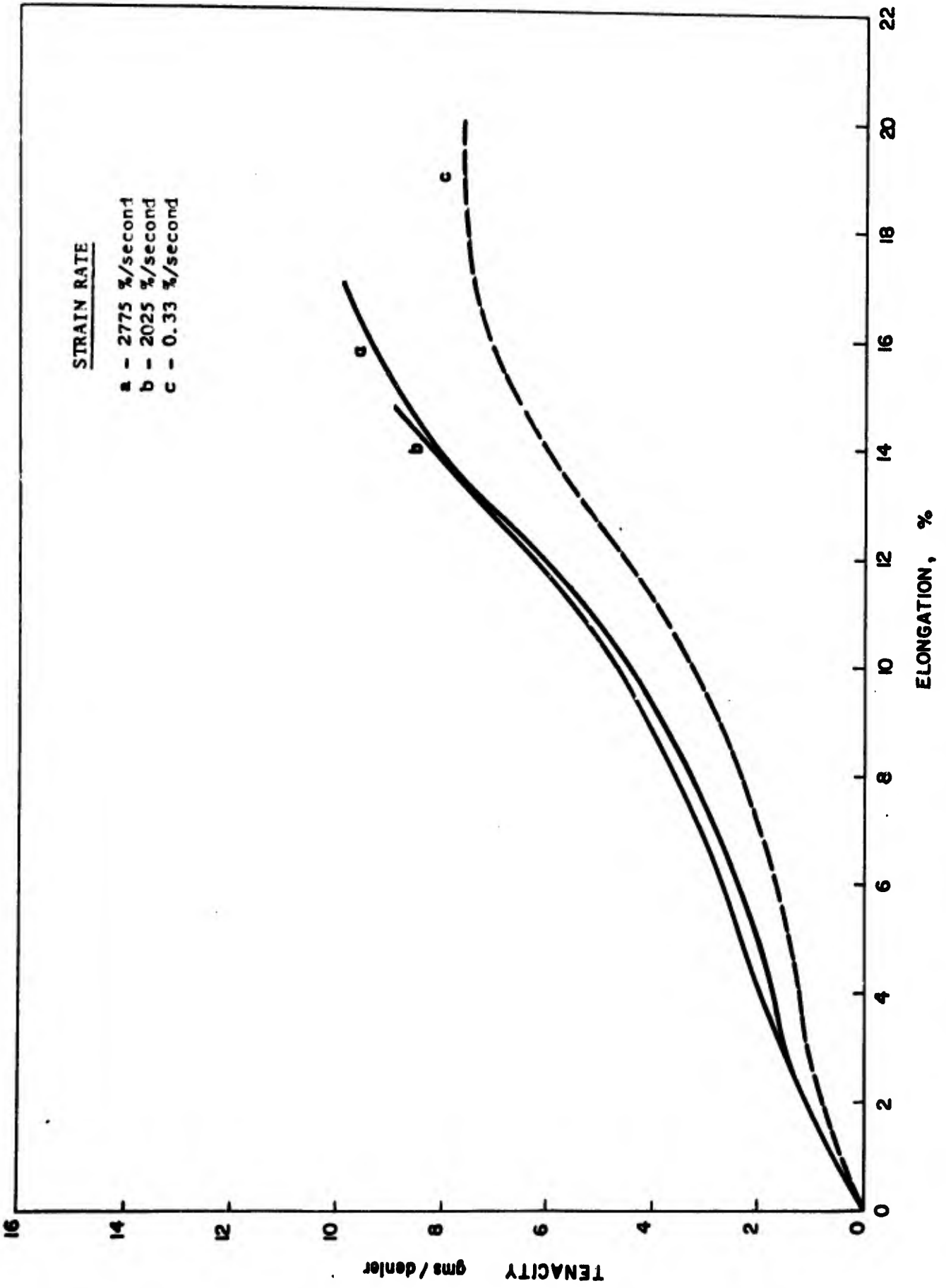


FIGURE E-10 : STRESS vs. STRAIN, Nylon, 210 - 34 - 0, -Type 305

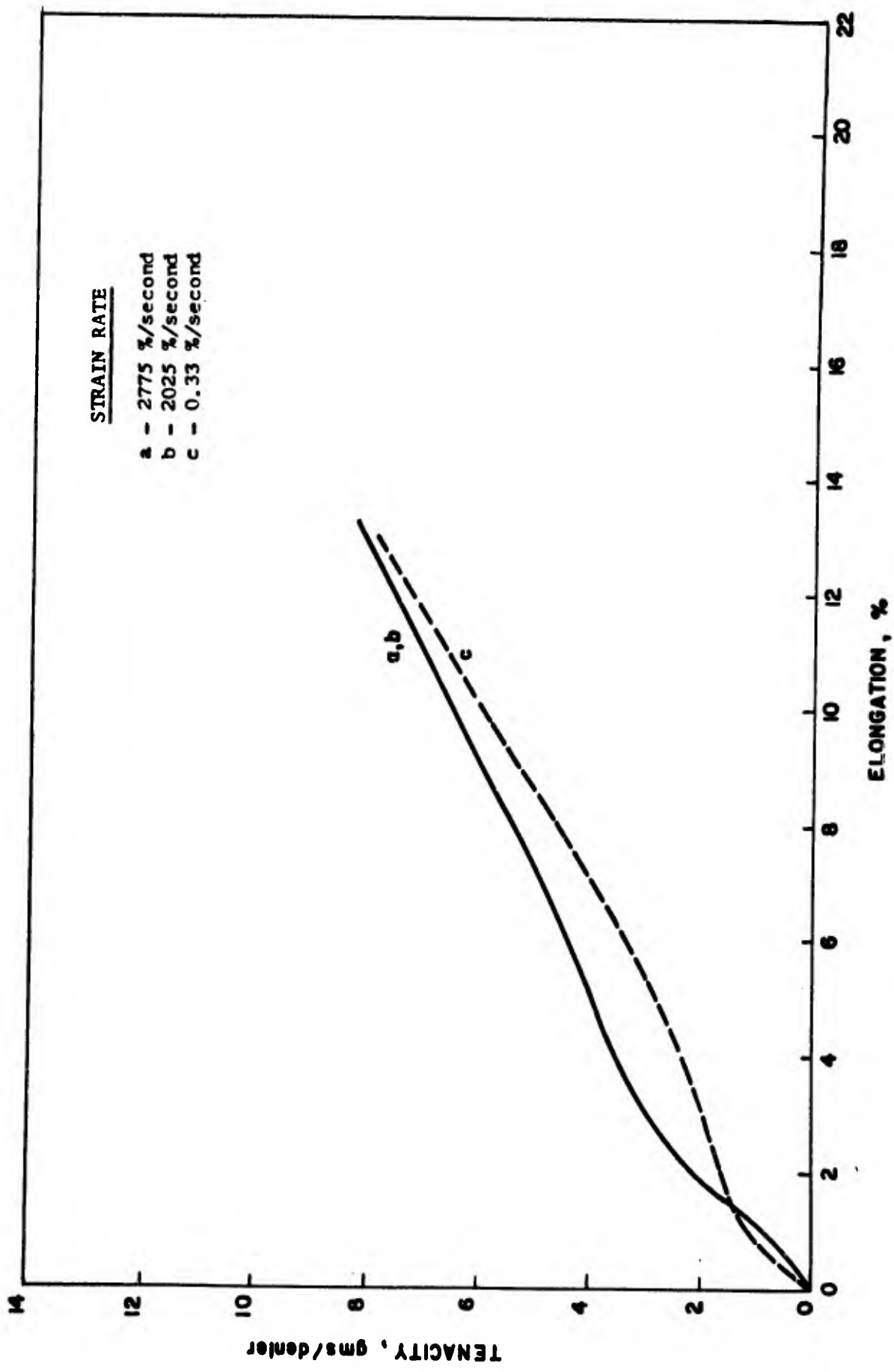


FIGURE E-11: STRESS vs. STRAIN, P V A (Vinal Fo). 1000 - 250 - 0

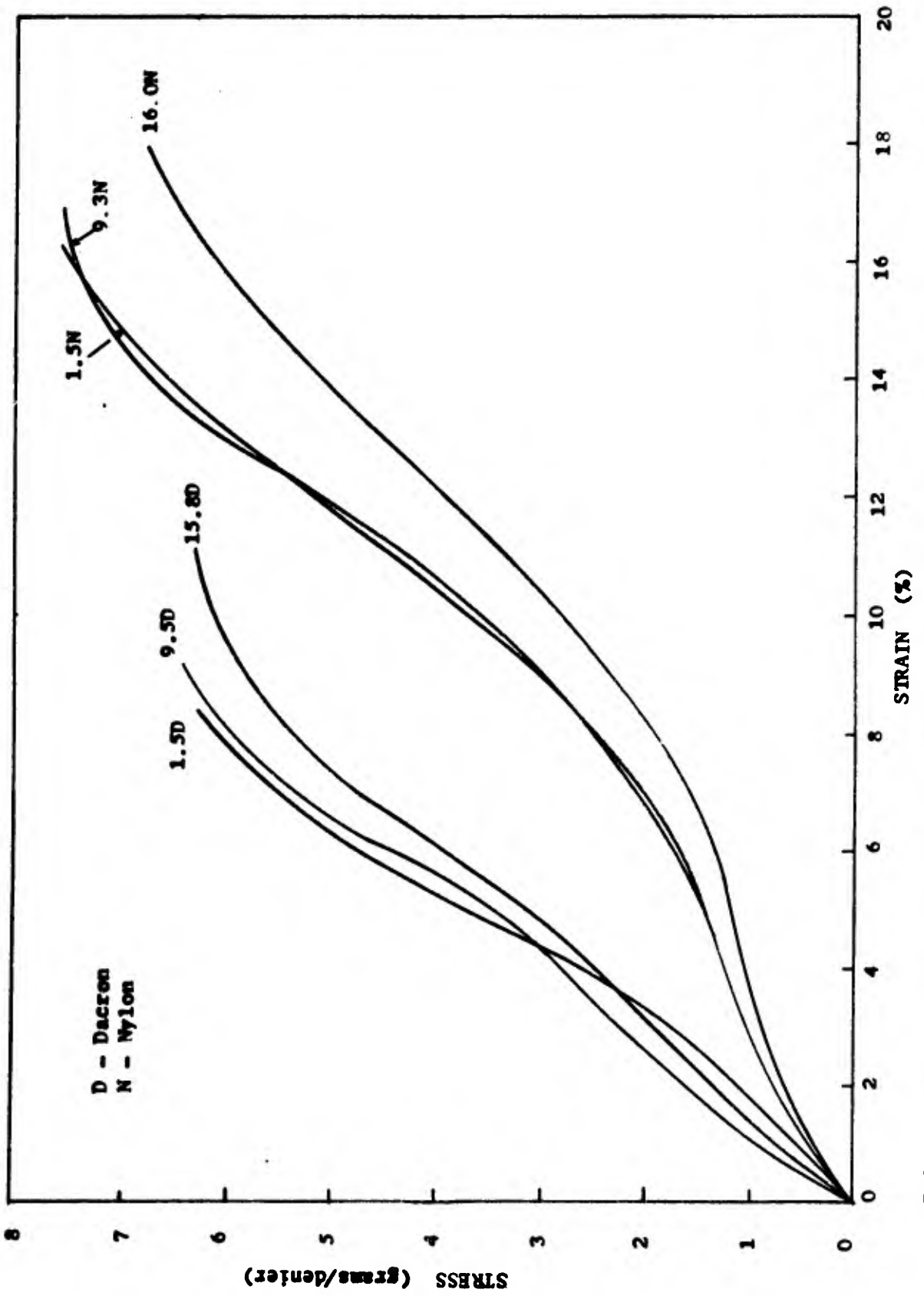


FIGURE E-12: 'Z' TWISTED DACRON, NYLON, STRESS vs. STRAIN AT 1 inch/minute

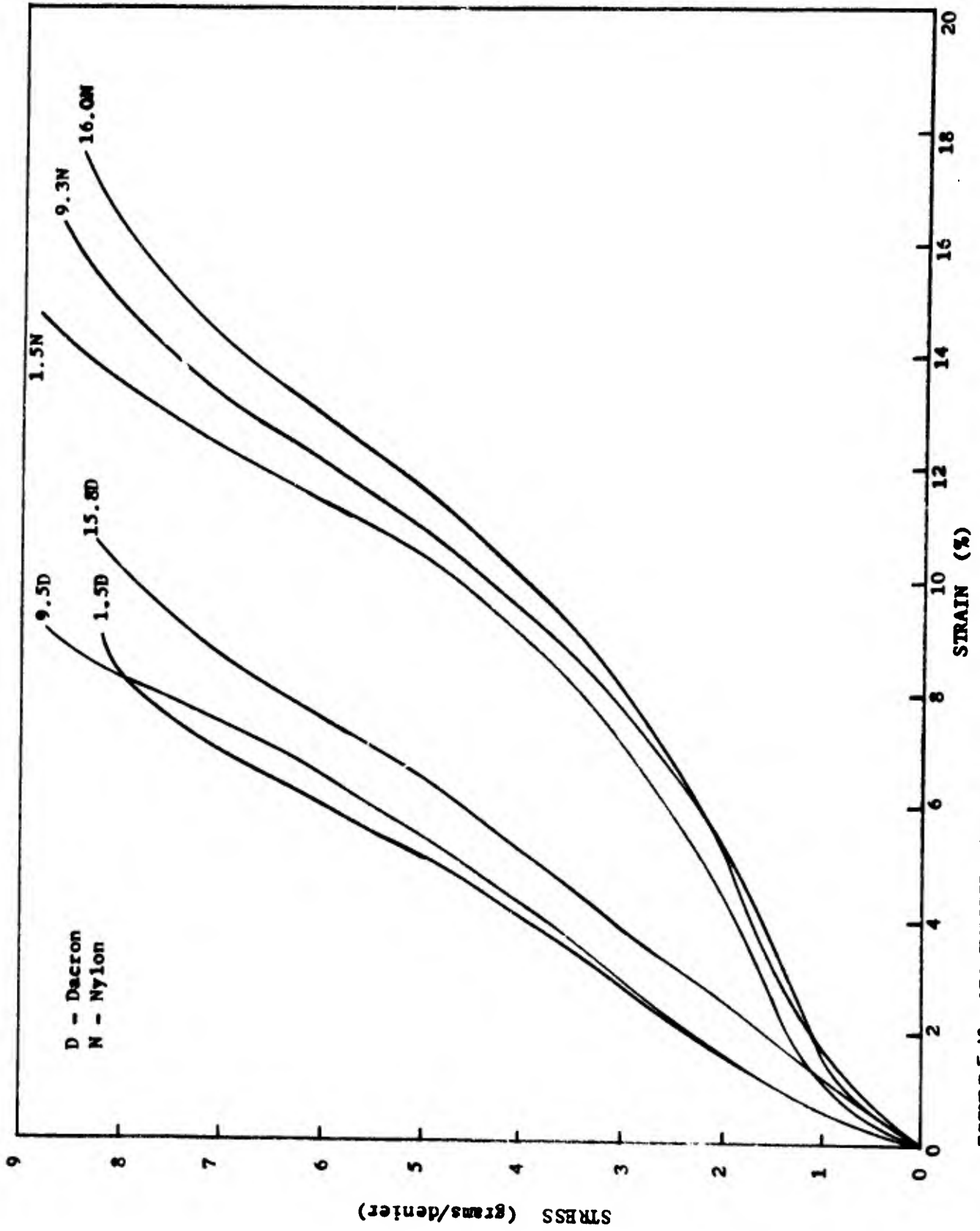


FIGURE E-13: 'Z' TWISTED DACRON, NYLON, STRESS vs. STRAIN AT 200 inch/second

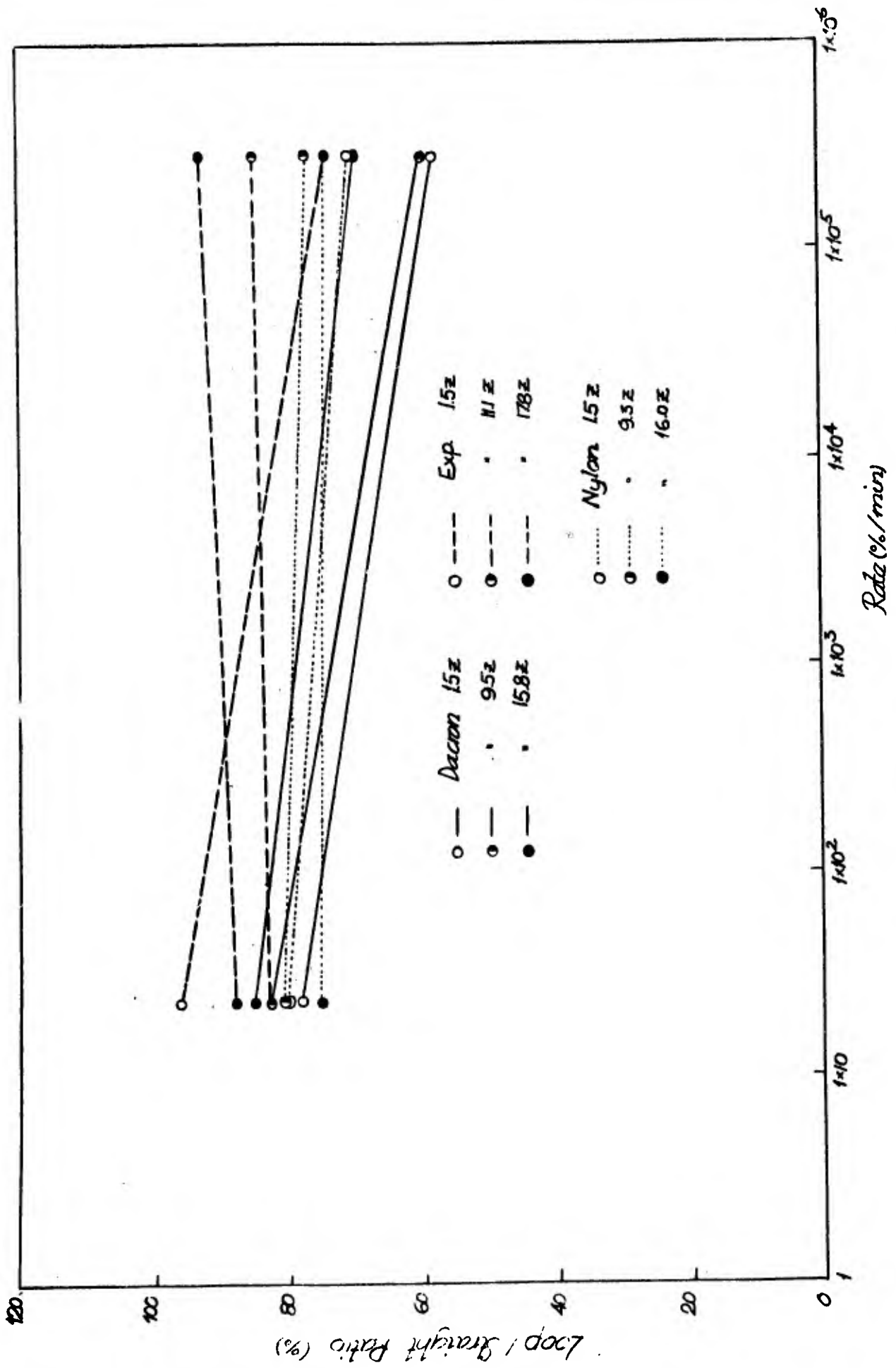


FIGURE E-14: LOOP/STRAIGHT RATIO vs. STRAIN RATE

## SECTION F

### IMPACT BEHAVIOR OF COMPLEX TEXTILE STRUCTURES

#### TRANSLATION OF YARN STRENGTH INTO FABRIC

The most routine of tensile tests of textiles provides for some stress concentration and therefore one may expect a reduction in efficiency of strength from test procedure alone. But some strength loss may be expected merely from the parallel loading of textile yarns, based on the theory of parallel structures with variable properties. On the other hand it may be expected that the weaving process may reinforce low twist yarns and improve their general mechanical behavior so as to manifest an increase in strength efficiency. Whatever the cause of yarn to fabric structural efficiency it is worth while knowing the effect of strain rate on such strength translation. This point provided the basis for a separate set of experiments described below.

The fabric used for the study was the light weight parachute material (125 x 117 threads/inch), with negligible crimp. A unravelled strip test was used to determine the strength of a 1 inch wide specimen. The breaking load was then divided by the number of threads present and the result was compared with the average breaking load of yarns taken from the same fabric. The specimen length was 8 inches as in the seam tests. The procedure was repeated for both warp and filling directions and at three rates of jaw speed; 1 inch/min., 10 inches/min., and 40 feet/sec. Owing to the low sensitivity of the dual trace scope at low loads, the single trace unit had to be used for single yarns, hence yarn strain could not be read. Both load and strain data were obtained for the fabrics. The data are reported in Table F-1 and show a tendency for the fabric efficiency to rise at the higher rates of test. But all in all the efficiencies are extremely high indicating that the fabric reinforcement is a major factor in the

TABLE F-1

TRANSLATION OF YARN STRENGTH INTO FABRICS

Direction	Jaw Speed	At Fabric Break		At Yarn Break		Load Efficiency (%)	Strain Ratio
		Load (lbs/in)	Strain (%)	Load (lbs)	Strain (%)		
WARP	1"/min.	43.86*	25.52	0.350	23.68	98.7%	1.077
	10"/min.	46.5	25.38	0.386	23.6	94.8	1.075
	28,800"/min.	62.83	21.8	0.408	24.14	123.0	
FILLING	1"/min.	40.7	34.16	0.344	33.98	101.5%	1.005
	10"/min.	42.3	34.28	0.368	33.14	98.2	1.034
	28,800"/min.	57.83	28.8	0.395	27.96	125.	

\*each figure is an average of 5 tests.

translation of the strength of these low twist yarns in parallel structures, and it would appear that the weave reinforcement is improved at the higher speeds of testing. It is of interest to observe the stress strain behavior of the fabric in question when tested at different rates of jaw movement in both warp and filling -- see Figure F-1.

The fabrics referred to above were all several years old and so it was deemed advisable to test newer nylon materials so as to avoid any possible aging effects. The material selected was the ballistic cloth procured for vests and helmets by the QMC. The yarn making up the fabric was nylon 66 of about 1000 denier, five ply. Two fabrics were evaluated, a standard QM fabric and an experimental cloth woven on a special loom. Constructional details of the fabrics are given in Table F-2. Test data for the fabrics follows in Table F-3. Impact tests were conducted on yarns removed from the fabrics only since the fabric strengths exceeded the capacity of the impact machine. Further tests were conducted on the original nylon 1085 yarn which is used in the ballistic cloth. Both Instron and impact tests were run and the results are reported in Table F-4. Strain rate effects are observed in the nylon yarn both before and after weaving. Significant differences in strain levels are attributable to crimp and heat setting of the woven fabric.

TABLE F-2

Fabric and Yarn Particulars of QM Standard & RA#2

	Q.M. Standard	RA#2
1. Threads per inch		
Warp	48(3)	54(3)
Filling	40(3)	39(3)
2. Weave	2X2 Basket	2X2 Basket
3. Fabric Weight per sq. inch	13.23 oz.	14.26 oz.
4. Denier Warp, Filling	1122/175/5 1119/160/5	900/170/5 1150/170/5
5. Twist per inch in the ply		
Warp	3.6 (ply)	3.7 (ply)
Filling	3.5 (ply)	4.1 (ply)
6. Crimp		
Warp	7% (5)	6% (5)
Filling	5% (5)	5% (5)

(no.) indicates the number of observations averaged to give reported data.

TABLE F-3

Load-Strain Behavior of QM Fabrics

Sample and Direction of test	Jaw Speed (in./min.)	Fabric		Yarn	
		Load* (lbs/in)	Strain (%)	Load (lbs)	Strain (%)
QM Standard Warp	1	760(1)	42(1)	17.0(4)	40(4)
	28,800			18.8(3)	29(3)
	1	610(1)	33.2(1)	18.0(3)	37(3)
	28,800			18.9(3)	25(3)
RA#2 Warp	1	443(3)	36.3(3)	15.3(3)	38(4)
	28,800			15.3(3)	25(3)
	1	663(3)	38.5(3)	17.0(3)	38(3)
	28,800			17.1(3)	28(3)

( ) indicates number of tests averaged  
 \* ravelled strip tests gage length 5 inches.

TABLE F-4

Instron and Impact Tests on Ballistic Yarn

<u>Jaw Speed</u>	<u>Breaking Load</u>	<u>Breaking Strain</u>
1"/min.	14.0 lbs.(5)	22.6% (5)
10"/min.	14.5 lbs.(5)	21.5% (5)
28,800 in/min.	17.5 lbs.(5)	17.8% (5)

(5) indicates number of observations on 8" gage lengths.

Sample geometry and sample size are of importance in the study of fabric failures, as they introduce strain distributions, a biaxial stress field and, in some cases, a localized stress concentration. Depending on the parameters under observation different sample geometries are selected.

If yarn orthogonality in the center of the sample is required, a grab sample should be used. This type of sample, on the other hand, necessitates nonslipping jaws (large loads must be expected). Biaxial stress fields are also present in the grab sample. If negligible biaxial stress is the order of the day and nonuniform strain distribution across the sample is of little importance, a 'strip' specimen can be employed. In this sample geometry large loads of the longitudinal yarns are found in the center of the sample and the outside yarns carry lower loads due to the crimp relief. A cut in the transverse direction in any of the standard type specimens will create a stress concentration with large nonuniform stress fields and varied amounts of biaxial stress.

In selected experimental studies of this program, ravelled strip samples and modified strip samples with two cross cuts were tested. The first supplied information on yarn strain distribution at failure. The two together indicated that the overall failure mechanism of a loosely woven fabric is controlled (1) by the strain distribution to failure of individual yarns, (2) by the sample stress field, (3) by the relief of strain energy of a broken yarn and its transfer to the other yarns and (4) by the crimp relief in the vicinity of a break and the effective reduction of local yarn gage lengths. All these factors contributed to failure propagation. Their relative importance can only be inferred at present. We assume that a normal distribution exists for strains at failure of individual yarns (tested separately) and for yarns as they lie in the fabric. It can be expected that

these two distributions will not be identical. Single yarns break at various strains when tested separately and one yarn failure does not contribute in any manner to failure of another yarn. In a fabric, the cross yarns transfer locally at least a part of the breaking load of each yarn (as it ruptures) to neighboring longitudinal yarns and therefore, it can be reasoned, the mean strain at failure of a fabric will be lower than that of a population of single yarns. Similarly a decrease of the standard deviation of strain would be expected. Attempt was made to substantiate these expectations by experiments.

Cargo parachute fabric (600 lbs/in) was used in this study on strain distribution at failure. All samples were tested in the filling direction.

The strain distribution at failure of a population of single yarns was obtained by testing each yarn separately. The sample yarns were removed from a strip of fabric which carried two gage marking lines in the warp direction and which were separated by 5". These marks established the gage length of the tests. It was found that the yarn removal from the fabric did not change the separation of the marks, that is no crimp relief or yarn straining took place. In total 10 samples were stressed in the Instron and strain at failure was computed from the jaw displacement, assuming that the gage length was constant. In these tests this assumption was valid because only negligible slippage was observed. In the plotted strain distribution (see Figure F-2), the strain magnitudes at failure did not include the crimp. The zero jaw displacement was taken at a point at which all crimp was removed. It was found that the crimp removal was achieved by a jaw displacement of approximately .25" or in terms of strain approximately 5%.

The question was raised, which of the two gage lengths

should be used for determination of strain at failure. The 5" gage length containing the crimp or the gage length without crimp. It was felt that the strain rate variation in the two sample lengths (5" and 5.25") can be neglected. It was therefore decided that the sample gage length of 5.25" should be used for determination of strain at failure. Should the crimp have been included in the initial sample length a fictitious strain of 5% would have been contained in the actual strain data. The crimp removal as far as the yarn fibers are concerned, cannot be considered as a strain.

The strain distribution at failure of individual yarns in a one inch wide fabric sample was determined from the jaw displacement of the Instron. (See Figure F-2). It was assumed the gage length of each individual yarn was 5" during the entire test duration. As the load built up in each tensile test, every sharp decrease of load on the recorder chart was taken as evidence of a break in the fabric. The magnitude of each such a load drop was used to estimate the number of yarns broken at each instant. It was known that a load of approximately 12 lbs was required to rupture one yarn. There was no doubt that the jaw displacement measurement was correct, but considerable doubt existed in the computations of yarn strain based on this displacement.

The assumption of constant gage length is open to question. Some slippage took place in the jaws. Strain nonhomogeneity of the sample reduced the gage length at some locations of the sample. After the first yarn failure the crimp relief of the neighboring few yarns, on the other hand, increased the actual gage length of those yarns. For those reasons the cited method for determining the "in-fabric" yarn strain distribution at failure is on weak ground. Nonetheless it was carried through to provide a semi-quantitative picture of the mechanism of failure.

Two by five inch grab samples with two cuts of .5" from the edges in the center were also tested in the Instron. The strain distribution of individual yarns at failure was calculated as described above and was plotted (See Figure F-2). This type of specimen did not slip in the jaws but contained two large stress concentrations at the two slits and a moderate biaxial stress field, at the jaws. It was expected that the strain distribution for yarn rupturing in this specimen would have a lower mean than for the singly tested yarns. This was found to be the case. The data suggests that this distribution was also much broader than the population of singly tested yarns. This widening was probably due to a minor cutting damage of the edge yarns and on the large strain side of the distribution to slippage of a few individual yarns. All failures took place on the edges of the sample and in the center of the gage length.

Progress of this type of a rupture is shown in Figure F-3. The first picture in the left corner represents the sample prior to the initiation of a test. Opening of the slits was caused by a small pretensioning. The sequential pictures from left to right show the initial edge yarn breaks. The trigger load cell can be seen. Back lighting was used in these photographs and the light source is seen in the background on each picture.

The failure observation made to date on loosely woven fabric indicated that a failure mechanism changed a little in the two types of samples. The straight sample initiated its failure inside of the sample while the cut sample broke from the edges. Stress nonuniformity determined the location of the first yarn failure. The straight sample carried the largest load in the center and the slitted specimen on the edges. The first failure in both samples was dictated by the low side of the strain distribution at failure. In samples with a large stress concentration the first break takes place at lower strain than indicated

by the single yarn strain distribution because "in fabric" yarn strain is computed from jaw displacement and the actual "effective" gage length of that particular yarn is not known. As stated above it was assumed equal to the initial jaw separation. A stress concentration implied that nonuniformity of strain and stress is present. In a fabric this nonuniformity is created or maintained by local yarn jamming and local crimp relief. The effective gage length of a yarn whose crimp removal is unrestrained by cross yarns is much larger than another yarn whose crimp cannot be removed. The first yarn failure in the straight sample, it is reasoned, allows the neighboring yarns to relieve some of their strain (increase their effective gage length). In this fashion the existing nonuniform stress field is changed and the location of its maximum can be transferred to a different point on the sample. The strain energy of the broken yarn contributes to the location and magnitude of the stress concentration. It is felt that each yarn failure in this type of sample is determined by the location of a stress concentration and the single yarn strain distribution at failure. This rupture mechanism can be visualized as a sequence of yarn failures followed by stress-field rearrangement coupled with additional external application of strain. It is expected that this type of failure will be strain rate sensitive. At high speeds the nonuniform stress field (which is made up by the mobility of the longitudinal and cross yarns) might not have enough time to reach an equilibrium state and thus at high speeds a different failure mechanism may be expected.

The cut sample shown in Figure F-3 fails in the same manner as the straight sample. However, at break, the location of stress concentration in the vicinity of the two cuts is still maintained. The crimp relief phenomena in this case is of lower importance because at the edges not much crimp is present to start with.

### SEAM BEHAVIOR

The ability of textile materials to perform in parachutes is obviously related to fabric stress strain behavior and to the capacity of the seam to transmit stresses. The ratio of seam strength to strength of the straight fabric has been termed seam efficiency and is a measure of the ability of the cloth to transmit an extremely complicated stress pattern. Cloth performance in non homogeneous stress fields is related to uniformity of the yarns, to their stress strain curve and to fabric geometry. Little is known as to the changes in behavior of cloth in a seam when tested at slow speeds as compared to impact tests. This phase of the program was therefore carried out on actual parachute fabrics (1.1 oz. 126 x 115 T.P.I.) to observe the strain rate effect on seam efficiency.

In the initial tests specimen gage length was taken to be 8 inches, with specimen width of 2 inches. Only the center 1 inch section of the specimen was gripped, much as is done in the 'grab' test. It was found that the seam running across the center of the specimen (the full 2 inches) slipped badly in the static test leading to unusually low results. No slippage occurred however in the impact test at 40 feet per second. This suggested that in the high speed test with no time allowed for slippage sufficient stress concentration was built up as to cause fabric rupture. An alternate geometry was required to permit successful tests at both static and dynamic speeds. It consisted of an 8 inch gage length and a 2 inch sample width. But at the sample edges, just above and just below the seam, a horizontal slit was cut into the fabric, each  $\frac{1}{2}$  inch long, leaving the center 1 inch strip of the fabric intact. A similar geometry was used

for the unseamed sample. It was found possible in this way to run seam tests without slippage and to determine a measure of seam efficiency at different test speeds. Extra fabric was used as jaw lining to reduce jaw breaks.

The test results for the light weight parachute fabric are listed in Table F-5 and show in general a decrease in seam efficiency as the test speed is increased from 1 inch/minute to 10 inches/minute to 40 feet/second.

TABLE F-5

Effect of Strain Rate on Efficiency of Parachute Seams

<u>Jaw Speed</u>	<u>Strength (w/seam)</u>	<u>Strength (w/o seam)</u>	<u>Efficiency</u>	<u>Strain Ratio</u>
1 "/min.	30.5 lbs.	27.5 lbs.		
	35.0	28.5		
	<u>30.5</u>	<u>28.5</u>		
	<u>32.0 Av.</u>	<u>28.1 Av.</u>	114%	1.31
10"/min.	37.5 lbs.	34.5 lbs.		
	38.5	37.5		
	<u>31.5</u>	<u>33.0</u>		
	<u>35.8 Av.</u>	<u>34.6 Av.</u>	103%	1.37
40'/sec.	25.2 lbs.	34.8 lbs.		
	27.6	38.4		
	<u>25.2</u>	<u>37.2</u>		
	<u>26.0 Av.</u>	<u>36.8 Av.</u>	70%	.81

It may seem strange to note seam efficiencies exceeding 100%, but it should be remembered that the straight fabric test is not a ravel strip nor a grab test. It is in itself a special form

of tear test selected primarily because its geometry allowed localization of the breakz both with and without the seam in place. And it is quite likely that the seam actually reinforced the fabric rupture during the slow tests. In Figure F-4 we present a photographic history of the seam failure showing the pullout of the warp yarns where the fabric joins the seam, the slippage of the filling yarns along the warp at each stitch line, the pinching of the warp yarns by the sewing thread at each stitch, the riding up of the whole seam surface layer as slippage takes place at each stitch line, the bunching of the stitch lines, the progressive rupture of warp yarns pinched within stitch loops at the outside line of stitches and at the inside line, the total collapse of the seam. It is clear that if the extensive elongation and slippage of the nylon parachute fabric were not operative, the seam would have failed at the outside row of stitches with a much lower strength than was recorded in the case at hand.

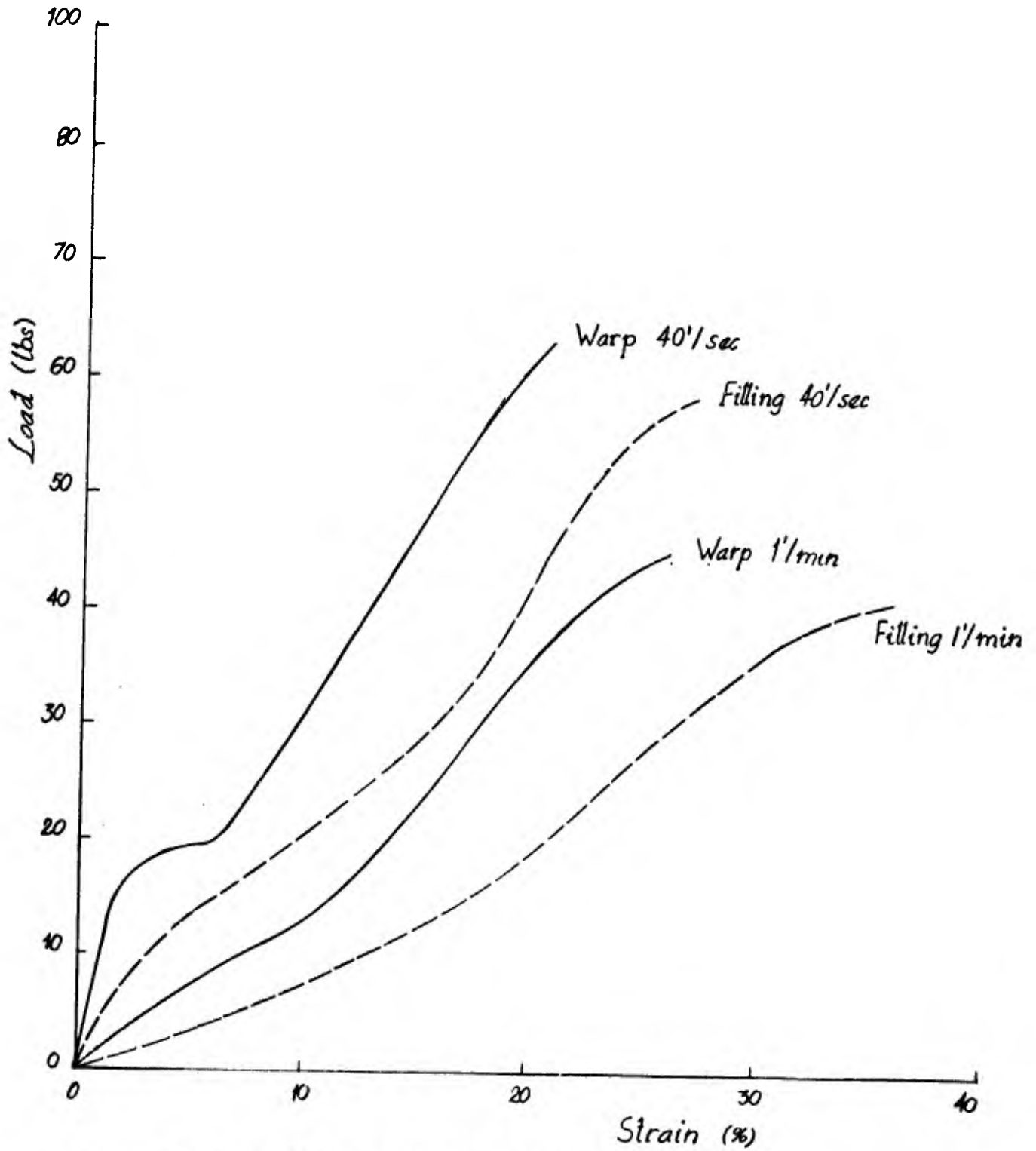


**Figure F-1. Load Extension - Behavior of Parachute Cloth (8" X 1" ravel strip) Static vs. Impact.**

# Yarn Strain Distributions at Failure



Fig. F-2

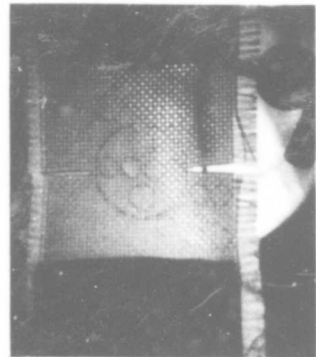
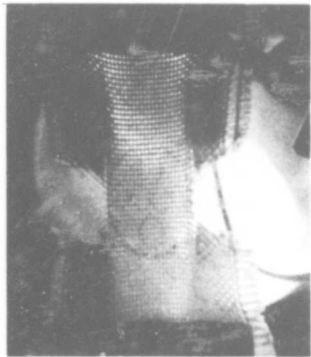
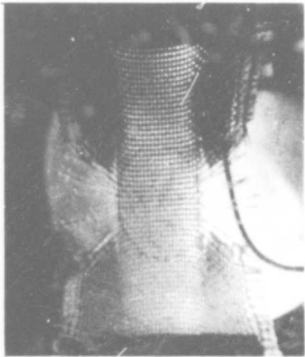
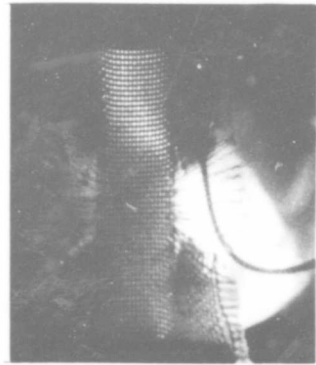
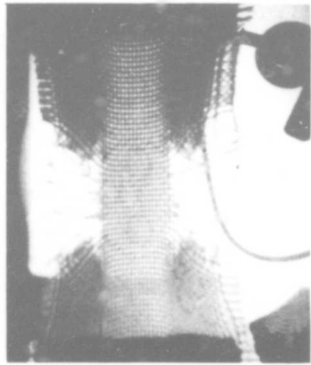
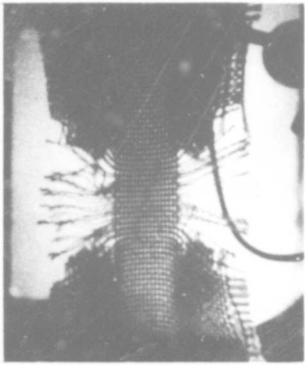


Figure No. F-3.

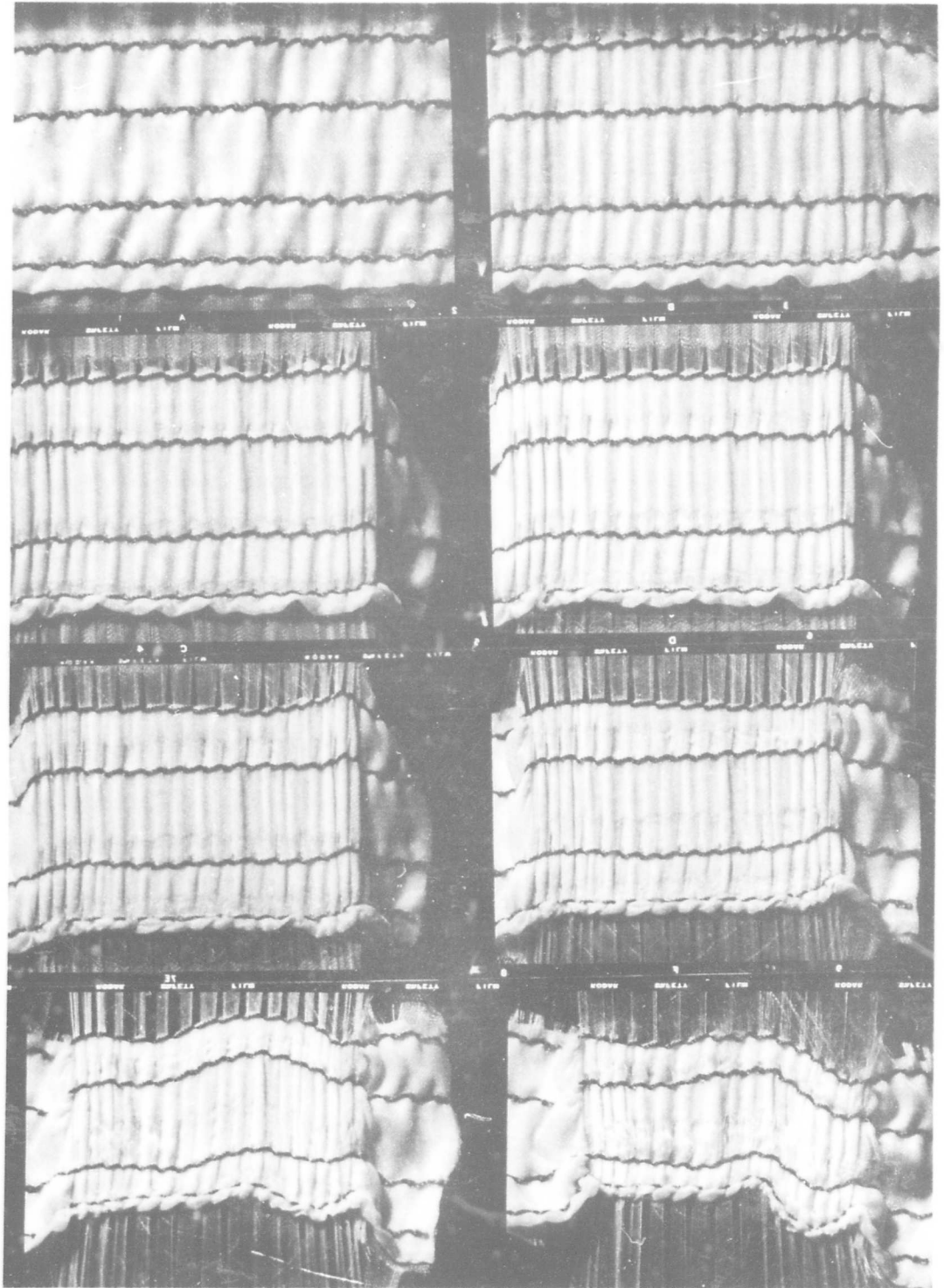


Figure F-4. - Photographic History of Seam Failure

SECTION G  
THE MITEK IMPACT TESTER

As a part of the QM Impact study at M.I.T., a new impact testing instrument has been designed, constructed, checked out operationally and delivered to the QM Laboratories in Natick. Titled the MITEK Impact Tester, the instrument operates on a pneumatic-hydraulic system with the specimen being pulled by a rod attached to the main cylinder piston. The load cell is a piezzo electric type and registers load increases via voltage output to an oscilloscope screen. The strain reading on the specimen is accomplished by attaching a premarked magnetic tape either to specimen or to lower jaw and registering its movement through a recorder head which shows the passing of premarked tape peaks as impulses on the scope screen.

Velocity of the tester can be adjusted from 1 inch per second to 20 feet per second. The load capacity of the unit is set at 500 lbs. The lower jaw movement is restricted to 8 inches and the sample length is made adjustable through use of a screw jack at the head of the instrument.

A block diagram of the instrument is shown in Figure G-1. A brief description of the parts is provided below. The panel diagram of the tester is shown in Figure H-1. The instrumentation block diagram is shown in Figure G-2, and the wiring diagram of the control switches in Figure G-3. The assembly drawing of the MITEK tester is provided in Figure G-4. A sub-assembly showing the structural elements of the tester and the oil reservoir made at M.I.T. is given in Figure G-4a. The numbered parts in Figure G-4a are detailed in Figures G-5 to G-15 inclusive. All other parts of the instrument (excluding the cabinet housing) were

commercially produced and purchased on the open market. Only the main driving cylinder required a slight modification in porting with respect to the standard 2" bore cylinders produced by the manufacturer. A list of major parts and components, both hydraulic and electrical is included in Section H.

A series of check tests on the instrument showed the displacement-time relationship to be linear within  $\pm 5\%$ . A typical set of tests under two conditions of operating pressure (360 psi and 200 psi) is shown in Figure G-5.

The MITEX tester operates on the principle of pressuring two sides of a piston -- one side pneumatically (nitrogen), the other side hydraulically (viscosity 100 - 200 SSU at 100°F). The piston rod supports the low instrument jaw. The upper instrument jaw is supported on a screw jack as pictured in Figure G-4. Upon mounting of the specimen and adjustment of the strain measuring tapes the test system can be activated with the following steps. The pneumatic pressurized side of the piston is connected with the main pressure reservoir and this connection remains open during the test. The hydraulic fluid side is suddenly ported via a large hand operated valve and the fluid is permitted to exhaust into the oil reservoir. (This reservoir is about half filled, and the air above the oil is at atmospheric pressure at the beginning of the test).

The port of the cylinder serves as a large orifice which meters the fluid flow in accordance with the pressure drop across its faces'. The use of the large nitrogen reservoir assures full movement of the piston with no more than 5% reduction in the pneumatic driving pressure. Thus with essentially constant pressure across the orifice, the hydraulic fluid flow provides constant piston velocity within the desired limits. The mass of

piston and oil reach constant velocity after approximately one inch of free running. Provision of sample slack permits testing in the constant velocity range of the stroke. The last inch of stroke introduces deceleration as the cushioning is engaged.

Upon completion of the test the upper chamber of the cylinder is closed off from the main nitrogen reservoir and it is then exhausted to the atmosphere. The gas pressure above the oil in the oil reservoir is then built up slowly to force the piston back to its starting position for a new test.

IT SHOULD BE EMPHASIZED THAT EVERY PRECAUTION AND DESIGN HAS BEEN INCLUDED IN THIS APPARATUS TO MAKE IT A SAFE EFFICIENT IMPACT TESTING INSTRUMENT FOR TEXTILES BUT THE HIGH PRESSURES AND HIGH SPEEDS INVOLVED IN ITS OPERATION MAKE IT ESSENTIAL THAT THE EQUIPMENT BE HANDLED ONLY BY TECHNICALLY TRAINED AND SAFETY CONSCIOUS PERSONNEL.

Brief Description of Components of the Pneumatic Hydraulic System of Figure G-1

(with pertinent comments on operational aspects)

Cylinder: 2" bore with enlarged ports. Cushioned on blind end only. Stroke 8". Cushioning can be adjusted. No maintenance.

Hand Valve (R): 1½" hydraulic valve. Spool type, designed for medium viscosity fluids. No oil in valve results in gas leakage in any valve position. The spool is machined to close tolerance ( $10^{-4}$  in.) and if it is removed from the body it should be handled with care to insure that surfaces are not damaged.

Needle Valve (N-1): Flow control needle valve. Adjustment of this valve sets the return speed of the piston or the down

stroke speed.

Oil Reservoir: Four inch diameter tubing with two caps sealed with a "O" ring. Half full oil level in this reservoir should be maintained. Periodic check is required. Do not fill too much. Filling plug on top.

Nitrogen Reservoir: Steel cylinder rated at 2000 psi.

Solenoid Valves (1-4): Two way  $\frac{1}{2}$ " normally closed 110 VAC. (occasionally these valves can get stuck and stay open. Should this happen they can be cleaned by blowing gas through in an open-close operation, or by disassembling the internal parts. Lines do not have to be disconnected. When the two hexagonal nuts are removed plungers and seats can be removed for cleaning. Special tool is required (supplied). Before disassembling be sure that there is no pressure across the solenoid valve.

Needle Valve (N-2):  $\frac{1}{2}$ " flow control valve. This valve is used to reduce gas flow to solenoid valve (1) and (3) to allow fast exhaust of solenoids (4) and (2). Thus the inflow is always exceeded by the outflow to the cylinder of oil reservoir. This valve also can be used as a shutoff valve.

Ball Valve (J): Pneumatically operated  $\frac{1}{2}$ " valve. The slot in the valve shaft indicates open and closed position. Handle is supplied for manual operation. Four way solenoid valve (5) operates this valve.

Oiler: Literature supplied.

Pressure Regulators: One pressure regulator located under right upper side panel is adjusted to 125 psi. This pressure level should not be readjusted to a higher one. Second regulator located on high pressure gas supply cylinder is adjustable **BOTH OF THESE REGULATORS MUST NOT BE USED WITH GAS OTHER THAN NITROGEN.**

Pressure Reliefs: The pressure relief valve which is adjusted to 300 psi is located under right upper side panel. This valve is a safety device and therefore THE TESTER MUST NOT BE OPERATED WITHOUT THIS VALVE. Second relief valve is located on the oil reservoir. The latter relief pressure is adjusted to 200 psi. It can be used for oil discharge.

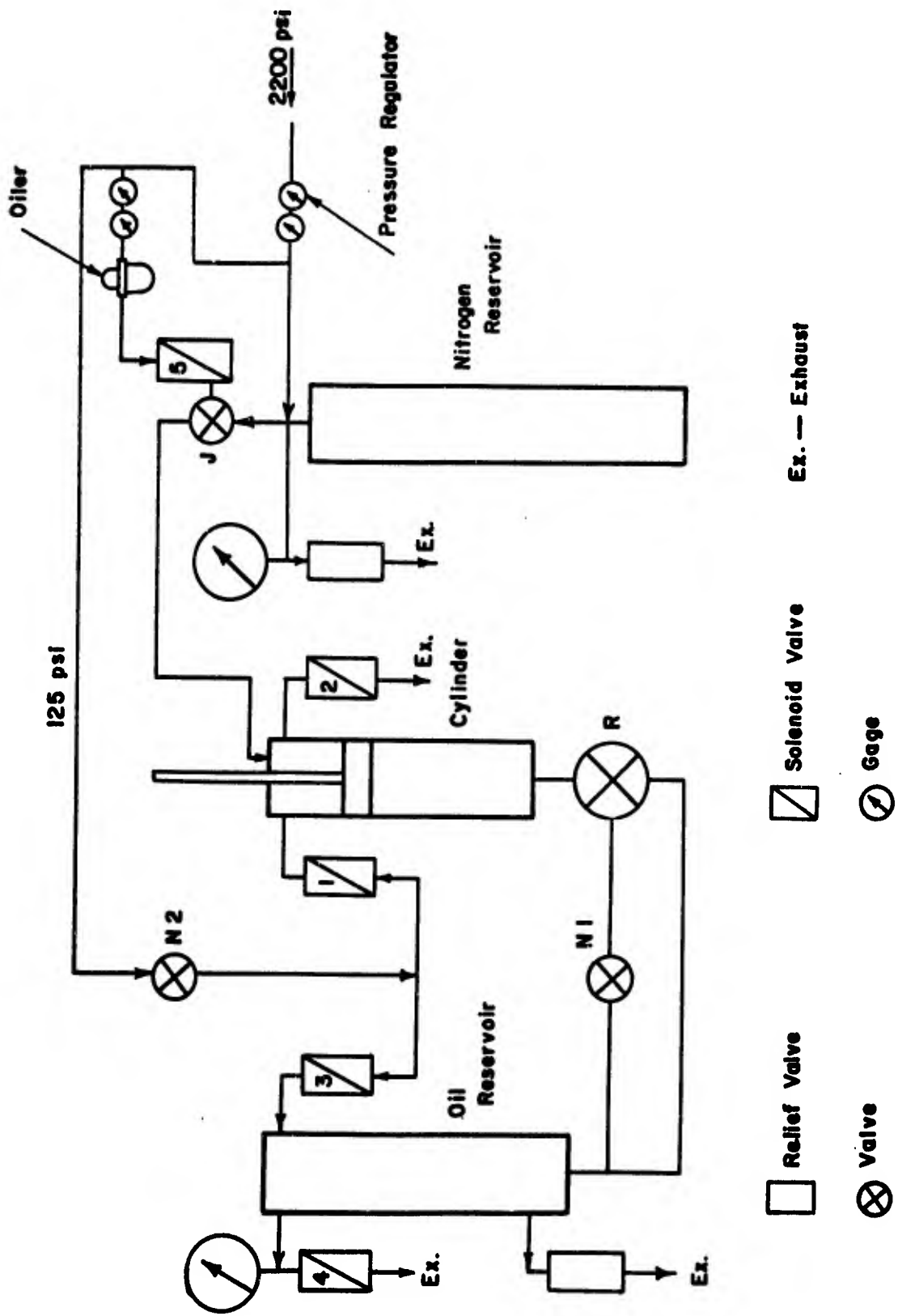
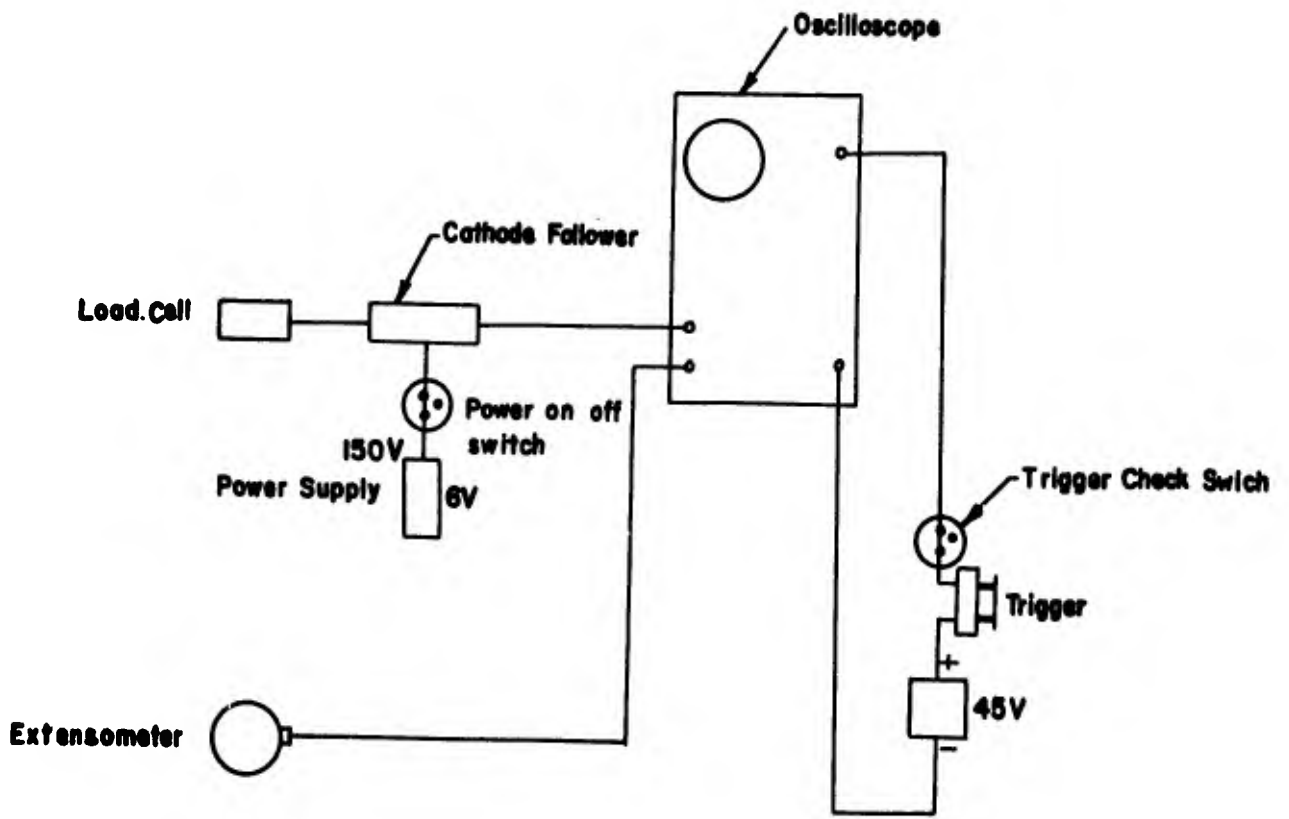
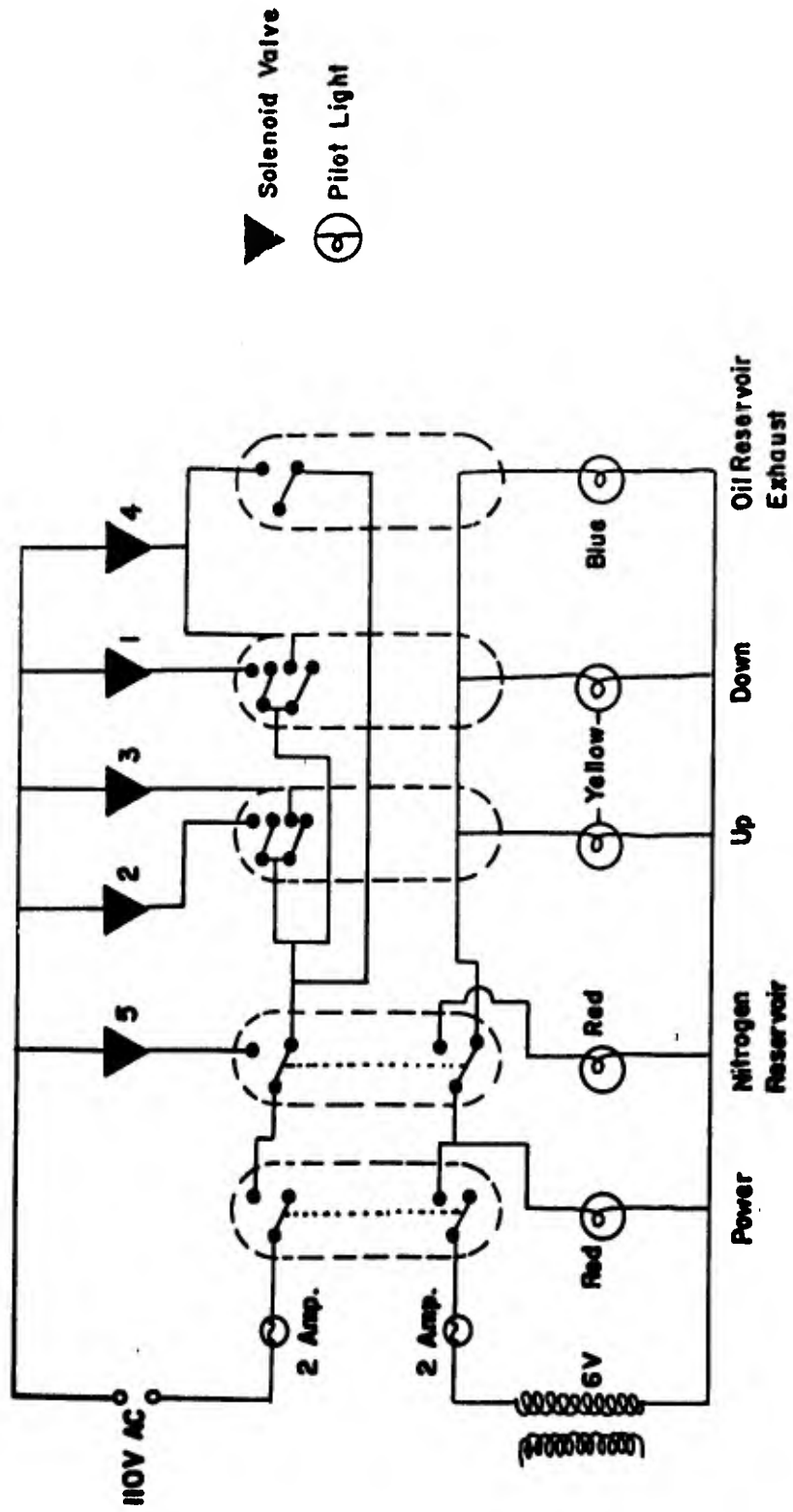


Figure: G-1. Schematic of MITEX Impact Tester.



**Figure: G-2. Instrumentation Block Diagram for MITEX Impact Tester**



**Figure: G-3. Wiring Diagram of Control Switches of MITEX Impact Tester**

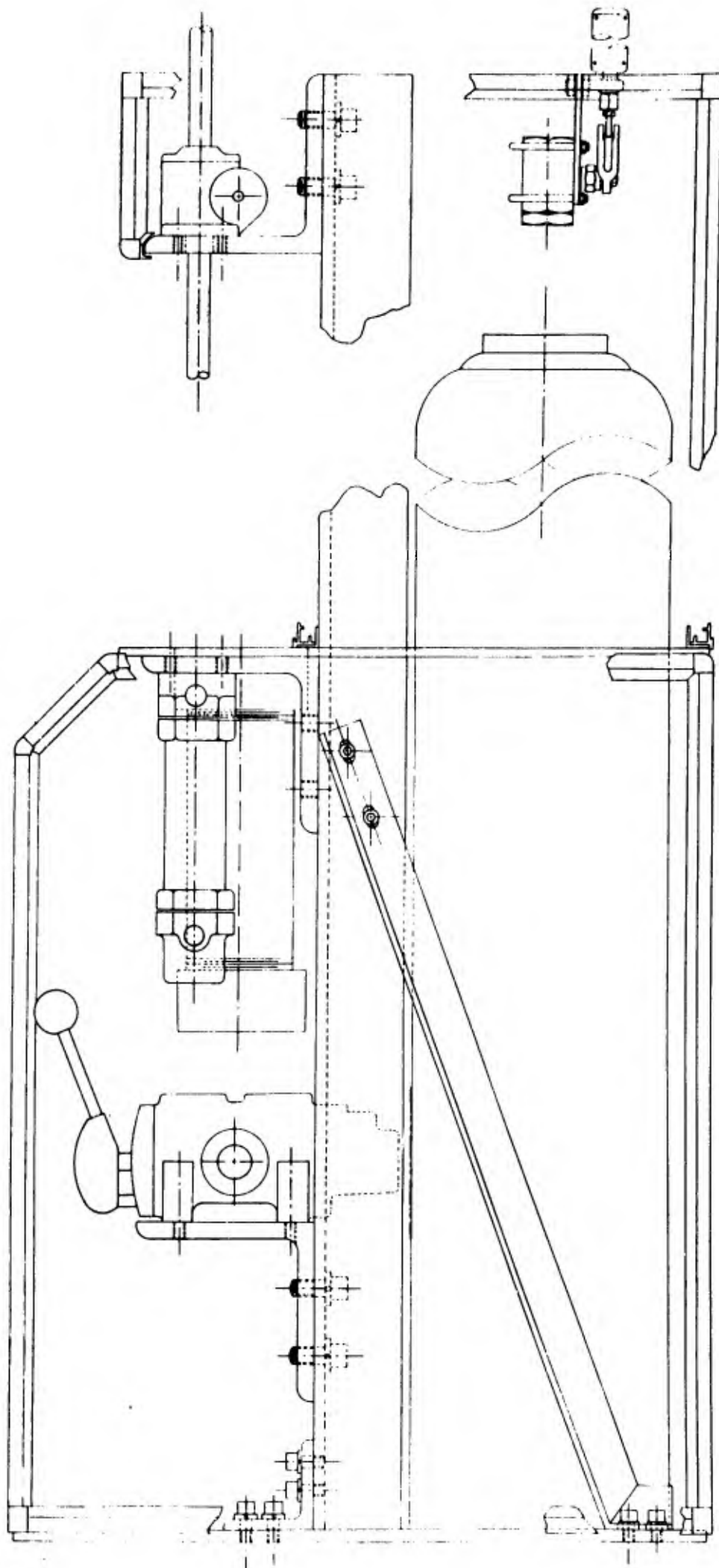


Figure G-4. Assembly of MITEX Impact Tester.

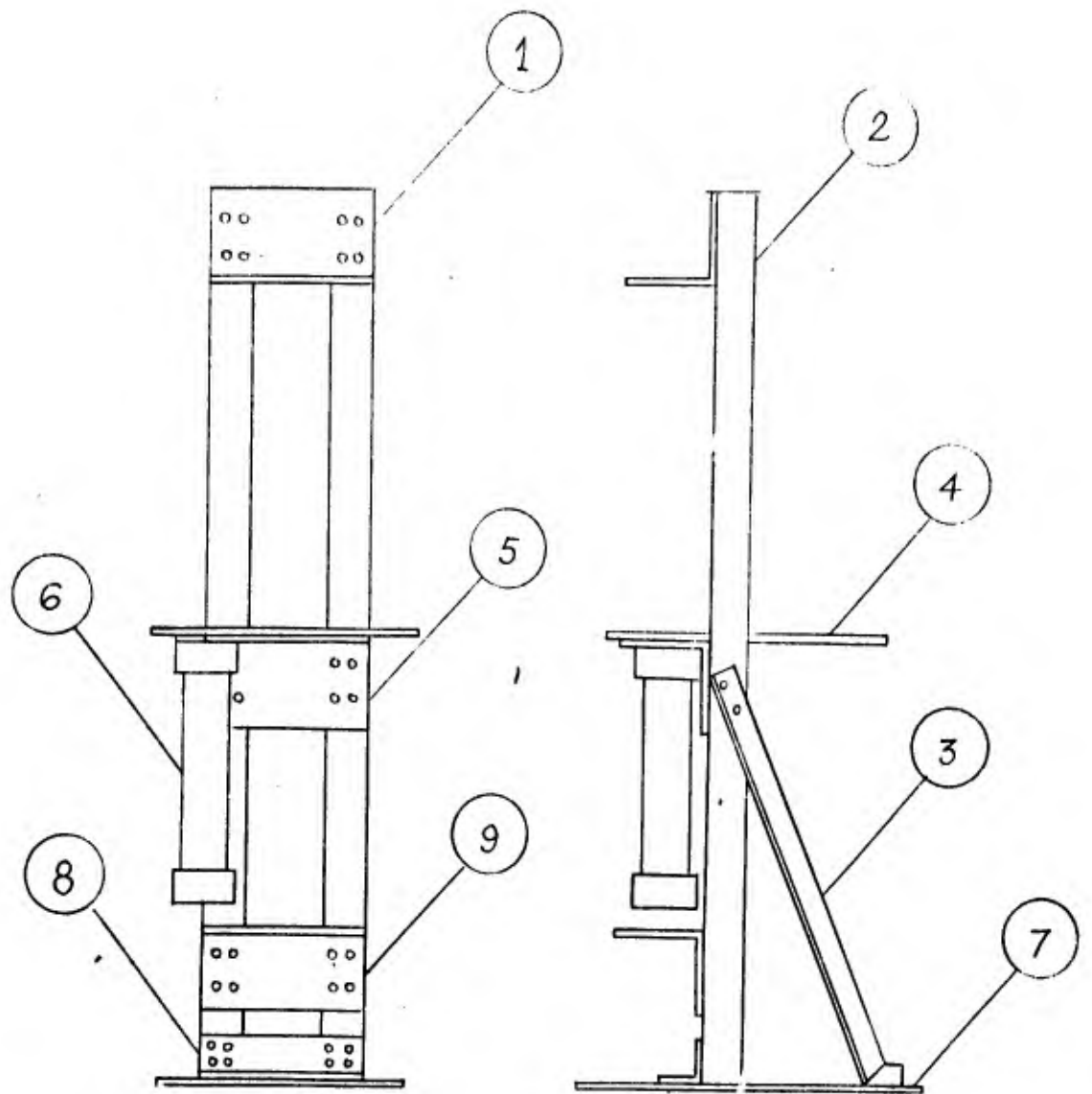


Figure: G-4a. Structure of MITEX Impact Tester

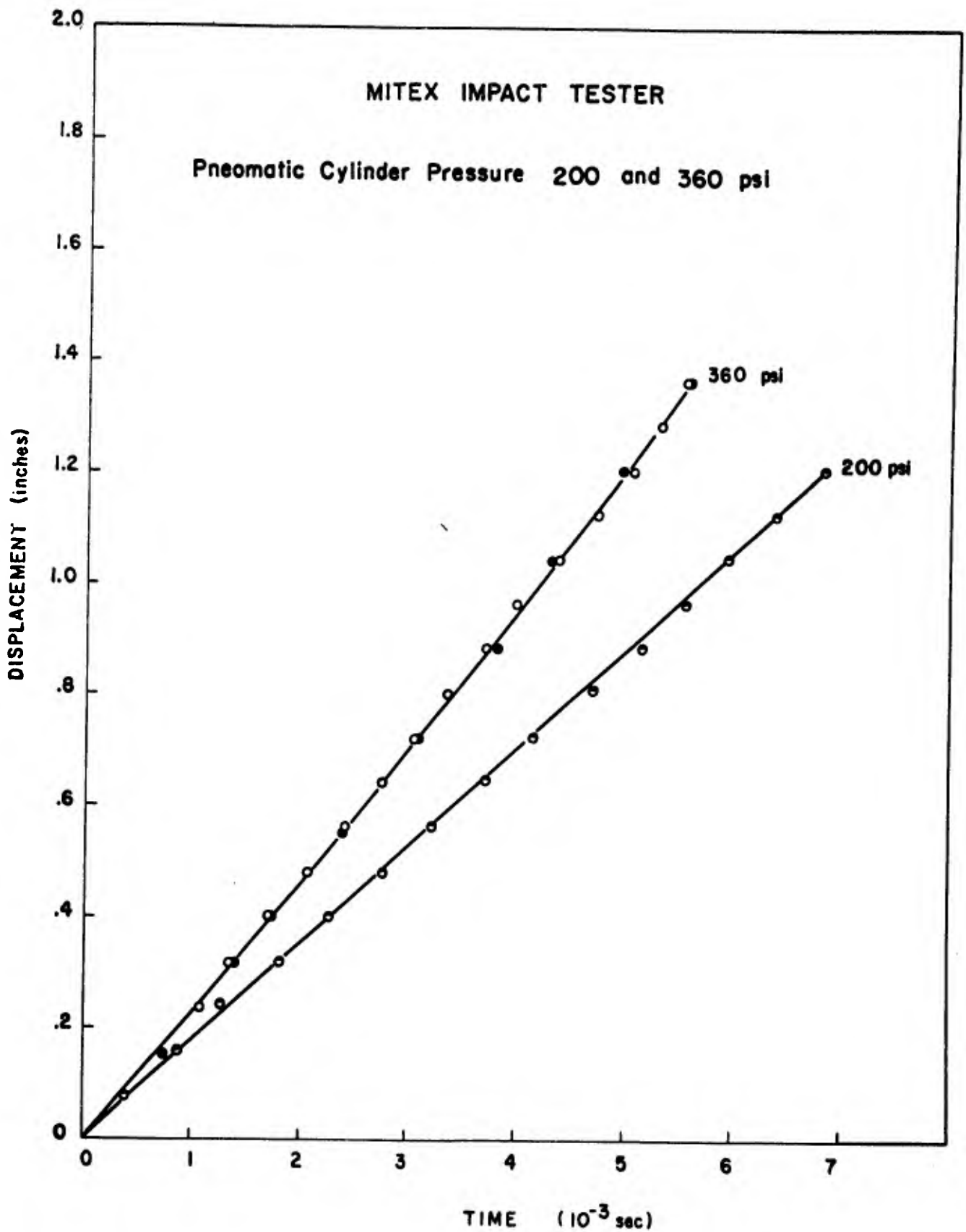


Figure: G-5. LOWER JAW DISPLACEMENT AS FUNCTION OF TIME.

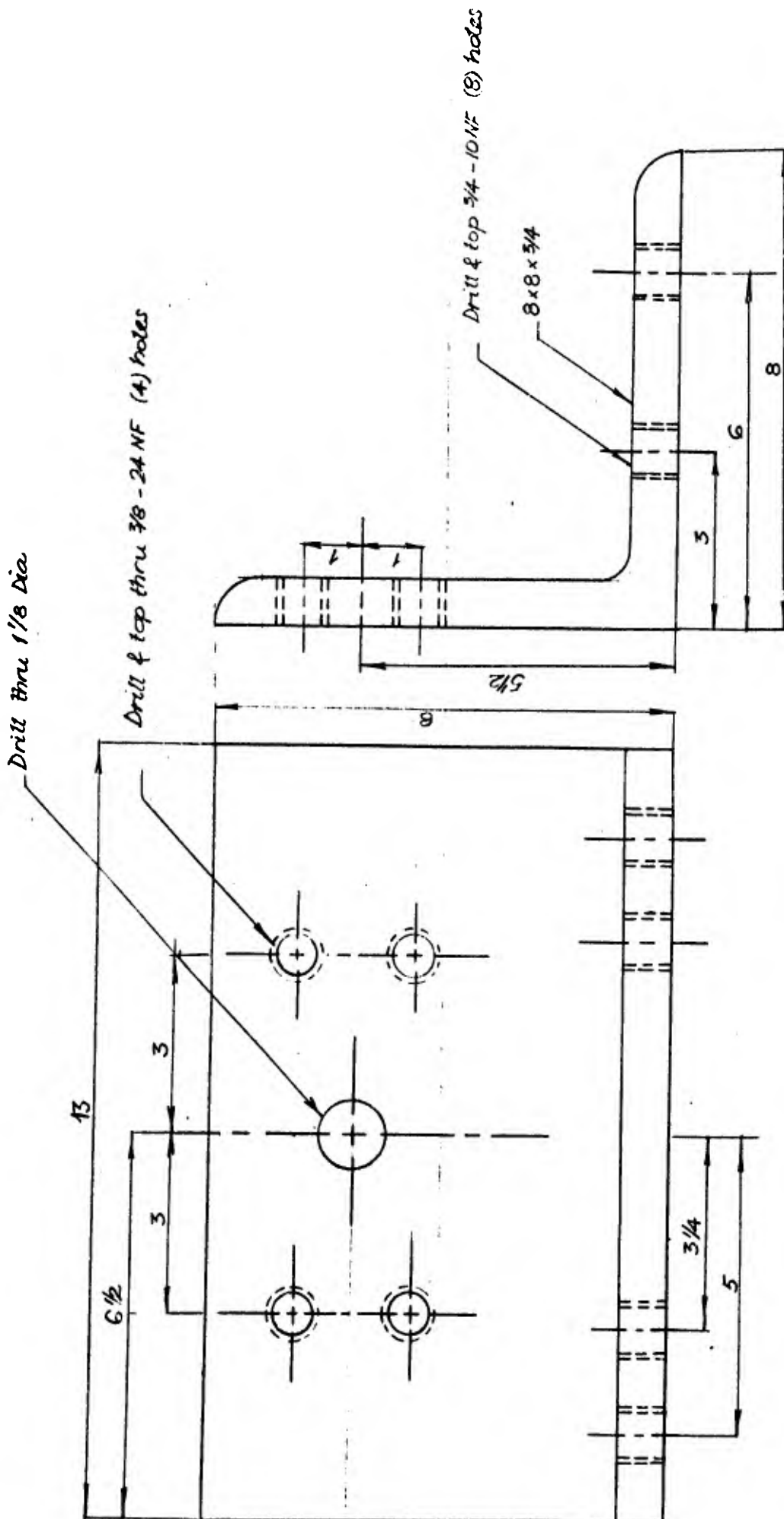


Figure: G-6. MITEX Impact Tester Part 1.

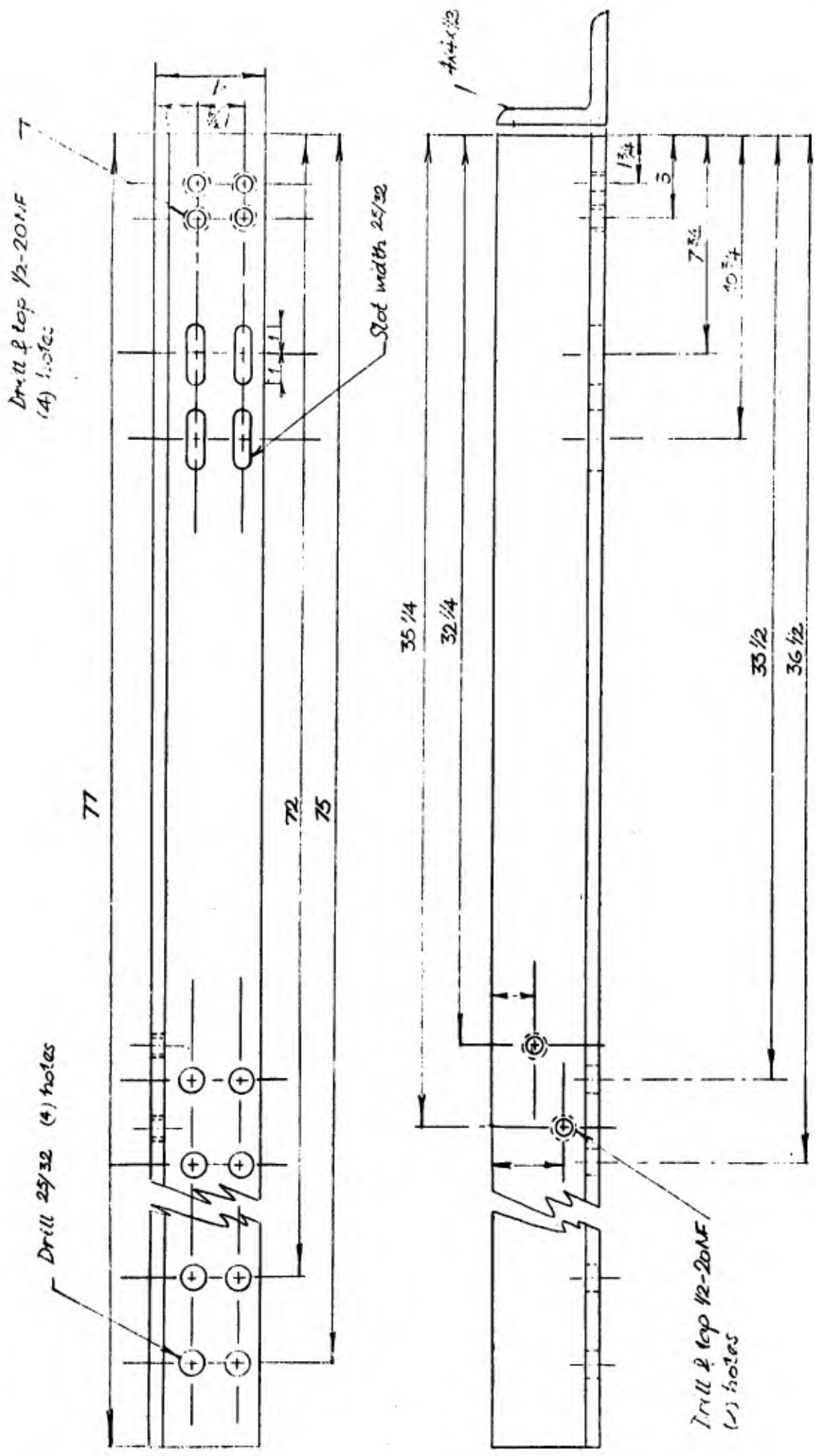


Figure: G-7. MITEEX Impact Tester Part 2.

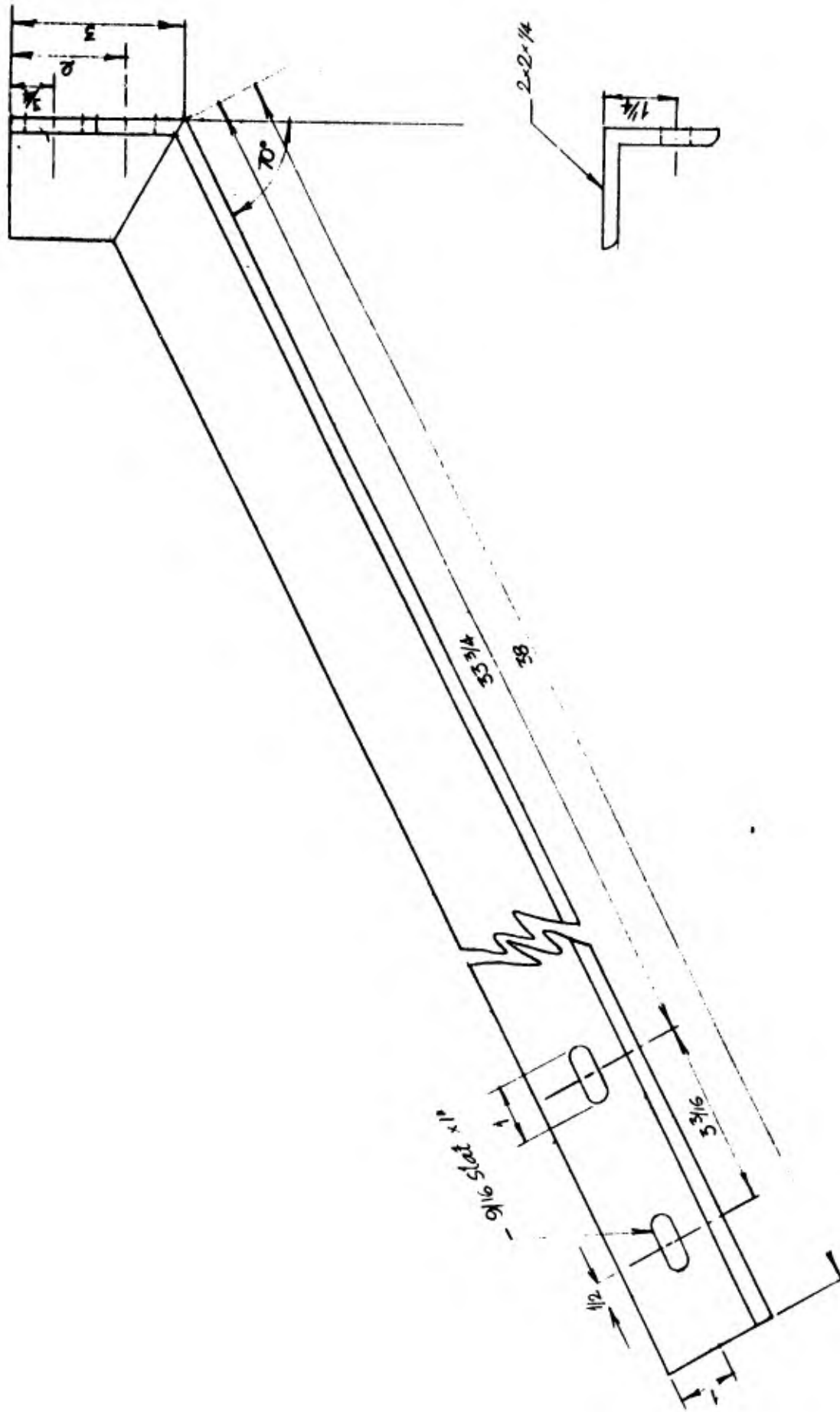


Figure: C-8. MITEX Impact Tester Part 3.

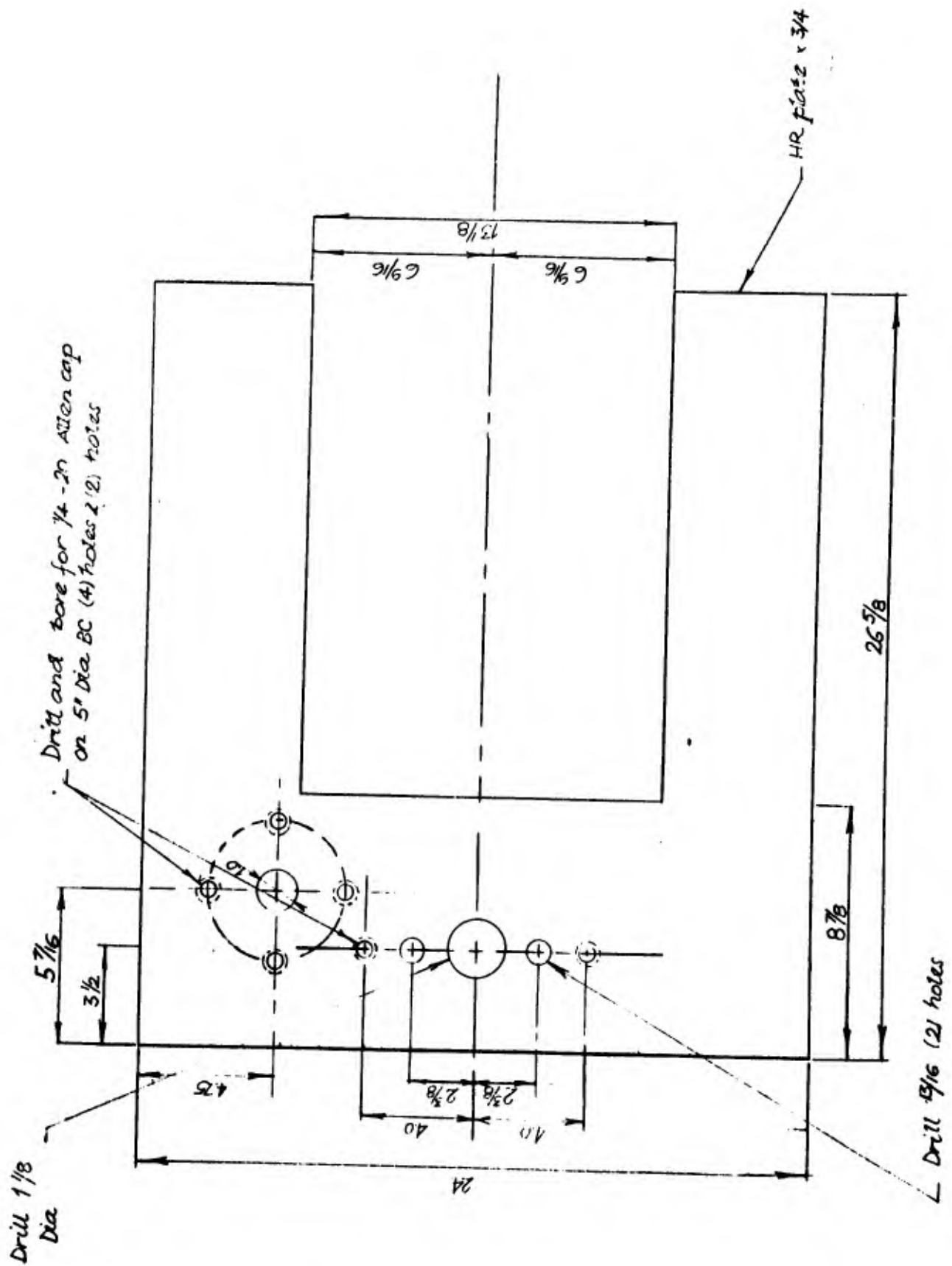


Figure:G-9. MITEX Impact Tester Part 4.

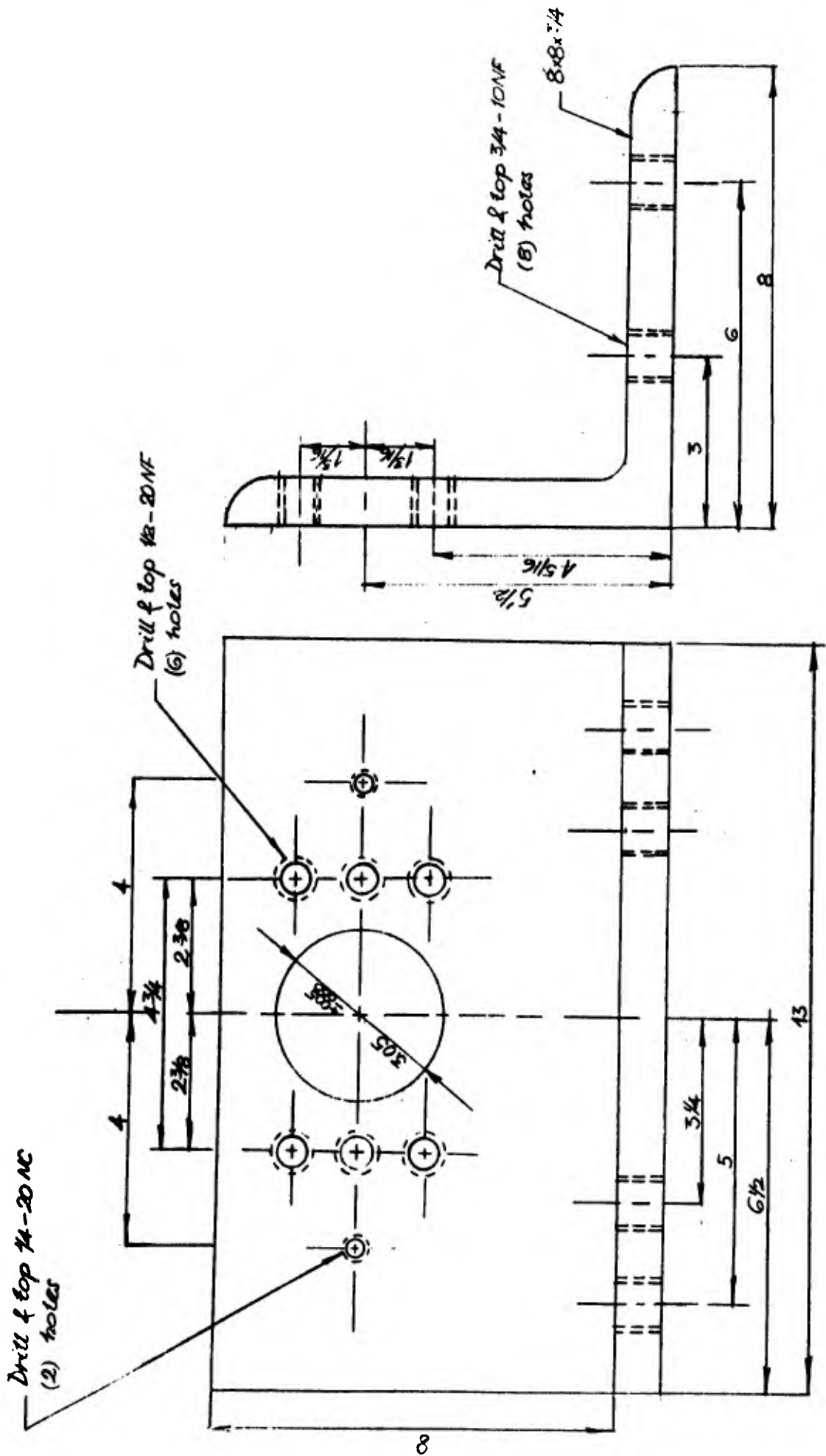


Figure : G-10. MITEEX Impact Tester Part 5.

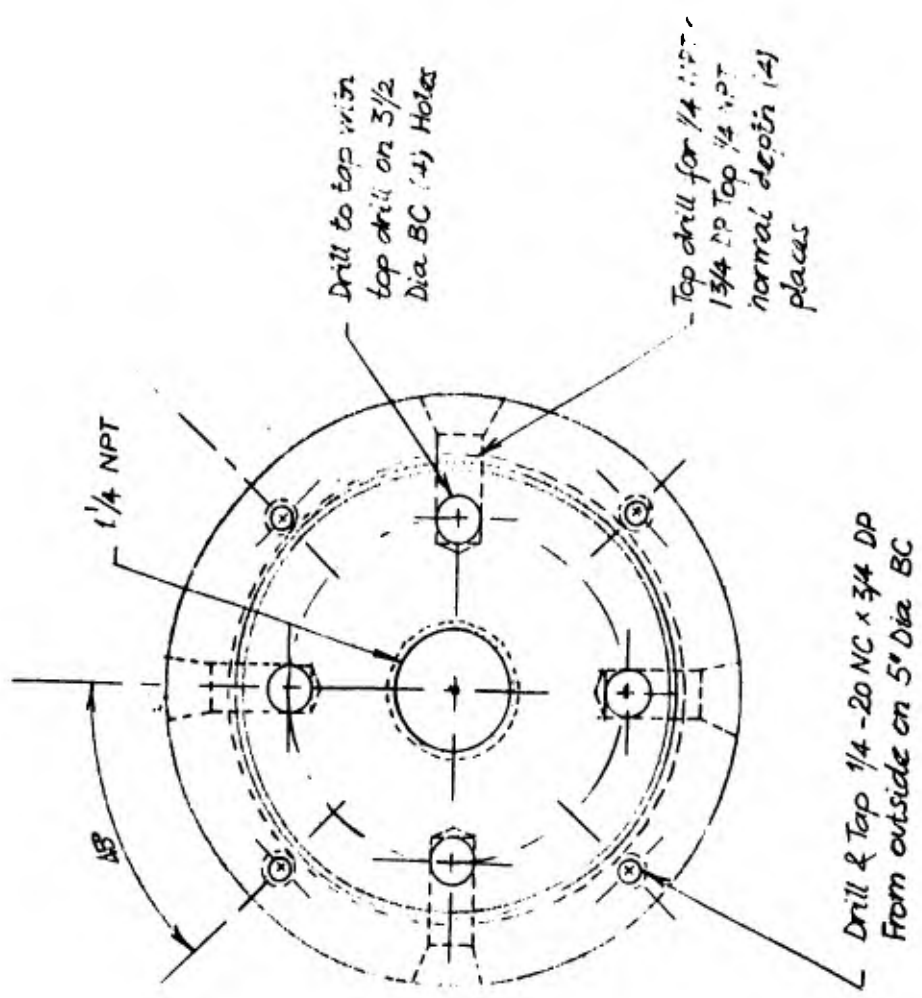
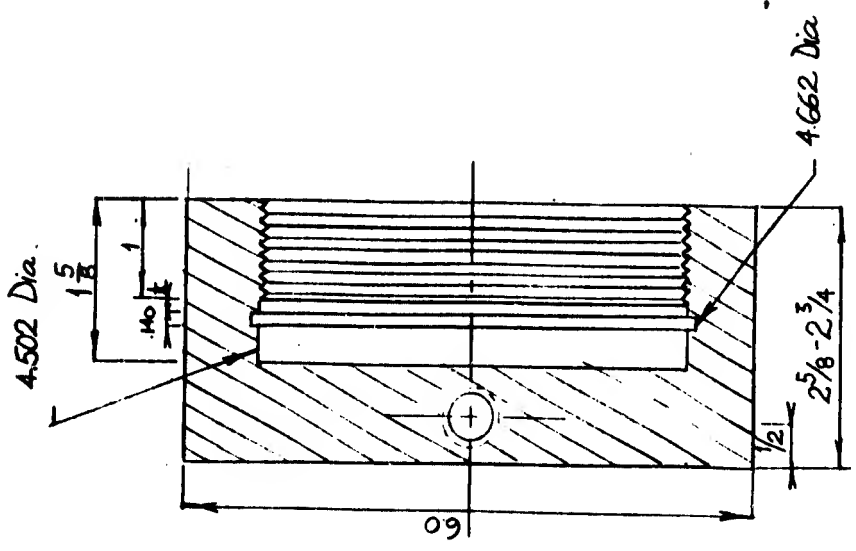


Figure G-11. MITEK Impact Tester Part 6a

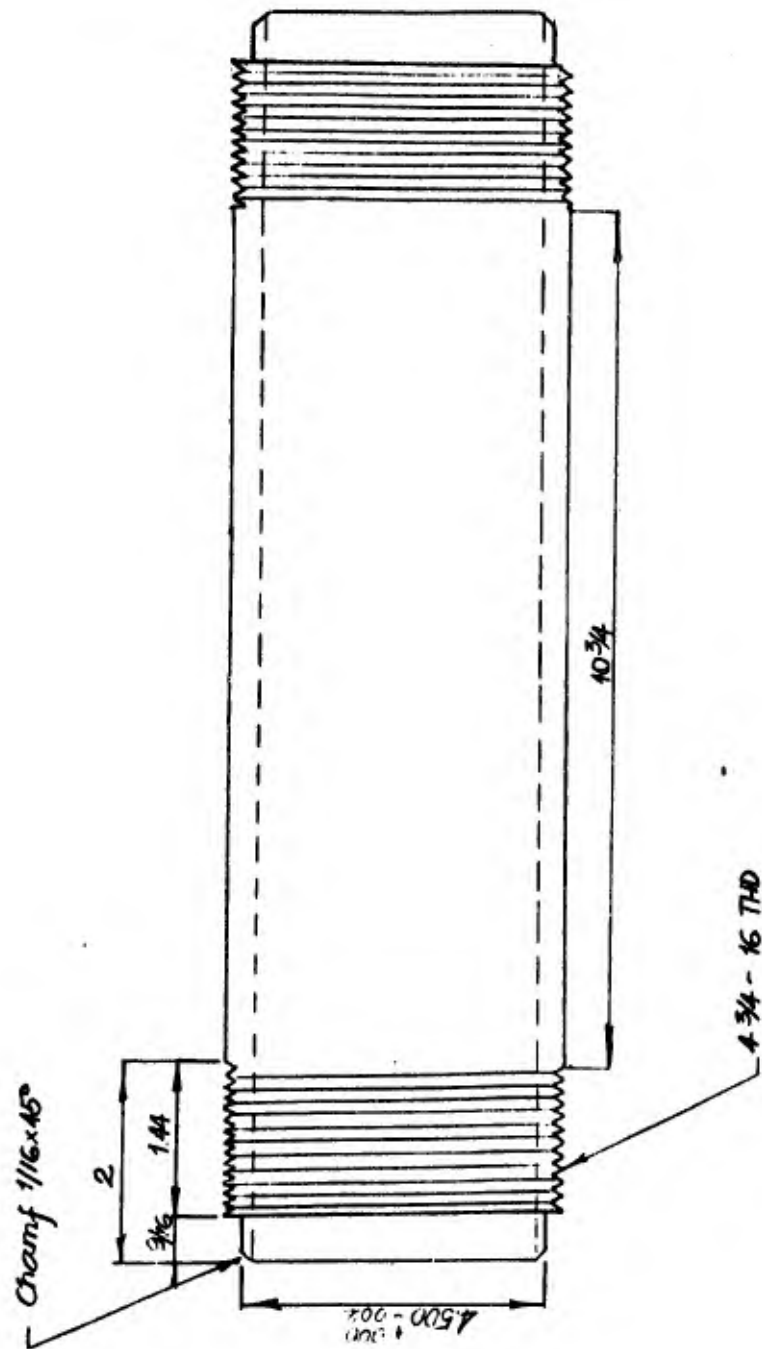


Figure: G-12. MITEX Impact Tester Part 6b.

7

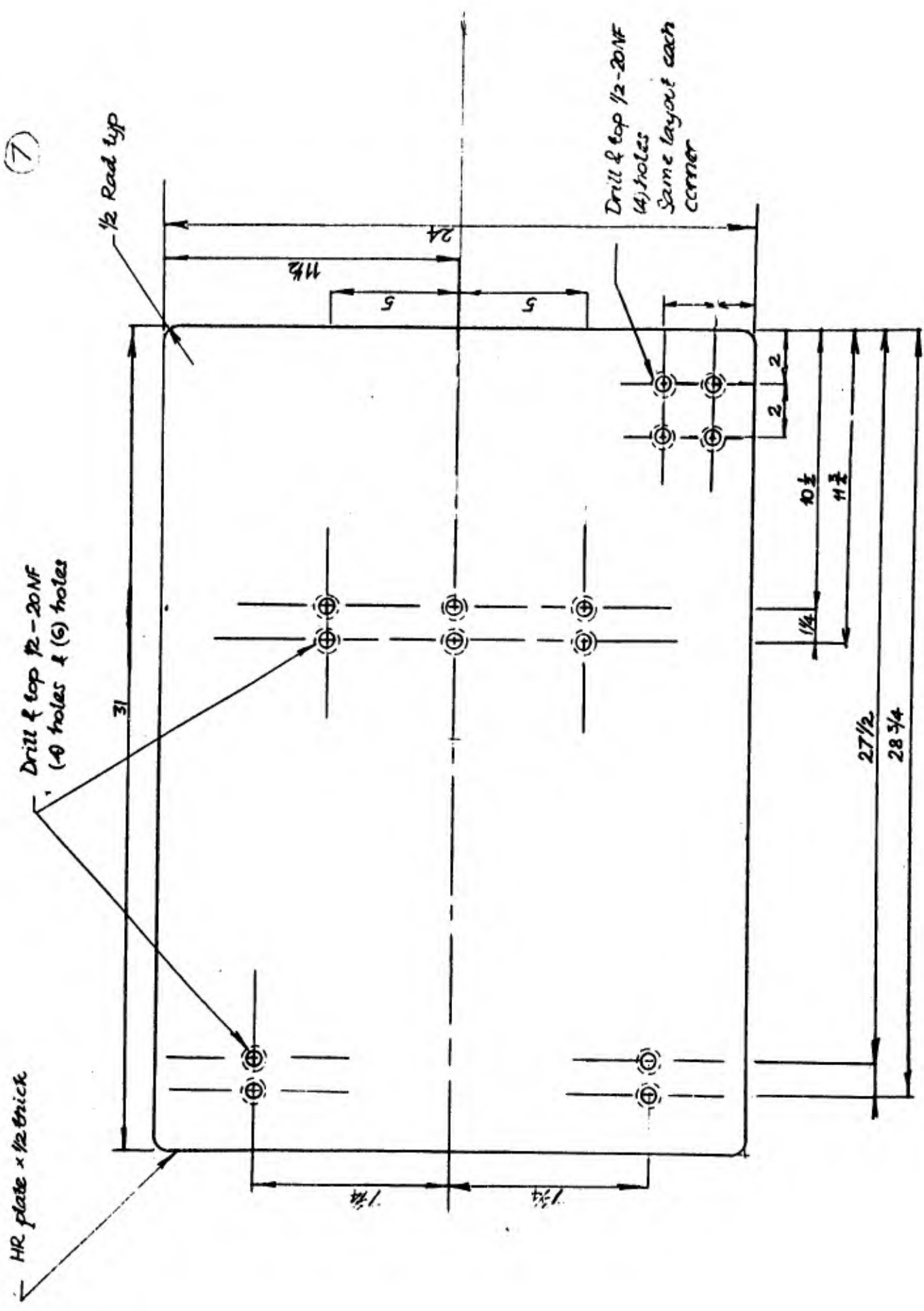


Figure: C-13. MITEEX Impact Tester Part 7.

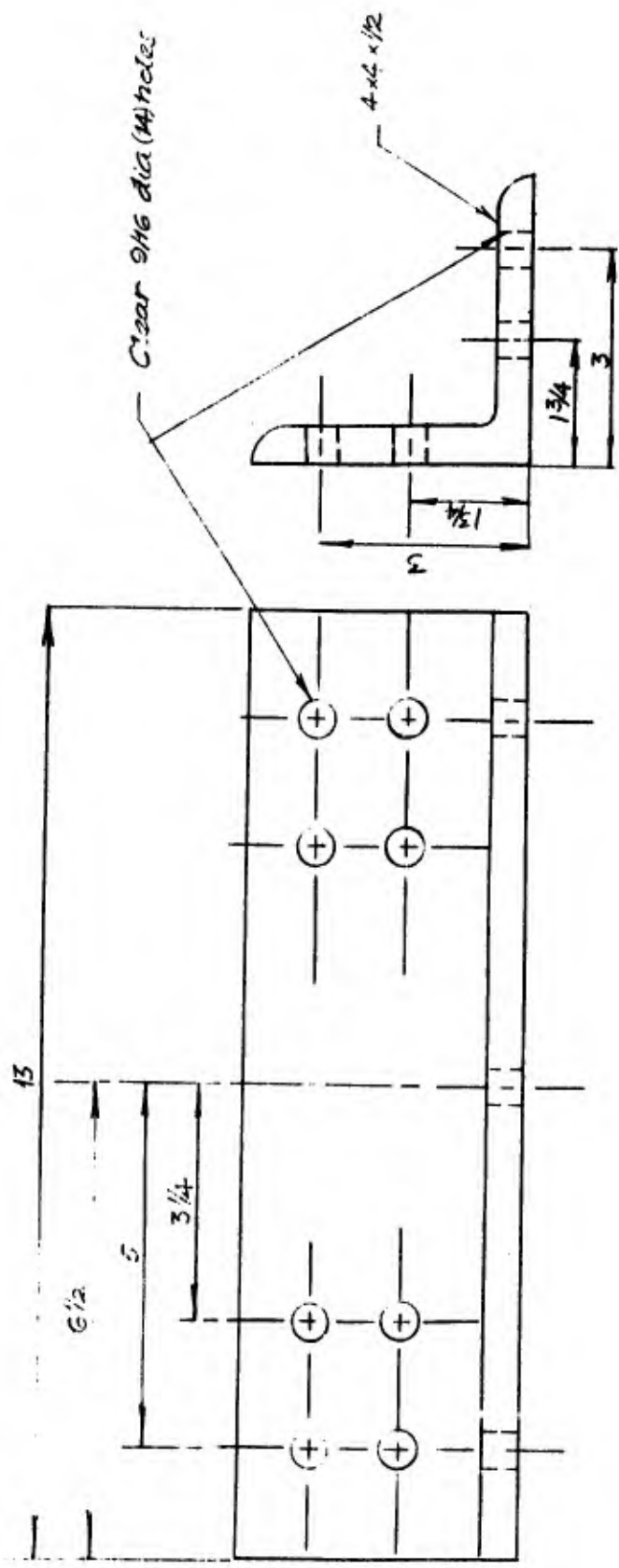


Figure: G-14. MITEEX Impact Tester Part 8.

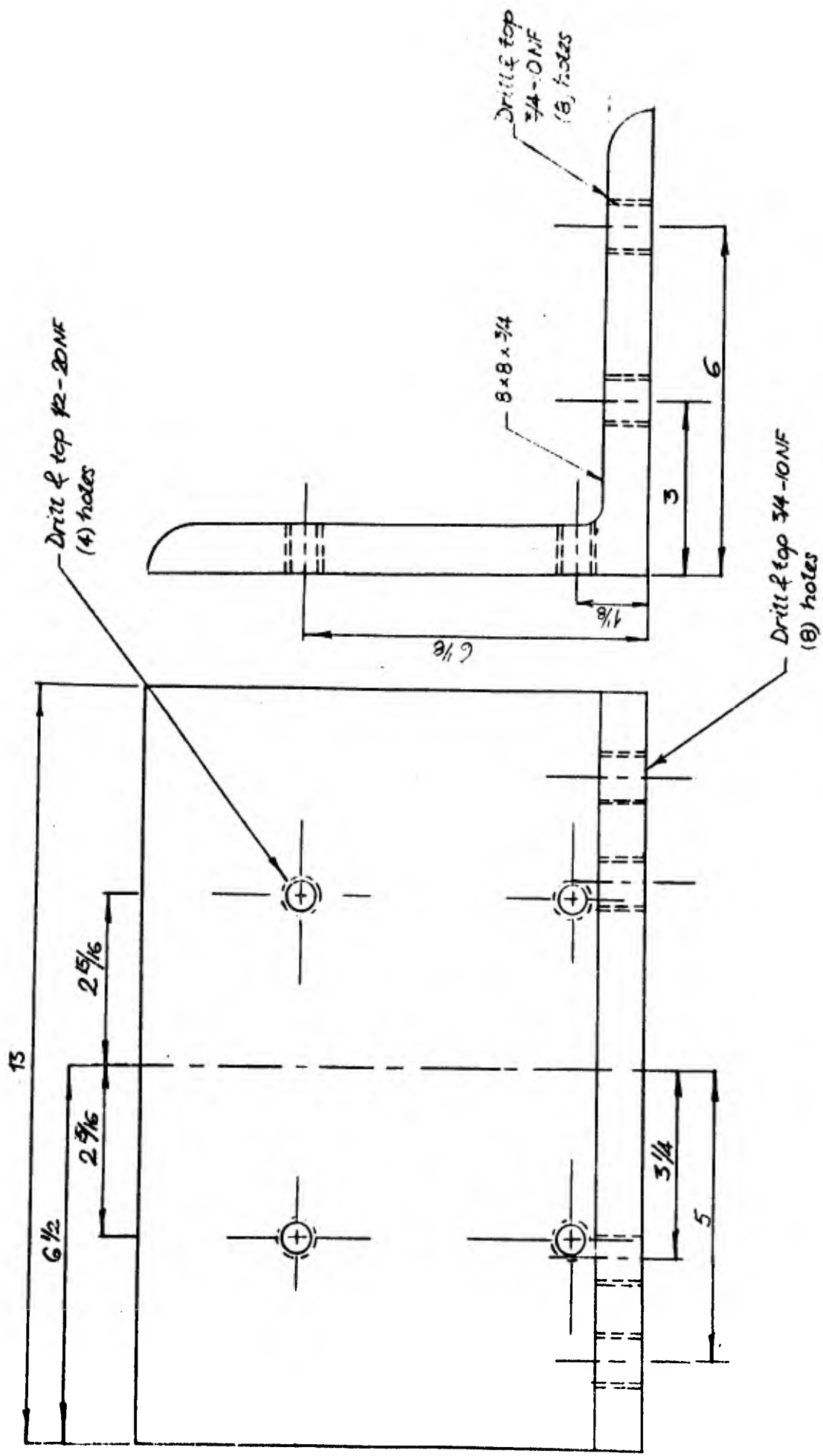


Figure: G-15. MITEEX Impact Tester Part 9.

## SECTION H

### OPERATIONAL INSTRUCTIONS FOR THE MITEX CYLINDER IMPACT TESTER

1. Connect high pressure nitrogen bottle to the tester (Right lower panel. Ball disconnect)
2. Turn green valve on the top of the gas reservoir counter clockwise to an angle of approximately 20-30°. (Valve can be reached from the top of the tester.)
3. Set main valve to its neutral position, which is the center position of the valve handle travel. (Front panel recess.)
4. Connect 110 V AC line to plug. (Lower left panel. Upper left corner.)
5. Press power switch. The pilot lights will come on. From left to right the following lights should be on: red, two yellow and blue. Should this color sequence be red, blue, red, press the second red button and the correct switching arrangement should result. (Power switch is the second red switch from left on the front sloping panel.)
6. Charge gas reservoir. Open main valve on high pressure nitrogen bottle. Turn regulator valve clockwise until steady hissing noise is heard. DO NOT LEAVE THE TESTER UNATTENDED DURING CHARGING OPERATION. The left pressure indicator on the regulator does not indicate the final reservoir pressure. It shows only the actual pressure at the gage pressure connection. The regulator valve can be adjusted to the required pressure only when this pressure is reached initially in the reservoir. Fine adjustment of regulator is accomplished in the following manner. First when the required reservoir pressure is reached (the gage on the right on the front panel is provided for this purpose) the regulator valve (brass) is closed (turn counter clock-

wise until no hissing is heard) and then the main valve of the nitrogen cylinder is also closed. The regulator gage on the right side indicates the pressure in the supply cylinder. When both valves are closed it will continue to point to the pressure level reached prior to valve closing. No pressure drop should be observed on this gage. Now the regulator valve should be slowly turned clockwise until the right supply bottle gage starts showing a decrease of pressure. At this point the direction of valve turning should be reversed until no drop in pressure is observed. The main supply cylinder valve should then be opened. The pressure is now adjusted to the level indicated on front panel gage.

7. Turn yellow valve handle twice around (Right lower panel).
8. Push main valve to back position (Front panel recess).
9. Press down and hold upper yellow switch until piston rod reaches its top position. Approximately 70-100 psi pressure will be indicated on oil reservoir gage (second gage on front panel from the right).
10. Set main valve to its neutral position.
11. Mount sample.
12. Set trigger and extensometer tape.
13. Press down red switch on the extreme right. The two yellow pilots will go off and hissing of the gas reservoir solenoid will be heard. Red light of this switch will come on and stay on.
14. Press blue switch down and wait for oil reservoir pressure to reach zero.
15. CHECK INSTRUMENTS, SWITCHES, AND GAGES.
16. In a rapid motion pull main valve to its front position.
17. Place main valve into neutral.
18. Switch off right red switch (Close gas reservoir).
19. Repeat 8)9)10)11)12)13)14)15)16)17)18).

20. Close both valves on high pressure supply.
21. Switch off power (Second red switch from left).

#### IN EMERGENCY

1. PRESS DOWN BLUE AND BOTH YELLOW SWITCHES SIMULTANEOUSLY.  
ALL EXHAUSTS WILL OPEN.
2. SHOULD A SOLENOID VALVE STICK FOLLOW (1).

#### CAUTION

DO NOT REMOVE LOWER LEFT, LOWER RIGHT, AND BOTH FRONT PANELS WHEN POWER IS CONNECTED TO THE TESTER.

WHEN LOWER PANELS (EXCLUDING BACK PANEL) HAVE TO BE REMOVED

REMOVE LARGE FRONT PANEL FIRST. DO NOT TOUCH THE SLOPING PANEL FROM UNDERSIDE. DISCONNECT 150 V AND 6 V BATTERIES. REMOVE REST OF PANELS AND DISCONNECT 45 V BATTERY.

OPERATE TESTER WHILE SITTING DOWN AT OSCILLOSCOPE - MAKE THIS A RULE.

#### SUPPLIES

##### HYDRAULIC:

High pressure hoses  $\frac{1}{2}$ " 2-wire braid  
Low pressure hoses  $\frac{1}{2}$ " 44 FN  
Steel tubing  $\frac{1}{2}$ ",  $\frac{3}{4}$ " and  $1\frac{1}{2}$ "  
Hand valves needle  $\frac{1}{2}$ "  
Solenoid Valves  $\frac{1}{2}$ " Skinner RZH DB2 1252  
Ball valve  $1\frac{1}{2}$ " Jamestury  
Spool valve  $1\frac{1}{2}$ " Rivett 5170- $1\frac{1}{2}$ "  
Cylinder Rivett 251-CB-PP-SS-2" x 8" special  
Relief valve 600 psi 51595-ZMP-600  
Relief valve 90-300 psi  
Lubricator Norgren #30-41-21

Hydraulic Engineering Co.  
2 Blanche Street  
Cambridge, Mass. UN 4-7922

**ELECTRICAL:**

Switches Microswitch Series 2 (2)

Cables small: Microdot (1)

Amphenol (2)

Connectors: Microdot and Amphenol

(1) Electrical Supply Corp.  
205 Alwfe Parkway  
Cambridge, Massachusetts

(2) Cramer Electronics  
811 Boylston Street  
Boston, Massachusetts

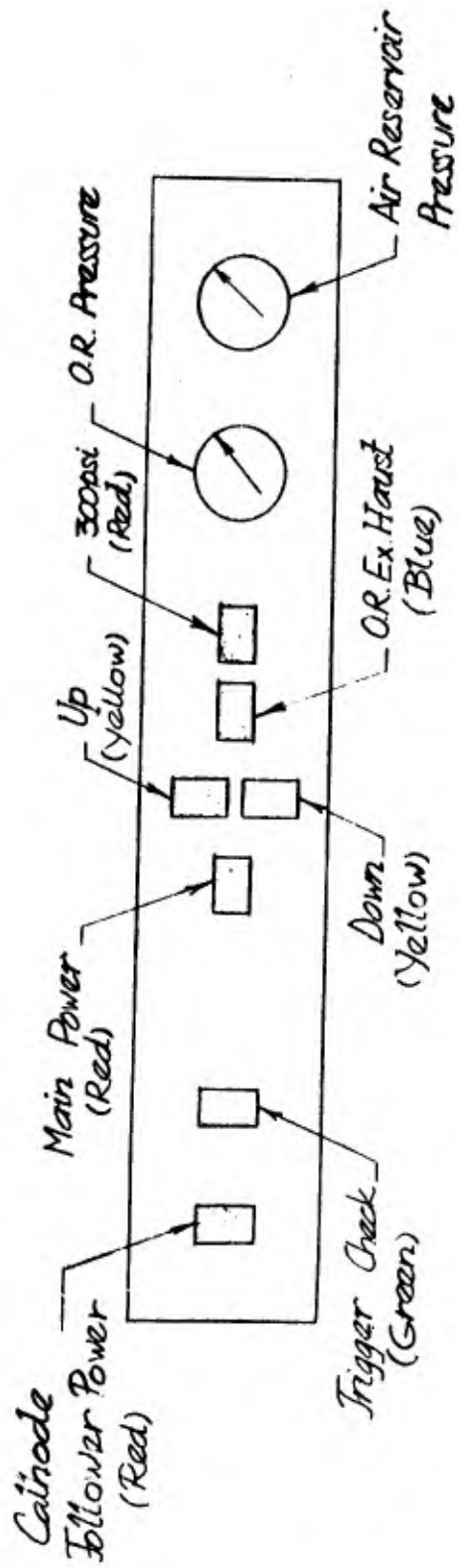


Figure H-1. Panel of MITEK Impact Tester

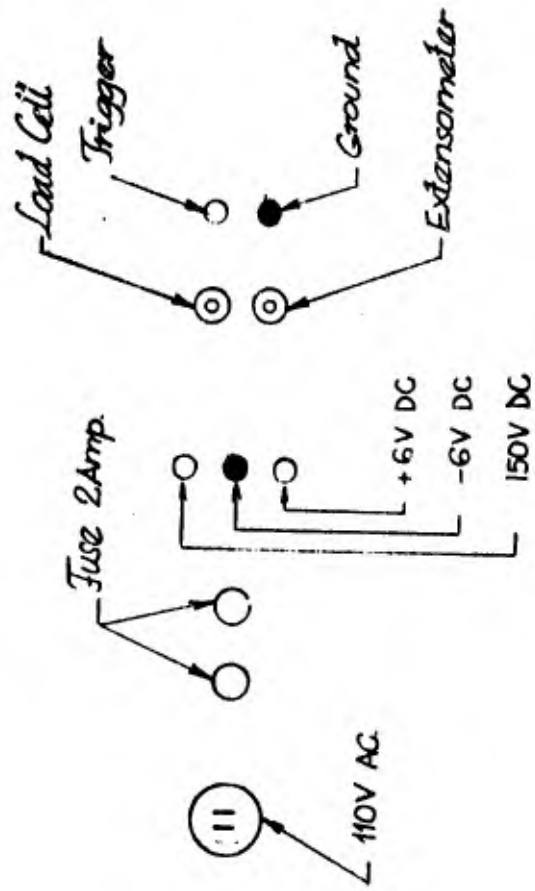


Figure H-2. Left Side Panel Outlets  
MITEX Impact Tester

<p>UNCLASSIFIED</p>	<p>TEXTILE DIVISION, MASSACHUSETTS INSTITUTE OF TECHNOLOGY, Cambridge, Mass. DYNAMIC TESTING OF SMALL TEXTILE STRUCTURES AND ASSEMBLIES by J.G. Krizik, D.M. Mellien, S. Backer, January 1961. 106p. incl. figs. and tables. (Project 7-93-18-019) (Contract No. Da-19-129-QM-1308)</p> <p>Unclassified Report</p> <p>Reports a study of the high (over)</p>	<p>UNCLASSIFIED</p>	<p>UNCLASSIFIED</p>
<p>UNCLASSIFIED</p>	<p>UNCLASSIFIED</p>	<p>UNCLASSIFIED</p>	<p>UNCLASSIFIED</p>
<p>UNCLASSIFIED</p>	<p>speed mechanical behavior of textile structures with a view to determining factors controlling translation of fiber yarn and fabric properties into impact performance of the end product. Mechanical behavior of stored and exposed materials was studied at impact speeds up to 40ft/sec. A pneumatic-hydraulic test unit was developed in the study and served to accelerate the test procedures over earlier drop weight methods.</p>	<p>UNCLASSIFIED</p>	<p>UNCLASSIFIED</p>

<p>UNCLASSIFIED</p> <p>TEXTILE DIVISION, MASSACHUSETTS INSTITUTE OF TECHNOLOGY, Cambridge, Mass. DYNAMIC TESTING OF SMALL TEXTILE STRUC- TURES AND ASSEMBLIES by J.G. Krizik, D.M. Mellen, S. Backer, January 1961. 106p. Incl. figs. and tables. (Project 7-93-18- 019) (Contract No. Da-19-129- QM-1308)</p> <p>Unclassified Report</p> <p>Reports a study of the high (over)</p>	<p>UNCLASSIFIED</p> <p>TEXTILE DIVISION, MASSACHUSETTS INSTITUTE OF TECHNOLOGY, Cambridge, Mass. DYNAMIC TESTING OF SMALL TEXTILE STRUC- TURES AND ASSEMBLIES by J.G. Krizik, D.M. Mellen, S. Backer, January 1961. 106p. Incl. figs. and tables. (Project 7-93-18- 019) (Contract No. Da-19-129- QM-1308)</p> <p>Unclassified Report</p> <p>Reports a study of the high (over)</p>	<p>UNCLASSIFIED</p>
<p>UNCLASSIFIED</p> <p>speed mechanical behavior of textile structures with a view to determining factors control- ling translation of fiber yarn and fabric properties into impact performance of the end product. Mechanical behavior of stored and exposed materials was studied at impact speeds up to 40ft/sec. A pneumatic hydraulic test unit was devel- oped in the study and served to accelerate the test procedures over earlier drop weight methods.</p>	<p>UNCLASSIFIED</p> <p>speed mechanical behavior of textile structures with a view to determining factors control- ling translation of fiber yarn and fabric properties into impact performance of the end product. Mechanical behavior of stored and exposed materials was studied at impact speeds up to 40ft/sec. A pneumatic hydraulic test unit was devel- oped in the study and served to accelerate the test procedures over earlier drop weight methods.</p>	<p>UNCLASSIFIED</p> <p>UNCLASSIFIED</p>